Damage Repair Mechanisms in Sensory Hair Cells

Submitted for the degree of Doctor of Philosophy

Nicola Jayne Allen

April 2015

Declaration

I hereby declare that this thesis has not been and will not be submitted in whole or in part to another university for the award of any other degree.

Signature,

Nicola Jayne Allen

This thesis is dedicated to the loving memory of Betty Grace Case.

ACKNOWLEDGEMENTS

Thank you to Action on Hearing Loss for giving me the opportunity and funding to pursue my PhD.

I owe my deepest gratitude to my supervisors Guy Richardson and Richard Goodyear for their continued support and guidance throughout the course of my PhD. I also thank my fellow members of the Hearing Group at Sussex, in particular, Kevin Legan and Lindsey Welstead for being there to answer my endless questions and for training me in genotyping.

Special thanks to Julia Korchagina and Terri Desmonds for sharing the early stages of my PhD with me and Terri Roberts and Freya Crawford for advice during the final stages.

I cannot end without thanking my mum, dad, family and friends for their continued support during my education.

Finally, thank you to Ash Robinson for being by my side. I don't know how I would have made it this far without you.

UNIVERSITY OF SUSSEX

NICOLA JAYNE ALLEN

SUBMITTED FOR THE DEGREE OF DOCTOR OF PHILOSOPHY

DAMAGE REPAIR MECHANISMS IN SENSORY HAIR CELLS

SUMMARY

Aminoglycoside antibiotics are a class of drug used to treat bacterial infections but have the unfortunate side effect of being both oto- and nephro-toxic. Deafness caused by aminoglycoside ototoxicity results from a loss of sensory hair cells from the inner ear. In vitro, two early effects of aminoglycoside exposure can be observed. First, membrane blebs are formed around the perimeter of the hair-cell apical surface. Secondly phosphatidylserine (PS), an aminophospholipid that is normally restricted to the inner leaflet of the plasma membrane, flops to the outer leaflet. This membrane damage occurs rapidly, within 90-120 seconds of drug exposure and can be completely reversed. The aim of this thesis was to determine the molecular mechanisms underlying damage repair in sensory hair cells recovering from aminoglycoside damage. TEM studies using cationic ferritin as a tracer indicates the repair process involves membrane internalisation, but recovery cannot be blocked by inhibitors of macropinocytosis, the clathrin-independent carrier (CLIC) pathway, PI3 kinase, PKC, Pak1 or of the clathrin-coated pit pathway. Damage repair is, however, prevented by the actin stabiliser jasplakinolide and the inhibitor of Protein kinase A, H-89. In addition, the CLIC pathway inhibitor EIPA has been uncovered as a reversible blocker of aminoglycoside entry into hair cells.

LIST OF ABBREVIATIONS

ALC	ankle-link molecular complex
AP2	adapter protein complex 2
ARP2/3	actin-related protein 2/3
BAPTA	1,2-bis (o-aminophenoxy) ethane-N,N.N',N'-tetraacetic acid
BIM I	Bisindolylmaleimide I
CCV	clathrin-coated vesicle
Cdh23	cadherin 23
CK2	casein kinase 2
CLIC	clathrin-independent carrier
CTx	cholera toxin
DDSA	dodecenyl succinic anhydride
DMEM	Dulbecco's Modified Eagle's Medium
DMP-30	2,4,6-tri (dimethylaminomethyl) phenol
DMSO	dimethylsulphoxide
E	embryonic
EGTA	ethylene glycol tetraacetic acid
EH	epidermal growth factor receptor substrate 15 (Eps15) homology
EHD3	Eps15 homology domain containing 3

EIPA	5-(N-Ethyl-N-isopropyl)amiloride
ELK-1	ETS domain-containing protein
FBS	fetal bovine serum
F-actin	filamentous actin
FM1-43	*N*-(3-triethylammoniumpropyl)-4-(4-(dibutylamino)styryl)pyridinium dibromide
GEEC	GPI-AP-enriched early endosomal compartments
GPI-AP	glycosylphosphatidyl-inositol anchored proteins
GRAF1	GTPase regulator associated with focal adhesion kinase-1
GTTR	gentamicin Texas Red
H-89	(E)-N-(2-(4-bromocinnamylamino)ethyl)isoquinoline-5-sulfonamide dihydrochloride
HBHBSS	Hepes buffered Hank's balanced salt solution
HIP1	huntingtin interacting protein 1
HIP1R	huntingtin interacting protein 1 related protein
HS	horse serum
IHC	inner hair cell
IPA 3	1,1'-Disulfanediyldinaphthalen-2-ol
JIP-1	c-jun-interacting protein-1
JNK	c-jun NH_2-terminal kinase

KT5720	protein kinase A inhibitor
LY294002	2-(4-morpholinyl)-8-phenyl-4*H*-1-benzopyran-4-one
MDCK	Madin-Darby canine kidney
MET	mechanoelectrical transducer
$MgCl_2$	magnesium chloride
MNA	methyl nadic anhydride
N-WASP	neural Wiscott-Aldrich syndrome protein
NPF	nucleation-promoting factor
OHC	outer hair cell
P	postnatal
PAK1	p21 activated kinase
PBS	phosphate buffered saline
Pcdh15	protocadherin 15
PCR	polymerase chain reaction
PE	phosphatidylethanolamine
PI3K	phosphatidylinositol-4,5-biphosphate 3-kinase
PKA	protein kinase A
PKC	protein kinase C
PS	phosphatidylserine

PtdLns(4,5)P_2	phosphatidylinositol-4,5-biphosphate
Ptprq	protein tyrosine phosphatase receptor Q
RCM	rat culture medium
ROCK1	Rho-associated kinase 1
ROS	reactive oxygen species
SEM	scanning electron microscopy
TBE	tris borate EDTA
TBS	tris buffered saline
TEM	transmission electron microscopy
TMEM16F	Transmembrane protein 16F
Tween-20	polysorbate 20
UV	ultraviolet
Vlgr1	very large G-protein-coupled receptor 1

TABLE OF FIGURES

TABLE OF TABLES

TABLE OF CONTENTS

1 INTRODUCTION

The aminoglycoside antibiotics are an important class of drug used to treat infections caused by gram negative bacteria. These drugs have unfortunate side effects and can cause deafness due to the permanent loss of sensory hair cells from the inner ear. Whilst these effects are irreversible, it has been shown that hair cells are able to repair the damage caused by short-term exposure to high doses of aminoglycosides in vitro (Goodyear et al., 2008). Membrane damage in sensory hair cells can also be caused by other insults that result in temporary or permanent hearing loss. Therefore, understanding the repair process may lead to development of strategies for preventing drug-induced hair cell death and ameliorating recovery from temporary deafness that might otherwise become permanent.

1.1 The ear

Our sense of hearing provides us with a wealth of information about our environment and is essential for communication and human interaction. Sound is detected by the peripheral auditory system which comprises the outer, middle and inner ear (Figure 1.1). The inner ear consists of the cochlea, which is a part of the auditory system, and the vestibular apparatus which detects head acceleration and rotation. The cochlea is a coiled tube which is partitioned along its length by the basilar membrane. Sitting on top of the basilar membrane is the organ of Corti, a structure containing sensory hair cells- polarised epithelial cells that have a mechanosensory hair bundle composed of multiple stereocilia at their apical ends (Purves, 2008).

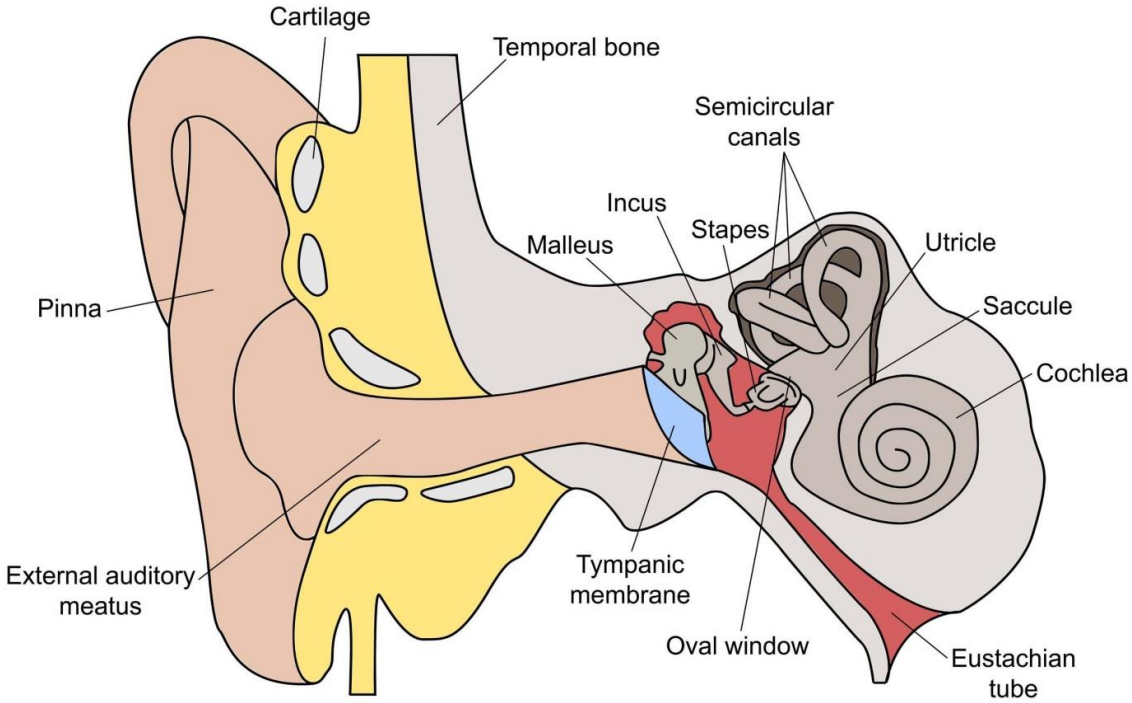

Figure 1.1. Anatomy of the outer, middle and inner ear.

1.2 The organ of Corti

The sensory hair cells of the cochlea are arranged in rows with one row of inner hair cells (IHCs) on the modiolar side of the tunnel of Corti and three rows of outer hair cells (OHCs) on the opposing side (Figure 1.2) (Pickles, 1988). Specialised types of supporting cells called Deiters' cells, are situated at the basal pole of the OHCs and send phalangeal processes between the OHCs. On the lateral side of the organ of Corti, there is another row of supporting cells known as Hensen's cells. The tectorial membrane is an extracellular matrix situated above the hair cells and is attached to the spiral limbus. The OHCs are attached by their longest stereocilia to the tectorial membrane and the stereocilia of the IHCs are in close apposition to a ridge on the underside of the tectorial membrane called Hensen's stripe (Pickles, 1988). Movement of the basilar membrane in response to sound pressure leads to a shearing motion between the organ of Corti and the tectorial membrane (Purves, 2008).

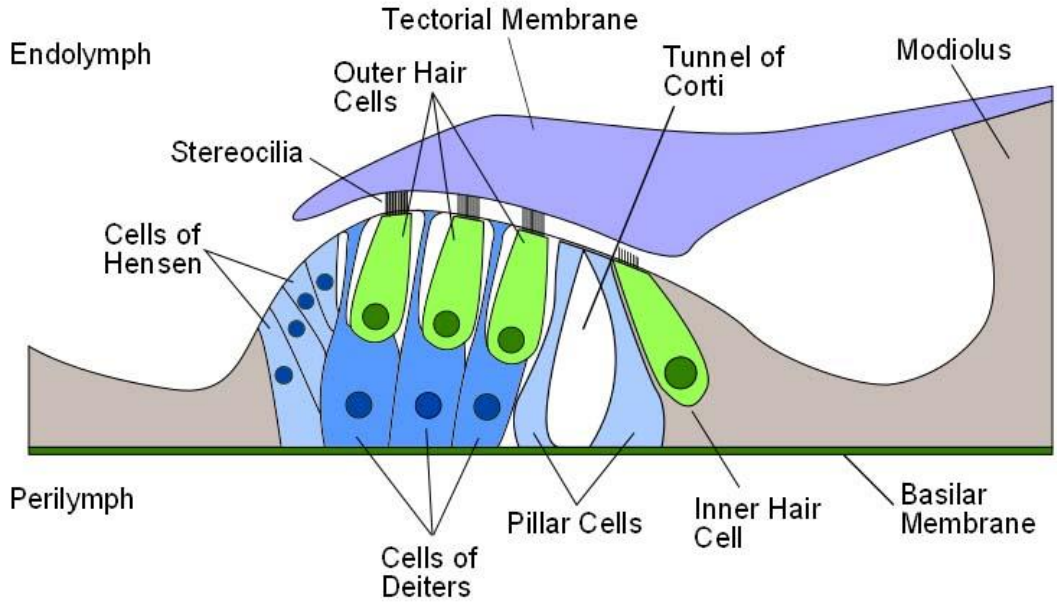

Figure 1.2. A cross section through the organ of Corti.

1.3 Hair cells

1.3.1 The hair bundle

The hair bundle is composed of two or more rows of stereocilia that are arranged in order of increasing height. These numerous stereocilia are packed with highly-cross linked filamentous actin giving them rigidity and are connected to adjacent stereocilia via stereociliary links which include tip links and horizontal top connectors (Goodyear et al., 2005; Osborne et al., 1988). The actin filaments within each stereocilium are polarised and arranged with the preferred end for actin monomer addition located at their distal tips. A number of actin filaments within a single stereocilium project from the taper region at the base of the stereocilia into the cuticular plate to form rootlets. The cuticular plate is located just below the hair bundle within the cytoplasm and is comprised of cytoskeletal proteins that form a dense meshwork. The cuticular plate allows stereocilia to be anchored into the top end of the cell (Pickles, 1988).

Deflections of the hair bundle toward the tallest row of stereocilia leads to opening of the mechanoelectrical transducer (MET) channels, whilst deflections in the opposite direction causes a closing of the MET channels. The nucleus of the hair cell is located towards the basal pole of the cell, a region contacted by afferent and efferent nerves. A single type 2 afferent nerve fibre innervates many OHCs whereas a single IHC is innervated by many highly myelinated type 1 afferent fibres (Purves, 2008).

1.3.2 Stereociliary links

The stereocilia of the hair bundle are connected to one another via various link types comprised of discrete proteins (Figure 1.3). A single kinocilium is present within the hair bundles in the cochlea of early postnatal mice and is joined to the tallest adjacent stereocilia via kinocilial links (Figure 1.3) (Goodyear et al., 2005). Kinocilial links within avian hair bundles are composed cadherin 23 (Cdh23) and protocadherin 15 (Pcdh15) in an asymmetric distribution, with the latter associated with the kinocilial membrane (Goodyear et al., 2010). Adjacent stereocilia are connected to one another by ankle links located at the base of the stereocilia (Figure 1.3). Ankle links are present in all vertebrate hair bundles but are only detected within the mouse hair bundle between the ages postnatal (P) 2 and P9. Ankle links comprise of very large G-protein-coupled receptor 1 (Vlgr1) (McGee et al., 2006) and usherin (Michalski et al., 2007). In mouse OHC bundles between embryonic (E) 17 and P15 shaft connectors are transiently expressed linking adjacent stereocilia (Figure 1.3). One component of the shaft connectors is a receptor-like inositol lipid phosphatase known as protein tyrosine phosphatase receptor Q (Prprq) (Goodyear et al., 2003). It has been suggested shaft connectors function to prevent fusion of stereocilia by acting as a spacer (between adjacent stereocilia) as opposed to providing hair bundle cohesiveness (Goodyear et al., 2003).

Horizontal top connectors are a type of stereociliary link located towards the apical end of the stereocilia. They form a zipper-like structure (Figure 1.3) and in mice, are thought to be formed of the protein stereocilin and maintain cohesion of the hair bundle (Verpy et al., 2011).

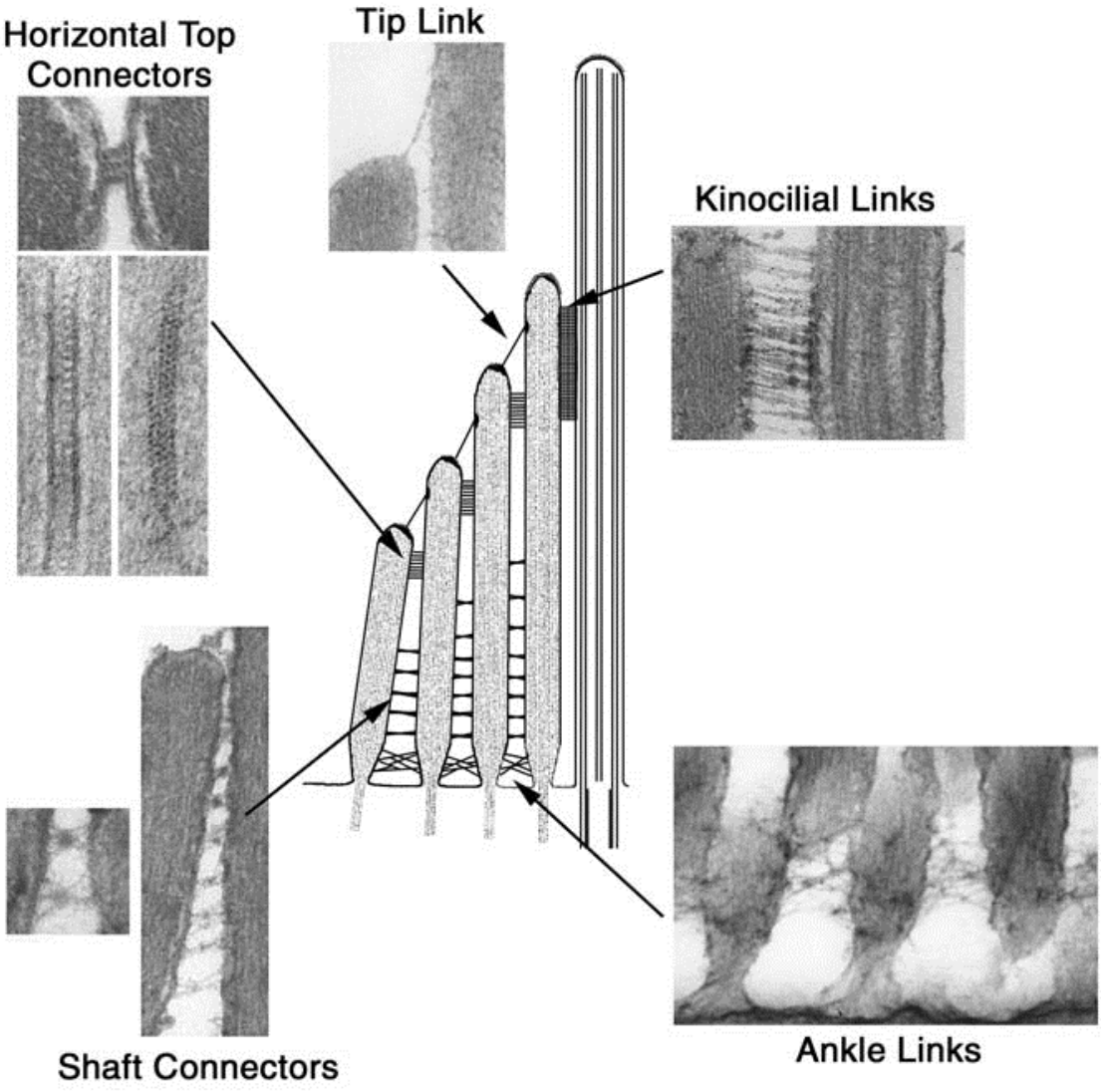

Figure 1.3. Link types present in the hair bundle of hair cells from the mammalian cochlea. From Nayak et al., 2007.

Tip links are a type of stereociliary link joining the tip of one stereocilium to the side of an adjacent stereocilium in a taller row (Figure 1.3) (Goodyear et al., 2005). Changes in tip link

tension alter the opening probability of the associated MET channel. Tip links therefore have a vital role in mechanotransduction. Tip links are composed of a pair of helically arranged protofilaments which bifurcate, at each end, into single filaments that attach to the membrane surface (Kachar et al., 2000). The proteins which form the tip link are cadherin 23 (Siemens et al., 2004) (Tsuprun et al., 2004) and protocadherin 15 (Ahmed et al., 2006) (Figure 1.4). The upper tip link density is a protein-dense region at the upper end of the tip link containing myosin VIIa which is thought to maintain tension on the tip links as well as containing the scaffolding proteins Sans and harmonin-b (Grati and Kachar, 2011). The MET channel is known to be associated with the lower tip link density (Figure 1.4).

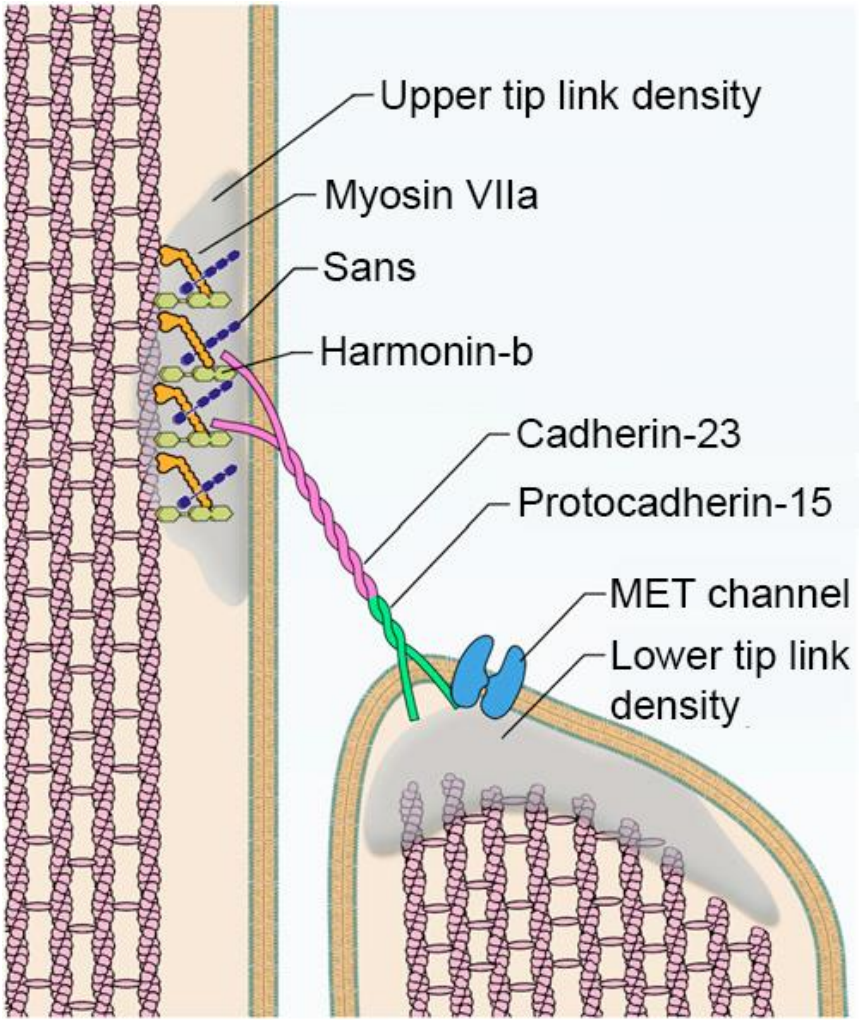

Figure 1.4. Tip link proteins and the MET channel. Adapted from Grati and Kachar, 2011.

1.4 Ototoxic compounds

Certain classes of drugs are known to be ototoxic and in many cases cause a permanent hearing loss. Ototoxic drugs include, but are not limited to, anti-malarials, loop-diuretics, aminoglycoside antibiotics and chemotherapy agents such as cisplatin (Rybak and Ramkumar, 2007). In addition, the active ingredient in aspirin, salicylate, is known to cause hearing loss and tinnitus (Sheppard et al., 2014).

1.4.1 Aminoglycoside antibiotics

Since their discovery in the 1940's (Schatz et al., 1944), the aminoglycoside antibiotics have been widely used for the treatment of infections caused by gram negative organisms. Aminoglycosides are currently administered to patients with severe infections caused by multi-drug resistant tuberculosis and for the treatment of urinary tract infections with complications (Xie et al., 2011). The aminoglycosides are also frequently used for the treatment of life threatening sepsis in neonates (van den Anker, 2014). Unfortunately, the aminoglycoside antibiotics are both oto- and nephro-toxic. The ototoxic effects of aminoglycosides cause the irreversible loss of sensory hair cells from the inner ear, leading to permanent deafness (Forge et al., 2000). Due to their low cost when compared to other antibiotics with less severe side effects, aminoglycosides are used in developing countries in unrestricted dosages as a first-line treatment for less severe infections including otitis media and bronchitis, (Schacht, 1993).

1.4.1.1 Antimicrobial effects

For the treatment of severe infections, aminoglycoside antibiotics are usually administered intravenously as they are poorly absorbed by the gut (Rizzi and Hirose, 2007). Aminoglycosides exert antimicrobial effects by inhibiting protein synthesis. All aminoglycoside antibiotics are positively charged due to the presence of multiple amine groups (Figure 1.5). These polycationic molecules are thought to enter gram negative bacteria by firstly displacing cross-links between adjacent lipopolysaccharides within the outer plasma membrane (Peterson et al., 1985). This displacement compromises the membrane structure and leads to the formation of blister like protrusions known as membrane blebs (Martin and Beveridge, 1986). The formation of membrane blebs in the bacterial plasma membrane results in emergence of holes in the cell wall which allows further entry of aminoglycosides. Aminoglycosides cross the inner plasma membrane and enter the bacterial cytosol. The mechanism by which aminoglycosides cross the inner plasma membrane is not yet clear but recently it has been suggested they enter via the mechanosensitive channel of large conductance (MscL) (Iscla et al., 2014). Upon entering the cytosol, aminoglycosides bind to the 30S ribosomal subunit at the A-translational site of the 16S rRNA, thus causing misreading of mRNA. This disruption of protein synthesis leads to the accumulation of defective proteins which ultimately results in bacterial cell death (Schacht et al., 2012).

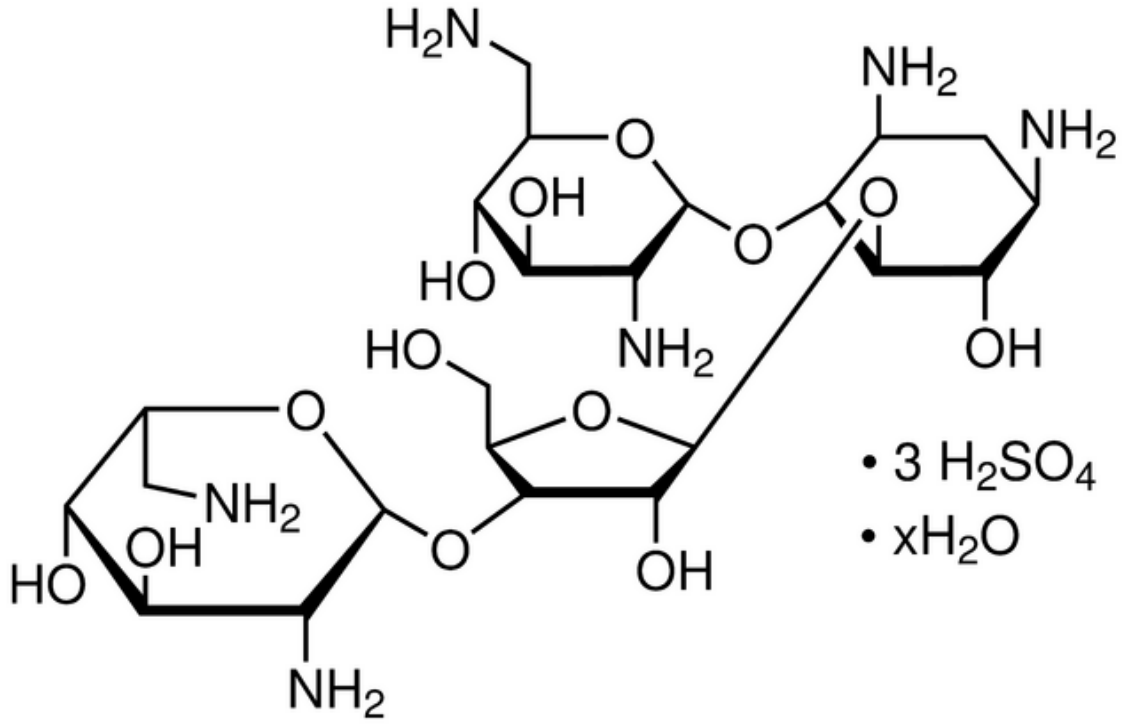

Figure 1.5. The chemical structure of neomycin showing multiple amine groups. Image from Sigma Aldrich.

1.4.1.2 Clinical presentation

Nephrotoxicity results from the aminoglycoside accumulating within the proximal tubules of the kidney and is usually reversible with hydration therapy (Heller, 1984). All aminoglycosides are ototoxic with some preferentially causing damage to the cochlea (cochleotoxic) and some to the vestibular system (vestibulotoxic). The ototoxic effects of aminoglycosides were uncovered following the initial clinical trials of streptomycin. Streptomycin appears to be more vestibulotoxic than cochleotoxic whereas a modified form, dihydrostreptomycin, preferentially causes more damage to the cochlea. Symptoms of vestibulotoxicity include loss of balance when turning the head, an ataxic gait and in some cases vertigo (Rizzi and Hirose, 2007). The main regions of vestibular damage include the sensory hair cells in the apical region of the cristae and the striolar region of the saccular maculae and utricular region (Rizzi and Hirose,

2007). Cochleotoxicity presents itself as a bilateral sensorineural hearing loss within the high-frequency range. This is due to damage to the outer hair cells within the basal region of the cochlea (Rizzi and Hirose, 2007). Reported statistics of patients suffering from hearing loss as a result of aminoglycoside treatment vary widely with hearing loss occurring in up to 50% of patients treated (Chen et al., 2007). Variation is likely to be the result of different regimens of administration combined with different methods for testing hearing function. Of the patients receiving a 5 to 7 day course of aminoglycoside treatment for acute infections, 20% reportedly had a hearing loss. Moreover, testing of the high-frequency hearing range reveals 47% of patients acquire a hearing loss following short term aminoglycoside treatment (Xie et al., 2011). These data indicate hearing loss in the high-frequency range may be missed during hearing tests which do not target the very high frequencies.

1.4.1.3 Aminoglycoside entry into hair cells

Although the ototoxic effects of aminoglycosides have been well studied, there has been much debate regarding mechanisms of aminoglycoside uptake into hair cells. Transmission electron microscopy (TEM) images taken from OHCs show an abundance of coated pits which can be seen across the apical surface of hair cells, suggesting aminoglycosides enter hair cells via endocytosis (Richardson and Russell, 1991). Another study (Hashino and Shero, 1995) supporting this used immunogold electron microscopy to study the ultrastructure of kanamycin accumulation within sensory hair cells. Kanamycin was shown to accumulate at the apical surface of hair cells following treatment, with accumulation also observed within vesicles containing the membrane tracer cationic ferritin (Hashino and Shero, 1995). These vesicles were located just beneath the apical surface of hair cells and the cationic ferritin labelling shows the membrane was initially located on the apical surface before becoming

internalised (Hashino and Shero, 1995). Endocytosis is an active process which is temperature dependent. Uptake of the fluorescently tagged aminoglycoside gentamicin Texas Red (GTTR) is, however, only weakly dependent on temperature, suggesting an alternate route of aminoglycoside entry into hair cells via a pore (Myrdal et al., 2005).

The current proposed mechanism for aminoglycoside entry into hair cells is via the MET channels. This was not initially thought possible as the diameter of the MET channel pore was estimated at 0.6 nm (Corey and Hudspeth, 1979) and the end-on diameter of dihydrostreptomycin is approximately 0.8 nm making it too large to pass through. However, a study using hair cells from the turtle inner ear provided an estimated pore size of 1.25 nm (Farris et al., 2004), revealing the MET channel pore is in fact large enough to permit aminoglycoside entry. Furthermore, electrophysiological recordings have shown dihydrostreptomycin permeates hair cells via open MET channels in OHCs and also acts as a permeant blocker of these channels (Marcotti et al., 2005). Entry via the MET channel is also supported by studies using the fluorescent stryl dye FM1-43. The structure of FM1-43 includes a positively charged ammonium head which allows it to pass through the MET channel as it is a non-selective cation channel. Studies have shown pre-treatment with FM1-43 reduces neomycin-induced ototoxic damage (Gale et al., 2001). Additional evidence supporting the MET channel as a route of entry comes from the use of calcium chelators. Calcium chelators including BAPTA and EGTA cleave tip links and consequently block mechanotransduction by closing MET channels. There is a reduction in ototoxic membrane damage in hair cells of cochlear cultures treated with calcium chelators (Goodyear et al., 2008). Mice lacking myosin VIIa have fewer open MET channels at rest which results in less aminoglycoside entering hair cells, therefore reducing the damage associated with aminoglycoside ototoxicity (Richardson et al., 1997).

1.4.2 Hair cell damage

Aminoglycoside antibiotics enter hair cells and exert their ototoxic effects by activating signalling pathways which contribute towards the initiation of programmed cell death, otherwise known as apoptosis (Rybak and Ramkumar, 2007). Hair cell death following aminoglycoside exposure results from the production of reactive oxygen species (ROS) (Clerici et al., 1996). ROS including hydrogen peroxide and superoxide are formed by an aminoglycoside-iron complex which reacts with electron donors, for example arachidonic acid, to produce ROS (Rybak and Ramkumar, 2007). ROS are produced as a primary metabolic product during normal physiological conditions and any detrimental effects of ROS are kept under control by maintaining a redox balance by cellular antioxidant systems. This balance can be disturbed by an increased level of ROS within the cell, producing highly ROS with the ability to initiate cell death (Xie et al., 2011). A reduction in aminoglycoside-induced ototoxicity is observed in the hair cells of mice overexpressing Cu/Zn-superoxide dismutase, a superoxide scavenging enzyme (Sha et al., 2001). This indicates elevated levels of ROS contribute towards the damage observed during aminoglycoside-induced ototoxicity. There are many proposed signalling pathways which mediate apoptosis following aminoglycoside exposure including the c-Jun N-terminal kinase (JNK) pathway (Figure 1.6). JNK is a MAP kinase and is activated by ROS during aminoglycoside-induced apoptosis. JNK is situated within the cytoplasm and is activated via phosphorylation by c-Jun-interacting protein-1 (JIP-1). This results in JNK activating various transcription factors in the cytoplasm (c-Jun, c-Fos, ETS domain-containing protein [ELK-1]) and in the mitochondria (Bcl-2). Elevated JNK, c-Fos, c-Jun and Bcl-2 are found in hair cells following aminoglycoside exposure (Huth et al., 2011). Inhibition of the JNK pathway by the peptide inhibitor D-JNKI-1 and CEP-1347, a derivative of the small molecule indocarbazole K252a (Pirvola et al., 2000), protects hair cells in the mouse cochlea from the ototoxic effects

of neomycin, highlighting the role of the JNK pathway in apoptosis following aminoglycoside treatment (Wang et al., 2003).

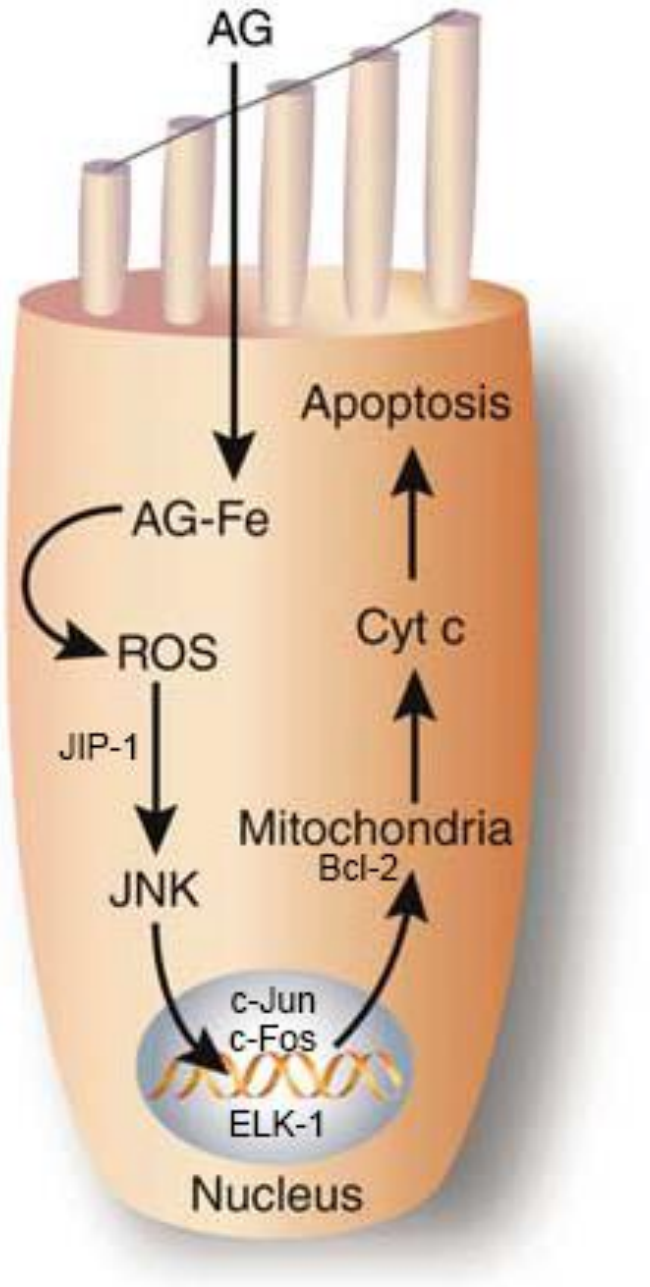

Figure 1.6. Aminoglycoside induced hair-cell death pathway. Aminoglycosides enter hair cells via the MET channel located at the tips of the stereocilia. Aminoglycosides form a complex with iron which produces ROS and activates the JNK pathway. Genes are activated in the nucleus which translocate to the mitochondria leading to cytochrome c leakage and activation of caspases which result in initiation of apoptosis. Adapted from Rybak and Ramkumar, 2007.

In addition to the JNK pathway, aminoglycosides have been shown to exert their ototoxic effects by altering levels of the phosphoinositides phosphatidylinositol-4,5-bisphosphate (PIP_2) and phosphatidylinositol-3,4,5-trisphosphate (PIP_3) (Jiang, Sha and Schacht, 2006). Following treatment with the aminoglycoside kanamycin, PIP_2 levels are increased in the apex and nuclei of OHCs due to an inhibition of the kinase reaction phosphorylating PIP_2 to PIP_3. The formation of a complex between histone H3 and PIP_2 is increased due to a rise in levels of PIP_2 in the nuclear membrane. The PIP_2 and histone H3 complex formation attenuates acetylation of histone H3 and induces gene transcription inhibition. The reduced level of PIP_3 is thought to inhibit the activity of the PIP_3/Akt pathway, contributing to death of OHCs (Jiang et al., 2006).

Exposure to the aminoglycoside neomycin in vitro leads to the occurrence of two events at the apical pole of sensory hair cells in mouse cochlear cultures. One event is the formation of blister-like protrusions (referred to throughout as membrane blebs for simplicity but see discussion) on the apical surface of hair cells (Richardson and Russell, 1991), the other is externalisation of the aminophospholipid phosphatidylserine (PS) which is usually restricted to the inner leaflet of the plasma membrane (Goodyear et al., 2008). The mechanisms underlying these two phenomena are not yet fully understood and may be entirely independent processes as PS externalisation can occur without membrane bleb formation following exposure of sensory hair cells to high levels of extracellular calcium (Goodyear et al., 2008). PS externalisation and the formation of membrane blebs are both universal signs of apoptosis that occur in many cell types including neutrophils, the T cell line Jurkat, the human leukemic cell line HL-60 and human embryonic kidney 293 cells (Bratton et al., 1997; Meshki et al., 2009).

1.4.2.1 Membrane blebbing

Membrane blebs are blister-like protrusions of the plasma membrane that can appear and disappear within a matter of minutes (Charras, 2008a). The formation of membrane blebs is a common occurrence in vitro and in vivo in different cell types and these protrusions have varying functions including apoptosis (Coleman et al., 2001), cytokinesis and cell movement (Fackler and Grosse, 2008). Apoptosis is necessary for the removal of damaged cells by phagocytes in a process called efferocytosis (Wickman et al., 2012). Following cell damage, an intrinsic mitochondrial pathway will be triggered leading to activation of caspases and formation of membrane blebs. In addition, PS externalisation occurs to act as an eat-me signal to attract macrophages. Once the signal is detected, cellular debris will be phagocytosed and translocated to lysosomes for degradation (Wickman et al., 2012) (Figure 1.7). The blebs formed during apoptosis are highly enriched with externalised PS, suggesting membrane blebs serve to focus PS and thereby assist recognition of damaged cells by macrophages (Wickman et al., 2012).

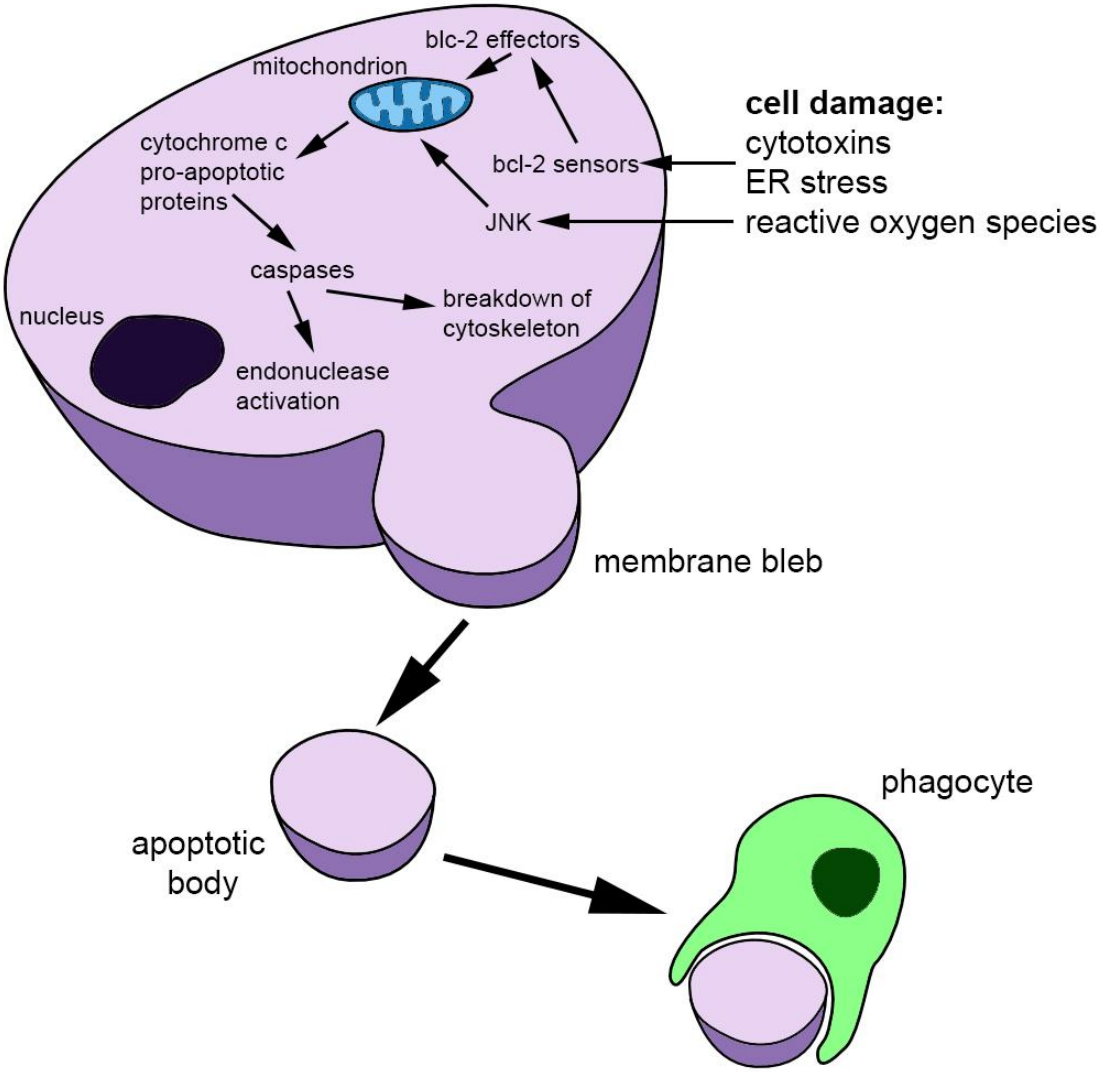

Figure 1.7. Membrane bleb formation during the process of apoptosis.

The formation of membrane blebs has been studied extensively and the molecular mechanisms underlying the life cycle of a bleb are well understood. Local formation of membrane blebs can be blocked by inhibiting myosin II-ATPase with blebbistatin or by inhibiting Rho-associated kinase 1 (ROCK1) with Y-27632 and 3-(4-pyridyl)indole, indicating the vital role of myosin II and ROCK1 in bleb formation (Charras et al., 2005). Membrane blebs are similar in all cell types and are initially formed when a region of plasma membrane becomes detached from the actin cortex (Figure 1.8). This plasma membrane detachment occurs when

the myosin II motor protein causes a local actin cortical contraction, leading to an increase in cytoplasmic pressure within the cell (Figure 1.8 A1) or an increase in actin cortex tension via local myosin movements (Figure 1.8 A2). Intracellular pressure causes the membrane to separate from the actin cortex (Figure 1.8 B1) or the cortex to simply rupture in a process called nucleation (Figure 1.8 B2). Cytosol then inflates the plasma membrane. Following this, the membrane bleb enters a growth phase by increasing in size and surface area as cytosol forces its way into the bleb to form a blister-like protrusion. The bleb is a blister that lacks actin and cytoskeletal components (Figure 1.8 C1,C2). Expansion of the bleb slows as cortical actin contractions are no longer able to drive more cytosol into the filling bleb. In addition to this, an actin cortex cage forms within the bleb (Figure 1.8 D). Finally, retraction of the membrane bleb occurs as myosin II powers the contractile process at the bleb rim (Figure 1.8 E) (Charras et al., 2008c).

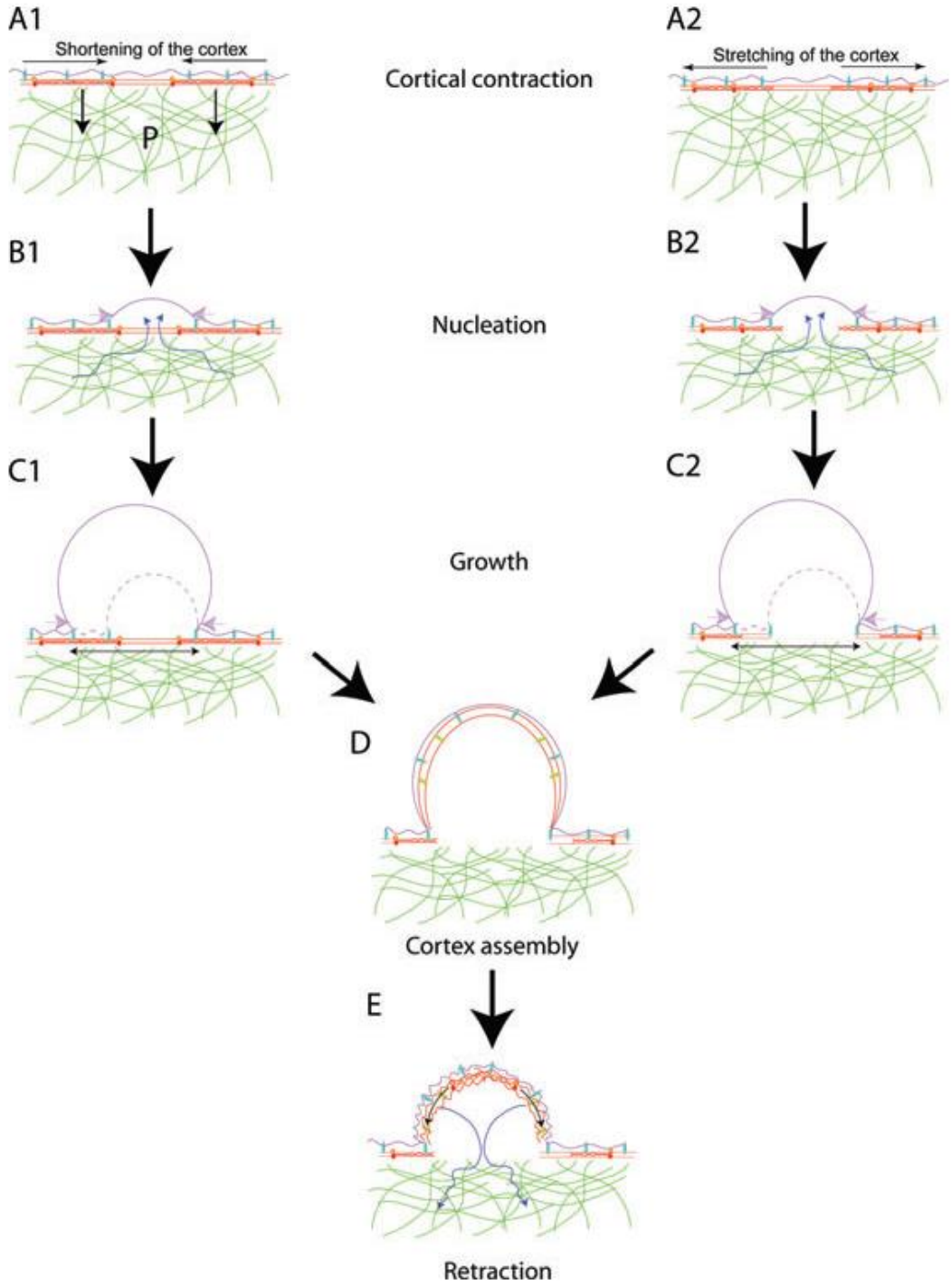

Figure 1.8. Formation and retraction of a membrane bleb. From Charras, 2008a.

When mouse cochlear cultures are treated with the aminoglycoside neomycin, membrane bleb formation is specific to hair cells (Figure 1.9). During neomycin exposure, membrane blebs appear rapidly, within 75 seconds of treatment (Goodyear et al., 2008), and are observed in a distinct gradient along the length of the cochlea. Hair cells from the high frequency basal end of the cochlea are more sensitive to neomycin damage than those at the low frequency apical end (Richardson and Russell, 1991). Neomycin-induced membrane blebs can reach diameters of up to 3 μm with a surface area of 28 μm^2 if the bleb is assumed to be smooth and spherical (Richardson and Russell, 1991). Membrane blebs also form on the apical surface of hair cells from the isolated mature guinea pig cochlea in response to sodium loading. This similarity in membrane bleb formation suggests immature mouse cochlear cultures are a good model system as they may be relevant to mature auditory hair cells (Shi, Gillespie, & Nuttall, 2005). In addition, a potential alternate system to study aminoglycoside-induced membrane damage is the mature vestibular system.

The formation of membrane blebs in response to neomycin insult is considered to be the result of new membrane being added to the plasma membrane. This addition of new membrane is likely as there is only a small stretch limit (2-4%) of the plasma membrane before the cell will lyse (Richardson and Russell, 1991). Further evidence supporting the addition of new membrane comes from capacitance recordings which show an increase in whole cell capacitance following neomycin treatment indicating an increase in surface area of the hair cell (Goodyear et al., 2008). Additional features of membrane blebs come from freeze fracture analysis which reveals neomycin-induced blebs are composed of atypical membrane. This membrane is lacking intramembrane particles and has a high concentration of unsaturated lipid in fluid phase (Forge and Richardson, 1993). Moreover, the content of membrane blebs include large vacuoles, membrane whorls, cytoplasm and vesicles (Goodyear et al., 2008).

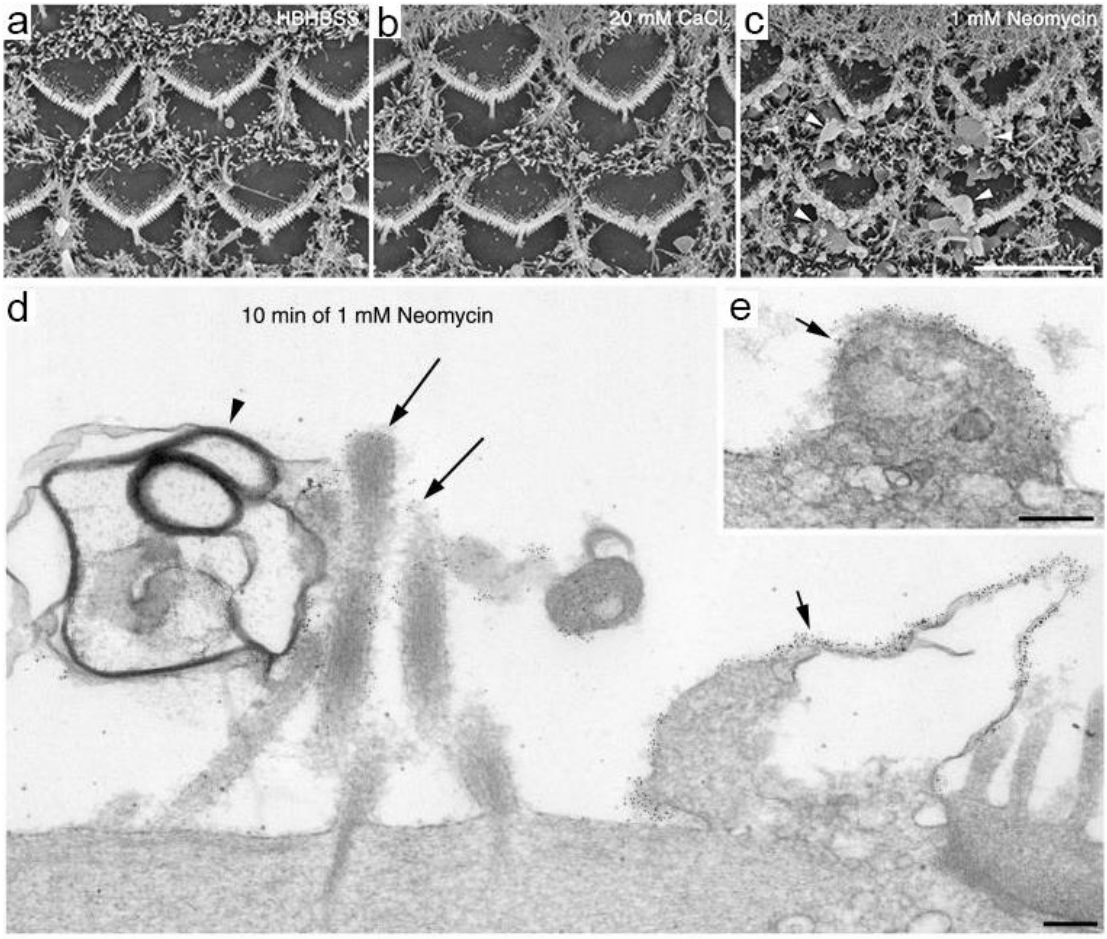

Figure 1.9. Scanning electron microscope (SEM) images showing the apical surface of OHCs from a cochlear culture treated with HBHBSS, $CaCl_2$ or neomycin (**a-c**). Transmission electron microscope (TEM) images showing membrane bleb formation in response to neomycin (**d,e**). Hair cells treated with $CaCl_2$ do not develop membrane blebs across the apical surface (**b**). Membrane blebs can be observed on the apical surface of hair cells treated with neomycin. Control cultures do not have membrane blebbing across the apical surface (**a**). The ultrastructure of neomycin-induced membrane blebs after 10 minutes treatment shows they contain large vacuoles, vesicles and cytoplasm (**d,e**). Arrows indicate annexin V labelling is seen on membrane blebs and stereocilia. Adapted from Goodyear et al., 2008.

1.4.2.2 Phosphatidylserine externalisation

In most cell types, a cell entering apoptosis will signal to macrophages via modifications of the affected cell's plasma membrane. In healthy cells, the plasma membrane has an asymmetric distribution of phospholipids with the aminophospholipids including PS and phosphatidylethanolamine (PE) usually restricted to the inner leaflet (Figure 1.10). The outer

leaflet of the plasma membrane houses the choline-containing phospholipids including sphingomyelin and phosphatidylcholine (Kleinegris et al., 2012). To maintain this asymmetric distribution, PS and PE are shuttled from the outer leaflet to the inner leaflet via an aminophospholipid translocase. Simultaneously a floppase pumps all phospholipids from the inner leaflet to the outer leaflet, but at a slower rate (Kleinegris et al., 2012).

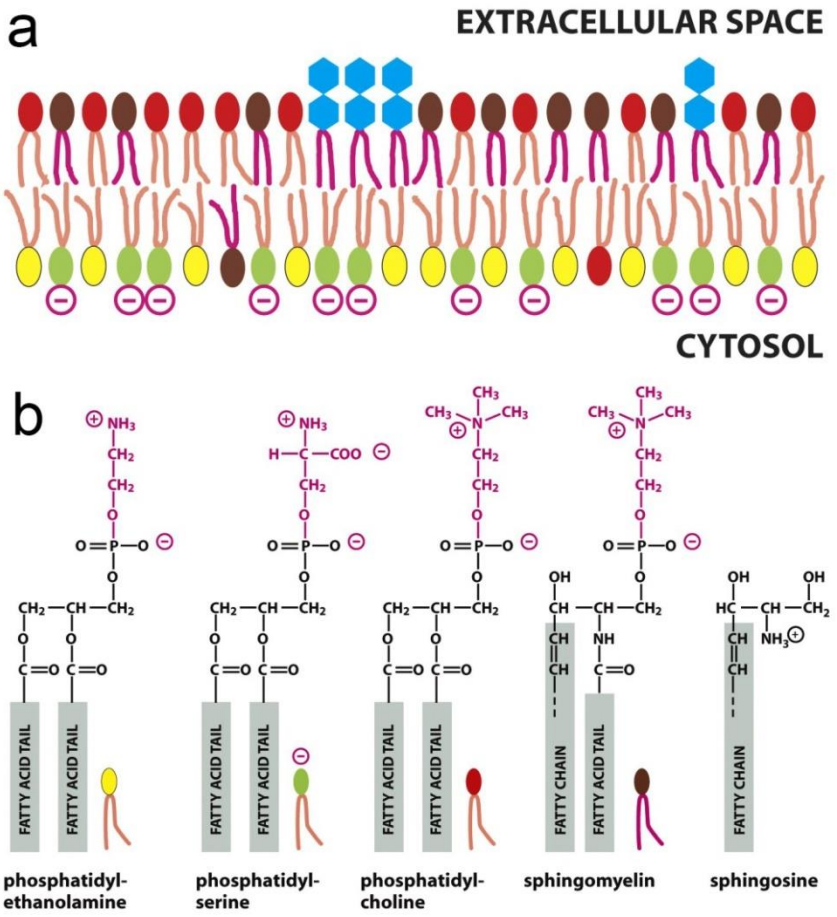

Figure 1.10. (**a**) A typical lipid bilayer with an asymmetric distribution of phospholipids. PS (coloured green) is mostly found on the inner leaflet. (**b**) The structure of different phospholipids found within a typical plasma membrane. Adapted from Alberts et al., 2008.

During cell damage by various insults, PS will translocate to the outer leaflet of the plasmalemma as a consequence of lipid scramblase activity. PS externalisation occurs early on

during the process of apoptosis, whilst the plasma membrane is still intact (Ravichandran, 2011). It is thought externalised PS is recognised by phagocytes in two different ways. Either receptors on the cell surface of phagocytes recognise externalised PS directly, known as direct binding, or phagocytic receptors detect bridging molecules which are bound to externalised PS (Figure 1.11) (Ravichandran, 2011). It is likely, however, these two processes are occurring at the same time during recognition of apoptotic cells. Externalisation of PS is mediated by Transmembrane Protein 16F (TMEM16F), an eight transmembrane spanning protein. When lymphoma cells were transformed with an active form of TMEM16F they exposed PS at a high level consistent with cells undergoing apoptosis. These PS exposing cells were not phagocytosed, indicating other eat me signals are required in addition to PS externalisation for engulfment by phagocytes to occur (Segawa et al., 2011).

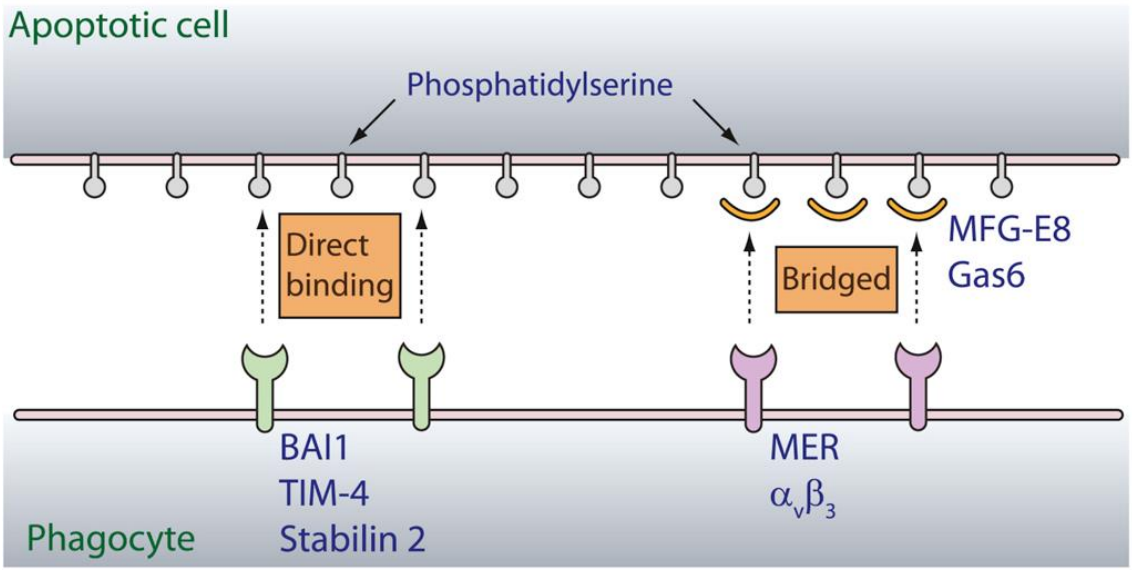

Figure 1.11. A schematic showing two types of externalised PS recognition by phagocytes. One mechanism involves direct recognition of PS via brain angiogenesis inhibitor 1 (BAI1), T cell immunoglobulin and mucin (TIM) family member TIM-4 and Stabilin 2 phagocyte receptors. Alternatively, the phagocyte receptors MER and $\alpha_v\beta_3$ recognise MFG-E8 and Gas6 which are bridging molecules bound to PS via indirect recognition. Figure from Ravichandran, 2011.

In contrast to most cell types, apoptotic hair cells are phagocytosed by supporting cells and not macrophages (Bird et al., 2010). An in vivo and in vitro study of avian vestibular hair cells shows an actin cable is formed by the surrounding supporting cells, which constricts and excises the hair bundle and underlying cuticular plate. The hair cell body is then engulfed and phagocytosed by supporting cells (Bird et al., 2010). It is possible the remaining hair cell debris including the excised hair bundle, is phagocytosed by macrophages providing a secondary role for this cell type (Bird et al., 2010).

PS externalisation in the hair cells of mouse cochlear cultures can be detected using fluorescent conjugates of Annexin V. In mouse cochlear cultures, externalised PS is detected in both OHCs and IHCs following neomycin treatment. A gradient of annexin V labelling occurs running from the basal end of basal-coil cultures to the apical end of apical-coil cultures, with more annexin V staining in hair cells in the basal region of the cochlea. A gradient of membrane blebbing is also observed with more blebbing in the basal-coil cultures than apical-coil cultures. These data show basal-coil hair cells are more susceptible to ototoxic damage than apical-coil hair cells (Lim, 1976; Anniko and Møller, 1978; McDowell, 1982). PS externalisation is detected specifically on the apical surface of IHCs and OHCs, on the hair bundle and in distinct punctae around the periphery of the apical surface of hair cells. PS externalisation is first detected on the hair bundle and then with some delay, is detected on the periphery of the apical surface of hair cells (Goodyear et al., 2008). The appearance of PS externalisation on the hair bundle before it occurs in the periphery could be due to aminoglycosides entering the MET channel and causing membrane disruption in the hair bundle first. The rapid occurrence of PS externalisation on the surface of aminoglycoside treated hair cells is likely due to the activation of lipid scramblase which can cause a fast accumulation of PS in the outer leaflet of the plasma membrane (Goodyear et al., 2008).

1.4.3 Hair cell damage repair

Interestingly, hair cells from cochlear cultures have a remarkably robust damage repair mechanism. If neomycin exposure of cochlear cultures is kept brief, the short term ototoxic effects (membrane blebbing and PS externalisation) are completely reversible. Following drug washout and incubation for 2 hours at 37°C, membrane blebs are no longer visible and externalised PS is no longer detected on the apical surface of hair cells (Goodyear et al., 2008). Internalisation of PS-annexin V complexes is temperature dependent, indicating this repair mechanism occurs via endocytosis (Goodyear et al., 2008). More recently, it has been shown that recovery from aminoglycoside insult occurs in less than 15 minutes (Richardson and Goodyear, unpublished observations). This rapid recovery suggests the mechanisms that restore membrane lipid asymmetry and regulate membrane surface area are very effective.

1.5 Mechanisms of endocytosis

During damage repair, internalised annexin V bound to PS becomes distributed in granules between the apical surface of the hair cell and the nucleus (as detected by confocal microscopy). Hair cells from mice containing a mutation in myosin VI are able to remove blebs and internalise PS-annexin V complexes. Internalised annexin V, however, remains just beneath the apical pole of the hair cell, indicating myosin VI plays an important role in transportation of internalised vesicles (Goodyear et al., 2008). There are a variety of different endocytotic pathways mediating uptake of various cellular components into cells. These mechanisms include, but are not restricted to clathrin-mediated endocytosis, caveolae-

dependent endocytosis, the clathrin-independent carrier (CLIC) pathway and macropinocytosis (Figure 1.12) (Doherty and McMahon, 2009).

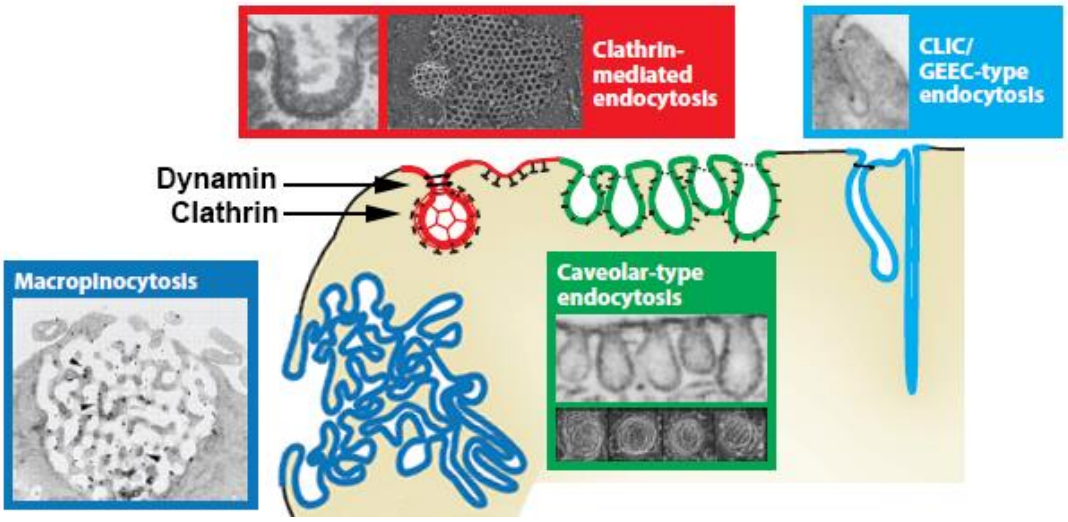

Figure 1.12. A diagram showing the mechanisms of endocytosis including dynamin-dependent and dynamin-independent pathways. Adapted from Doherty and McMahon, 2009.

1.5.1 Clathrin-mediated endocytosis

The molecular mechanisms underlying clathrin-mediated endocytosis are well understood, making it one of the best studied pathways. Clathrin-mediated endocytosis involves the formation of clathrin-coated vesicles (CCV) and occurs over a series of different stages. These stages include nucleation, cargo selection, coat assembly and finally scission (Figure 1.13) (Humphries and Way, 2013). The process of nucleation occurs in the plasma membrane at sites containing high levels of phosphatidylinositol-4,5-bisphosphate (PtdIns(4,5)P_2), clathrin and adapter protein complex 2 (AP2) (Humphries and Way, 2013). During the coat assembly stage, a lattice of clathrin triskelia is bound to the plasma membrane at the cytoplasmic surface by adapter proteins which include AP2. The clathrin lattice acts as a scaffold for the binding of

various proteins including epsin and endophilin which underlie budding of the CCV. Epsin 1 is involved in the early stages of CCV formation as it generates membrane curvature which is required for the formation of clathrin-coated pits (Horvath et al., 2007). In addition, endophilin and amphiphysin regulate later stages of CCV formation by producing deformation of the plasma membrane (Sorkin, 2004). During coat assembly, rim complex proteins are recruited to the edge of the vesicle. The rim complex proteins aid membrane invagination and promote further assembly of the clathrin lattice (Humphries and Way, 2013). Following lattice assembly, the CCV continues to invaginate, forming deep pits that eventually pinch off from the plasma membrane and become internalised within the cell. Vesicle scission requires the activity of both dynamin and actin at the neck of the invaginating clathrin-coated pit. Dynamin acts as a GTP-dependent 'pinchase' to constrict the neck of the invaginating vesicle, whereas actin polymerisation provides mechanical force during the invagination process. Branched actin filaments form a complex around the edge of vesicles and are comprised of actin-related protein 2/3 (ARP2/3). Dynamin, cortactin and neural Wiskott-Aldrich syndrome protein (N-WASP) regulate the activity of ARP2/3 (Humphries and Way, 2013). N-WASP is a type of nucleation-promoting factor (NPF) that regulates ARP2/3 by forming a complex with casein kinase 2 (CK2). The formation of a N-WASP-CK2 complex optimises clathrin-mediated endocytosis by integrating actin polymerising activity with kinase activity (Galovic et al., 2011). Actin polymerisation is also modulated by the interaction of HIP1 (huntingtin interacting protein 1) related protein (HIP1R) with cortactin (Humphries and Way, 2013). Following this, the final stage of clathrin-mediated endocytosis occurs with the removal of the assembled clathrin coat by coat-associated 5-phosphoinositide phosphatase synaptojanin 1, auxilin and Hsc70 (Sorkin, 2004).

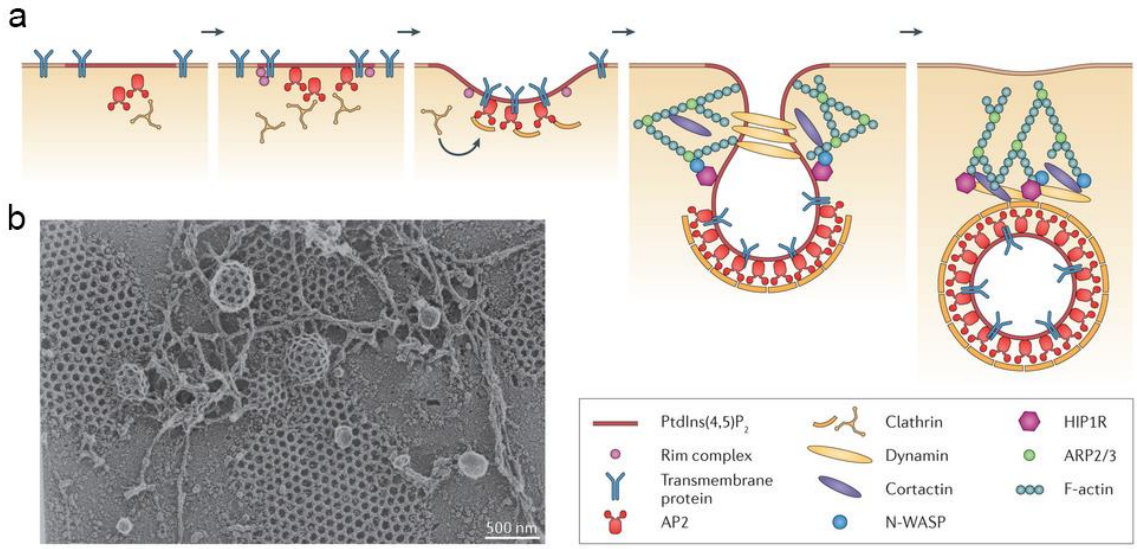

Figure 1.13. Clathrin-mediated endocytosis. From Humphries and Way, 2013.

1.5.2 Caveolae-type endocytosis

Although clathrin-mediated endocytosis underlies the majority of endocytotic activity, TEM shows that not all membrane buds have a clathrin coat (Doherty and McMahon, 2009). Caveolae are approximately 70 nm in diameter and have an appearance of flask-shaped plasma membrane invaginations which lack a clathrin coat (Doherty and McMahon, 2009). Caveolae are a subtype of cholesterol-rich lipid rafts, which are dynamin-dependent and distinguished from morphologically similar caveolae-like structures by the presence of the molecular marker caveolin-1 (Stan, 2005). Other components of caveolae include cavins, pacsin 2 and the ATPase EHD2 (Shvets et al., 2014). Pacsin 2 contains an F-BAR domain which generates and recognises membrane curvature. The loss of pacsin 2 function results in a disruption of normal caveolae morphology (Hansen et al., 2011). Caveolins and cavins but not pacsin 2 and EHD2 are located in an 80S complex which forms the caveolar coat complex. The

caveolar coat complex forms a striated lattice and is located around the caveolar bulb with EHD2 restricted to the neck of the caveolae (Ludwig et al., 2013).

1.5.3 CLIC/GEEC pathway

The process of endocytosis can also be both clathrin and caveolae-independent. One such mechanism of endocytosis is characterised by the formation of tubular invaginations called clathrin-independent carriers (CLICs). CLICs internalise cargo and delivers them to tubular compartments termed GPI-AP(glycosylphosphatidyl-inositol anchored proteins)-enriched early endosomal compartments (GEECs) (Doherty and McMahon, 2009). The CLIC/GEEC pathway is a recently proposed mechanism of endocytosis which is not yet fully understood. The CLIC/GEEC pathway of endocytosis is known to internalise the bacterial toxin, cholera toxin (CTx) (Kirkham and Parton, 2005). Formation of CLICs is dependent on the small G-proteins Cdc42 and Arf1. The GTPase regulator associated with focal adhesion kinase-1, GRAF1, is a marker of the CLIC pathway and is involved in membrane remodelling and formation of tubules (Doherty and Lundmark, 2009).

1.5.4 Macropinocytosis

Macropinocytosis removes large amounts of membrane from the surface of cells and is triggered by growth factors and cell remnants containing PS (Mercer and Helenius, 2012). The process is mediated by actin and involves the formation of large protrusions of plasma membrane in the form of membrane ruffles. The increase in actin polymerisation at the site of membrane ruffling is due to activation of receptor tyrosine kinases including platelet-derived

growth factor receptor and epidermal growth factor (Kerr and Teasdale, 2009). Following this, these membrane protrusions collapse and fuse with themselves or fuse back with the plasma membrane. This generates large fluid-filled vacuoles resulting in the engulfment of a multitude of extracellular components along with large areas of plasma membrane (Doherty and McMahon, 2009). Macropinocytosis can be blocked by inhibitors of phosphatidylinositol-4,5-bisphosphate 3-kinase (PI3K) and by disrupting actin using cytochlasins and latrunculins (Bohdanowicz and Grinstein, 2013). In addition, macropinocytosis is inhibited by amiloride and its derivative 5-(N-Ethyl-N-isopropyl)amiloride (EIPA) (Kerr and Teasdale, 2009). Once macropinosomes have matured, they tend to shrink progressively and fuse with lysosomes. Macropinosomes are also able to fuse with one another, thus increasing in size during maturation (Bohdanowicz and Grinstein, 2013). To date, little is known about the mechanisms underlying the fate of macropinosomes.

1.5.5 Protein kinases

Endocytosis is regulated by many different pathways and cellular mechanisms. One class of proteins regulating endocytosis are protein kinases. Endocytosis at the apical surface of polarised epithelial cells is known to be regulated by protein kinase A (PKA) and protein kinase C (PKC) along with calmodulin, phospholipase D and RhoA (Sandvig et al., 2008). PKA is a cAMP-dependent kinase and endocytosis of ricin in polarised MDCK cells is reduced following treatment with the PKA inhibitor H-89 (Eker et al., 1994). Furthermore, internalisation of the SV40 virus and cholera toxin b is dependent on PKC along with dynamin and actin. This mechanism of virus entry occurs via caveolae-dependent endocytosis (Parton and Simons, 2007).

1.6 Aims

Sensory hair cells have a very robust and efficient damage repair mechanism that is triggered following exposure to aminoglycoside antibiotics *in vitro* (Goodyear et al., 2008). The processes underlying membrane repair are, however, not yet understood. The aim of this thesis was to explore the mechanisms by which hair cells repair membrane damage caused by short-term exposure to aminoglycosides. Most experiments were performed on cochlear cultures prepared from early postnatal mice. The ultrastructural features present during the repair process were characterised using transmission electron microscopy and three-dimensional reconstructions. A combination of live cell imaging, confocal microscopy and scanning electron microscopy were used to probe the molecular mechanisms underlying damage repair. This was carried out using a range of inhibitors known to block different endocytic pathways, interfere with actin dynamics or inhibit protein kinase activity. In a second approach, mice with mutations in Atp8b1, Ptprq, TRPC3/6 and Eps8 were tested for their ability to repair membrane damage resulting from drug insult. Mice lacking Atp8b1, an aminophospholipid translocase that is required for membrane lipid asymmetry maintenance, were studied to see if hair cell repair in these mutants was impeded (for more detail see Section 3.3.1). Mice with a mutation in Ptprq were tested for their ability to repair membrane damage as the intracellular domain of Ptprq interacts with eps 15 homology domain 3, a protein involved in endocytosis (for more detail see Section 3.3.2). Eps8 is an actin capping protein which regulates actin dynamics and as endocytosis can be impaired by disruption of actin dynamics, mice with a mutation in Eps8 were tested for their ability to endocytose damaged membrane (for more detail see Section 3.3.3). Hair cell repair was also tested in mice with mutations in the non-selective cation channels TRPC3 and TRPC6. Entry of Ca^{2+} via these channels activates PS externalisation, therefore PS externalisation and membrane repair were tested in hair cells from TRPC3/6 mutant mice (for more detail see Section 3.3.4).

2 MATERIALS AND METHODS

2.1 Cochlear culture preparation

Cochlear cultures were prepared from wild-type CD-1 mice as described previously (Russell and Richardson, 1987). Two-day-old (P2) mouse pups were killed by cervical dislocation and surface sterilised by immersion in 80% ethanol for approximately 6 minutes. The heads were removed and placed in Hepes buffered (10 mM, pH 7.2) Hanks' balanced salt solution (HBHBSS) (Invitrogen). The heads were bisected midsagitally and the cochleae removed and placed in fresh HBHBSS. The cartilaginous capsule was removed and the stria vascularis dissected away. Cochleae were kept as whole coils or split into apical and basal coils. Two whole coils or two basal and two apical coils were placed on a collagen (BD Biosciences) coated round glass coverslip and the tissue pieces were oriented so the apical surface of the hair cells were pointing away from the collagen. Approximately 50 µl of rat cochlear culture medium (RCM) containing 93% DMEM/F12 (Dulbecco's Modified Eagle's Medium/F12) (Sigma), 7% fetal bovine serum (Labtech) and 10 µg ml^{-1} ampicillin was added and the coverslip was sealed in a Maximow depression slide. Cultures were maintained in the lying drop position at 37°C in an incubator for 24 hours.

All procedures involving animals were performed in accordance with UK Home Office regulations.

2.2 Transmission electron microscopy

To study recovery from neomycin damage at the ultrastructural level, cultures were transferred into 35 mm diameter plastic Petri dishes with 2 ml of HBHBSS and exposed to 1 mM neomycin (Sigma) for 15 minutes at room temperature. To label the apical plasma membrane of the hair cell prior to recovery, the cultures were washed twice with 2 ml ice cold HBHBSS, exposed to 0.5 mg/ml cationic ferritin (Sigma) for 30 minutes on ice, and washed once with ice cold HB-DMEM/F12 (Sigma). Following this, cultures were either fixed immediately with 2.5% glutaraldehyde (TAAB) in 0.1 M sodium cacodylate buffer pH 7.4 for 1 hour, or allowed to recover in 2 ml pre-gassed pre-warmed RCM at 37°C for 5 or 10 minutes and then fixed with 2.5% glutaraldehyde in 0.1 M sodium cacodylate buffer. Following glutaraldehyde fixation, cultures were washed three times with 2 ml of 0.1 M sodium cacodylate and, following separation of the apical and basal coils, transferred into Eppendorf tubes containing 1 ml of 0.1 M sodium cacodylate. Cultures were postfixed in 1% osmium tetroxide (TAAB) for 1 hour, washed three times with 1 ml 0.1 M sodium cacodylate, and dehydrated in ethanol (5 minute washes with 1 ml of 50%, 70%, 80%, 90% and two 10 minute washes of 100%). The cultures were equilibriated twice for 10 minutes in 1 ml propylene oxide and left in a 1:1 mixture of propylene oxide and Epon (TAAB 812 resin, dodecenyl succinic anhydride (DDSA), methyl nadic anhydride (MNA), (2,4,6- tri (dimethylaminomethyl) phenol) (DMP-30)) (TAAB) for 1 hour, then a mix of 1:3 propylene oxide:Epon for 3 hours. Finally cultures were infiltrated for 8 hours in pure Epon, embedded in Beem capsule lids (TAAB) and allowed to polymerise overnight at 60°C. Ultrathin sections at a thickness of 100 nm were taken with a Reichert-Jung (Leica) Ultra-cut E ultramicrotome using a Diatome diamond knife (TAAB) and collected in ribbons on either Formvar coated copper slot grids or non-coated copper mesh grids. The sections were stained with 1% aqueous uranyl acetate for 25 minutes,

washed 3 times, stained with lead citrate (45 µg/ml lead nitrate, 25 µg/ml trisodium citrate, 6 µg/ml sodium hydroxide) for 6 minutes and washed 4 times.

2.3 Three-dimensional reconstruction from serial sections

Serial sections were collected from some samples on copper grids and imaged using TEM. The images captured from 100 nm serial sections were processed for optimal contrast and brightness using Adobe Photoshop CS6. The stack of TEM section images to be reconstructed were imported into the Reconstruct software (Fiala, 2005). At least four correspondence points were specified using the stamp tool on adjacent sections to enable the programme to align each section in the stack. These correspondence points included features such as vesicles and mitochondria. Objects including vesicles and the hair-cell membrane were traced around by hand using the trace tool in Reconstruct. This was carried out on all sections in the stack. Cationic ferritin was represented by drawing spheres in the areas cationic ferritin particles were present. Once all features were traced in each section, a three-dimensional view of the object traces was produced in a three-dimensional scene which was rotated and images were captured at the desired orientation.

2.4 PS externalisation in cultures treated with inhibitors

To see if the inhibitors listed in table 2.1 alone elicited PS externalisation, cultures were transferred into 35 mm diameter plastic Petri dishes and incubated in 2 ml pre-warmed pre-gassed RCM at 37°C containing the inhibitor to be tested (Table 2.1) or an equal volume of DMSO as a control for 10 or 15 minutes. Cultures were washed twice, transferred to glass-

bottomed Perspex slide chambers with 0.5 ml HBHBSS and labelled with Alexa Fluor 488 annexin V (Molecular Probes) (annexin V-488) at a dilution of 1:100. Annexin V-488 labels PS when it flops from the inner leaflet of the plasma membrane to the outer leaflet. Alternatively, cultures were exposed to 0.1% DMSO or the inhibitor to be tested for 10 or 15 minutes at room temperature in 0.5 ml HBHBSS in glass-bottomed Perspex slide chambers before the addition of annexin V-488. Cultures were viewed and imaged 5 minutes after annexin V-488 was added. The pre-incubation step was initially used on all inhibitors tested but the protocol was later changed as this step was not deemed necessary.

Inhibitor	Target	Concentration	Repeats	Pre-incubation
Blebbistatin	Myosin II inhibitor	50 µM	N=5	Yes
Chlorpromazine	Inhibits clathrin coated pit formation	12.5 µM 25 µM	N=1 N=7	Yes Yes
Pitstop 2	Inhibits clathrin binding	30 µM 60 µM	N=1 N=3	No No
Dynasore	Inhibits dynamin	100 µM	N=8	No
Rhodadyn	Inhibits dynamin	7 µM 70 µM	N=1 N=5	No No
EIPA	Inhibits CLIC pathway and macropinocytosis	100 µM 200 µM	N=6 N=2	No No
LY294002	Inhibits PI3 kinase and autophagy	1 µM 10 µM 20 µM	N=1 N=3 N=1	Yes Yes Yes
Wortmannin	Inhibits PI3 kinase and autophagy	10 µM 20 µM	N=4 N=1	Yes Yes

Jasplakinolide	Stabilises actin filaments	5 µM 10 µM	N=15 N=1	Yes Yes
Staurosporine	Multiple kinases	10 nM 50 nM 100 nM	N=2 N=1 N=1	Yes Yes Yes
BIM I	PKC inhibitor	1 µM 5 µM 10 µM	N=1 N=2 N=1	Yes Yes Yes
IPA 3	PAK1 inhibitor	10 µM 100 µM	N=2 N=2	Yes Yes
KT5720	PKA inhibitor	1 µM 10 µM 50 µM	N=1 N=2 N=1	Yes Yes Yes
H-89	PKA inhibitor	10 µM 20 µM	N=3 N=6	Yes Yes

Table 2.1. Table of inhibitors tested, cellular targets, concentrations tested, number of times repeated and whether cultures were pre-incubated for an hour in the inhibitor used.

2.5 Testing the ability of inhibitors to block internalisation

When compounds were tested for their ability to block internalisation of PS-annexin V complexes and membrane bleb retrieval, cochlear cultures were transferred into 35 mm diameter plastic Petri dishes and pre-incubated in 2 ml pre-warmed pre-gassed RCM at 37°C for 1 hour with the compound to be tested or an equivalent volume of DMSO. The concentrations of all inhibitors tested can be found in table 2.1. The 1 hour pre-incubation step

was performed for the following compounds: the myosin II inhibitor blebbistatin (abcam), the actin stabiliser jasplakinolide (Tocris), the phosphatidylinositol (PI-3) kinase inhibitors wortmannin (Sigma) and 2-(4-morpholinyl)-8-phenyl-4*H*-1-benzopyran-4-one (LY294002) (Sigma), the general protein kinase inhibitor staurosporine (Calbiochem), the Protein kinase C inhibitor BIM I (Calbiochem), the p21 activated kinase (PAK1) inhibitor IPA 3 (Calbiochem) and the Protein kinase A inhibitors H-89 (Calbiochem) and KT5720 (abcam). The following inhibitors were tested without a pre-incubation step: the clathrin inhibitor Pitstop 2 (abcam), the CLIC pathway inhibitor 5-(N-Ethyl-N-isopropyl)amiloride (EIPA) (Sigma) and the dynamin inhibitors dynasore (abcam) and rhodadyn (abcam). After 1 hour pre-incubation, cultures were washed twice with HBHBSS and treated as described in section 2.6.

2.6 Live imaging of cultures treated with neomycin

Cultures were transferred to glass-bottomed Perspex slide chambers with 0.5 ml HBHBSS. Annexin V-488 was added to a dilution of 1:100 and neomycin to 1 mM. Five minutes after the addition of neomycin, images were captured from the mid-basal and mid-apical regions of the coils to confirm the hair cells were externalising PS and forming membrane blebs in response to neomycin. After a further 10 minutes (i.e. 15 minutes neomycin treatment in total), cultures were transferred to 35 mm diameter plastic Petri dishes, washed twice with 2 ml HBHBSS and allowed to recover for 30 minutes in 2 ml pre-warmed, pre-gassed RCM at 37°C and the compound to be tested or 0.1% DMSO. After the recovery period, cultures were washed twice with 2 ml HBHBSS and placed in glass-bottomed Perspex slide chambers with 0.5 ml HBHBSS and imaged in the mid-basal and mid-apical regions. Some cultures were also exposed to Alexa Fluor 594 annexin V (Molecular Probes) (annexin V-594) at a dilution of 1:100 after the

recovery step. The annexin V-594 enabled labelling of externalised PS which had not become internalised during the 30 minute recovery step.

2.7 Fixing cochlear cultures for fluorescence and confocal microscopy of annexin V internalisation

To examine the depth of annexin V internalisation, cultures from the live imaging experiments were washed twice with HBHBSS, and fixed for 1 hour with 3.7% formaldehyde in 0.1 M sodium phosphate buffer pH 7.3 (Sigma). After fixation cultures were washed 3 times with phosphate buffered saline (PBS), trimmed, transferred to Eppendorf tubes and preblocked and permeabilised for 15 minutes in PBS and horse serum (HS) with 0.1% Triton X-100. Cultures were labelled overnight with Texas Red phalloidin (Molecular Probes) at a concentration of 1:250 in PBS, washed 3 times in PBS and mounted on glass slides using Vectashield (Vector Laboratories).

2.8 Live imaging of bleb formation in jasplakinolide treated cultures

To study the effects of jasplakinolide on neomycin-induced membrane bleb formation, cultures were transferred to glass-bottomed Perspex slide chambers with 0.5 ml HBHBSS, DMSO as a control or 5 µM jasplakinolide and 1 mM neomycin. To compare membrane bleb formation between DMSO control cultures and jasplakinolide treated cultures, the diameter of membrane blebs in the kinocilial region of outer hair cells was measured from images using

Adobe Photoshop CS6. Volume was calculated from measurements of diameter, assuming membrane blebs to be spherical. An unpaired t test was used to determine if differences in membrane bleb volume were significant.

2.9 Scanning electron microscopy

To examine membrane bleb retrieval in cultures treated with jasplakinolide and H-89, cultures were transferred into 35 mm diameter plastic Petri dishes with 2 ml HBHBSS containing either 0.1% DMSO (as a control), 1 mM neomycin or 1 mM neomycin and the inhibitor. After 15 minutes of neomycin treatment, cultures were washed twice with 2 ml HBHBSS and fixed with 2.5% glutaraldehyde in 0.1 M sodium cacodylate pH 7.2 for 1 hour or allowed to recover for 30 minutes in 2 ml pre-warmed, pre-gassed RCM at 37°C plus 0.1% DMSO or the inhibitor. After 30 minutes recovery, cultures were washed twice with 2 ml HBHBSS and fixed as described above. After glutaraldehyde fixation, cultures were washed three times in 0.1 M sodium cacodylate and transferred into Eppendorf tubes. Cultures were postfixed in 1% osmium tetroxide for 1 hour, washed three times with 1 ml 0.1 M sodium cacodylate buffer and dehydrated in ethanol (5 minute washes each with 1 ml of 50%, 70%, 80%, 90% ethanol and two 10 minute washes of 100% ethanol). Cultures were critical point dried from liquid $C0_2$, mounted on aluminium stubs (TAAB) with double-sided sticky tape and sputter coated with silver.

2.10 Cholera toxin B labelling

To study Cholera Toxin B (CTxB) labelling, cochlear cultures were transferred into glass-bottomed Perspex slide chambers with 0.5 ml HBHBSS and labelled with Alexa Fluor 488 CTxB (Molecular Probes) at a dilution of 1:100 for 10 minutes. Cultures were washed twice with HBHBSS and fixed with 3.7% formaldehyde in 0.1 M sodium phosphate buffer pH 7.3 for 1 hour. The cultures were washed 3 times with PBS, trimmed, transferred to Eppendorf tubes and preblocked, permeabilised and labelled overnight with anti-Alexa Fluor 488 rabbit IgG (Molecular probes) at a dilution of 1:500 and Texas Red phalloidin at a dilution of 1:250 in PBS. Cultures were then washed again and labelled with the secondary antibody Alexa Fluor 488 goat anti rabbit (Molecular Probes) at a dilution of 1:500 and mounted on glass slides.

2.11 Antibody labelling

To study different markers of endocytosis in recovering hair cells, cochlear cultures were treated with 1 mM neomycin in the presence of annexin V-488, washed and allowed to recover for 10 minutes in 2 ml pre-warmed pre-gassed RCM at 37°C. After incubation, cultures were washed once with HBHBSS then fixed with 3.7% formaldehyde for 1 hour. Following fixation, cultures were preblocked and permeabilised as described. Following this, cultures were labelled overnight with antibodies to caveolin 1 or clathrin, washed 3 times with PBS and labelled with the secondary antibody Alexa Fluor 555 donkey anti-rabbit (Molecular Probes) at a dilution of 1:500 and 647 phalloidin for 3 hours.

2.12 Phenotypic analysis of Atp8b1 mutant mice

To examine hair-bundles in Atp8b1 mutant mice, inner ears from Atp8b1 mice aged P0, P3 and P7 and age-matched heterozygous controls were fixed with 3.7% formaldehyde in 0.1 M sodium phosphate pH 7.3 for 4 hours and then washed three times in PBS. The cartilaginous capsule, modiolus and stria vascularis were removed by dissection. The tissue was transferred to Eppendorf tubes, preblocked and permeabilised as described previously. Tissue was stained overnight with Texas Red phalloidin at a dilution of 1:250, washed three times with PBS and mounted on glass slides.

2.13 Imaging spontaneous PS externalisation

To determine if spontaneous PS externalisation was occurring in Atp8b1 mutant mice, cochlear cultures of 2, 3 and 4 days of age were transferred to a glass-bottomed Perspex slide chamber with 0.5 ml HBHBSS and annexin V-488 at a dilution of 1:100 for 15 minutes. After 15 minutes, cultures were washed twice with HBHBSS and fixed with 3.7% formaldehyde in sodium phosphate pH 7.3 for 1 hour. Following fixation, cultures were washed 3 times with PBS, trimmed, transferred to Eppendorf tubes and preblocked and permeabilised as described previously. Cultures were labelled overnight with Texas Red phalloidin, washed 3 times in PBS, mounted on glass slides using Vectashield and imaged with a Zeiss AxioPlan 2 microscope with Nomarski interference contrast optics using a 20× objective. Fluorescence images of annexin V-488 labelling (3 second exposure time) and Texas Red phalloidin labelling (1 second exposure time) were captured with a Spot RT slider digital camera from the cochlear cultures and assembled into a photomontage using Adobe Photoshop CS6. The percentage of annexin V-

488 positive hair cells was calculated from the number of annexin V labelled hair cells and the total number of phalloidin stained hair cells for each cochlea. Differences in numbers of labelled hair cells were compared to see if the differences were significant using an unpaired t test.

2.14 Neomycin treatment and recovery in cultures from Atp8b1, Ptprq, Eps8 and TRPC mutant mice

Atp8b1, Ptprq, Eps8 and TRPC mutant mice were tested for their ability to repair membrane blebs and internalise annexin V-488 by using the protocol outlined in section 2.6.

2.15 Genotyping Atp8b1 and Ptprq mutant mice

2.15.1 Extracting DNA from tail snip preparations

Tail snips (2-3 mm long) from mouse pups were added to 0.5 ml PCR tubes with 200 µl GNT-K buffer (10 mM Tris-HCL pH 8.5, 50 mM KCL, 1.5 mM $MgCl_2$, 0.45% Nonidet P40, 0.45% Tween 20, 100 $\mu g ml^{-1}$ proteinase K) and cooked in the PCR machine at 55°C for 2 hours, followed by 95°C for 15 minutes.

2.15.2 Atp8b1 genotyping

Once the tails were cooked, 23 µl of prepared PCR reaction mixture (Table 2.2) was aliquoted into the required number of PCR tubes (including one control tube for the PCR mixture), with 2 µl of tail prep DNA. In addition, 2 µl of tail prep control was added to a control tube and 2 µl of water was added to a PCR control tube.

Tail prep DNA was cycled in a PCR machine at the following temperatures and amounts of time:

95°C for 6 minutes

40 cycles of 94°C for 15 seconds, 55°C for 30 seconds, 72°C for 30 seconds

72°C for 5 minutes

After the PCR reaction was complete, the product was digested overnight at 37°C with 2 µl of NcoI reaction mixture (Table 2.3) added to each PCR reaction.

Reagents	**Volume in µl per reaction**
10 x PCR reaction buffer without $MgCl_2$	2.5
$MgCl_2$	2
dNTP mix (10 mM dATP, 10 mM dCTP, 10 mM dGTP, 10 mM dTTP in sterile water)	0.5
Sterile water (to 23 µl final volume)	12.65

Fast Start Taq DNA polymerase 5 U/µl	0.1
Primer Mix (250 pmol/µl ATP ATP8b1F1, 250 pmol/µl ATP8B1R2 in sterile water)	5
Total volume	23

Table 2.2. Atp8b1 PCR reaction mixture.

Reagents	**Volume in µl per reaction**
10 x Buffer 3	0.2 µl
Water	1.6 µl
NcoI (Promega)	0.2 µl

Table 2.3. NcoI reaction mixture.

2.15.3 Ptprq genotyping

After the tails have been cooked (described in section 2.15.1), 23 µl of prepared Ptprq PCR reaction mixture (Table 2.4) was aliquoted into PCR tubes, including one control tube for each PCR mix and 2 µl of tail prep DNA was added to each tube. In addition 2 µl of tail prep control was added to a control tube and 2 µl of water was added to 2 PCR control tubes.

Tail prep DNA was cycled in a PCR machine at the following temperatures and amounts of time:

	30°C for 15 minutes
	95°C for 6 minutes
40 cycles of	94°C for 15 seconds, 55 °C for 15 seconds, 72°C for 30 seconds
	72°C for 5 minutes

Reagents	**Volume in µl per reaction (Wild type)**	**Volume in µl per reaction (Mutant)**
5 x KAPA2G buffer A with $MgCl_2$	5	
dUTP mix (100 mM dATP, 100 mM dCTP, 100 mM dGTP, 100 mM dUTP in sterile water)	0.5	
Sterile water (to 23 µl final volume)	12.15	
Heat-labile Uracil-DNA glycosylase	0.25	
KAPA2G robust hot start Taq DNA polymerase	0.1	
Wild Type Allele Primer Mix	5	
Mutant Type Allele Primer Mix		5
Total volume	23	23

Table 2.4. Prptq PCR reaction mixture.

After the PCR reaction was complete, the product was loaded onto agarose gels as described below.

2.15.4 Gel electrophoresis of DNA

1 x TBE mini agarose gels with 100 bp ladder markers were used for electrophoresis. DNA samples were loaded into wells with 10x gel loading buffer (50% glycerol, 1 mM Tris-HCl, pH 8.0, 0.25% w/v bromophenol blue, 1 mM EDTA). Electrophoresis was carried out at 100 volts for 35 minutes. The gels were incubated for 30 minutes in 0.5 µg/ml ethidium bromide in water before imaging DNA bands using an ultraviolet (UV) transilluminator.

2.16 FM1-43 loading

Coverslips with adherent cultures were placed into Columbia jars with 8 ml HBHBSS and 100 µM EIPA or 0.1% DMSO for 5 minutes. Cultures were transferred into a second Columbia jar with 8 ml HBHBSS and 0.3 µM FM1-43 (Molecular Probes) for 10 seconds then transferred through a further three Columbia jars containing 8 ml HBHBSS for 10 seconds each. After the third HBHBSS wash, cultures were transferred into glass-bottomed Perspex slide chambers with 0.5 ml HBHBSS and imaged.

2.17 Texas Red neomycin and Texas Red dihydrostreptomycin loading

Texas Red ester (MWt = 641.15) was obtained from Invitrogen and dissolved at a concentration of 2 mg/ml in dry dimethylformamide (DMF). Neomycin sulphate was obtained from Sigma and dissolved at a concentration of 50 mg/ml (~50 mM) in 100 mM K_2CO_3 buffer pH 8.5. To prepare the conjugate, 1.5 ml (225 µMoles) of the neomycin solution was mixed with 0.5 ml (1.225 µMoles) of the Texas Red ester on a rotator overnight (i.e., at a 184:1 molar ratio of neomycin to Texas Red). As a control for the stability of neomycin in the presence of DMF, 1.5 ml of the neomycin solution was mixed with 0.5 ml DMF overnight, and as a control for the specificity of the Texas Red neomycin conjugate, 0.5 ml of the Texas Red ester was mixed with 1.5 ml of the K_2CO_3 buffer. The neomycin retained toxicity after overnight incubation in the presence of 33% DMF, and no labelling of hair cells was observed with the hydrolysed Texas Red ester. Hair cell labelling was only observed with the Texas Red neomycin conjugate.

To study the effect of EIPA on dihydrostreptomycin and neomycin entry into hair cells, cultures were transferred into 35 mm diameter plastic petri dishes with 2 ml HBHBSS and either 0.1% DMSO or 200 µM EIPA for 5 minutes. After 5 minutes, the cultures were treated with either 500 µM dihydrostreptomycin Texas Red or 500 µM neomycin Texas Red for 15 minutes, washed twice with HBHBSS and fixed with 3.7% formaldehyde in 0.1 M sodium phosphate buffer for 1 hour. Following fixation, cultures were washed 3 times with PBS and preblocked and permeabilised as described previously. Cultures were labelled overnight with FITC phalloidin (Molecular Probes), washed 3 times in PBS and mounted on glass slides.

2.18 Statistical analysis of fluorescent compound loading

Fluorescence intensity of FM1-43, Texas Red dihydrostreptomycin and Texas Red neomycin loading in outer hair cells was obtained by subtracting background fluorescence (F0) from the fluorescence in the cytoplasm of outer hair cells (F). The histogram tool in Adobe Photoshop CS6 was used to measure mean grey levels within a defined area. The background fluorescence was measured from images of three different regions in the basal-coil and apical-coil cultures and from the cytoplasmic region in the ten brightest outer hair cells. Differences in fluorescence intensity of control cultures and EIPA treated cultures were compared to see if they were significantly different. All statistical comparisons were performed using an unpaired t test. P values < 0.05 were considered significant. All statistics are presented in the text as (mean ± SEM, number of OHCs).

2.19 Short term EIPA block reversal

To study the ability of EIPA to block neomycin entry into hair cells, cochlear cultures were transferred into glass-bottomed Perspex slide chambers with 0.5 ml HBHBSS plus DMSO or 200 µM EIPA for 5 minutes. Following this, annexin V-488 at a dilution of 1:100 and 1 mM neomycin were for added for 15 minutes and images captured from the mid-basal and mid-apical regions. To see if the EIPA block is reversible at physiological temperature, cultures treated with 200 µM EIPA were transferred to 35 mm diameter plastic Petri dishes, washed twice with 2 ml HBHBSS and incubated for 30 minutes in 2 ml pre-warmed pre-gassed RCM at 37°C. Cultures were washed twice with HBHBSS, transferred to glass-bottomed Perspex slide

chambers with 0.5 ml HBHBSS, annexin V-488 at a dilution of 1:100 and rechallenged with 1 mM neomycin.

2.20 Treating cultures for 24 hours with EIPA

To study the effects of EIPA over a 24 hour period and its ability to block neomycin damage, cochlear cultures were transferred into 35 mm plastic Petri dishes using sterile forceps, with 2 ml pre-warmed pre-gassed RCM at 37°C and either 250 µM neomycin, 50 µM EIPA, both 250 µM neomycin and 50 µM EIPA or 0.1% DMSO as a control. Following 24 hours incubation, cultures were washed twice with HBHBSS and fixed with 3.7% formaldehyde in 0.1 M sodium phosphate pH 7.3 for 1 hour. Following fixation cultures were labelled with Texas Red phalloidin as described previously, mounted on glass slides, imaged and assembled into a photomontage as described previously.

2.21 Microscopy

Fluorescent images were viewed with a Zeiss AxioPlan 2 microscope with Normarski interference contrast optics using a 60x water-immersion objective, numerical aperture (NA) 0.90 or a 63x water-immersion objective, numerical aperture (NA) 0.95. Fluorescence images (3 second exposure time) were captured with a Spot RT slider digital camera. Images fixed for confocal microscopy were imaged with a Zeiss LSM 510 confocal microscope using a 100 x oil immersion objective or a 63x oil-immersion objective (NA, 1.4). Annexin V-488 and Alexa Fluor 488 CTxB were excited by the 488 nm laser line and annexin V-594, Alexa Fluor 555 and Texas Red phalloidin were excited by the 543 nm laser line and 647 phalloidin was excited by the 633

nm laser line. Samples prepared for transmission electron microscopy were viewed with a Hitachi 7100 transmission electron microscope (TEM) operating at 100 kV capturing images with a Gatan Ultrascan 1000 CCD camera. Samples prepared for scanning electron microscopy were viewed using a Leica Leo S240 scanning electron microscope (Leica).

3 RESULTS

3.1 Ultrastructure of the damage repair process

Blebs form on the apical surface of hair cells in cochlear cultures that are treated with neomycin. Bleb formation is rapid and occurs within minutes of aminoglycoside application (Goodyear et al., 2008). The process is also reversible following drug washout. Transmission electron microscopy (TEM) was used to study the ultrastructural features of the formation and retrieval of blebs in cochlear cultures from 2 day old (P2) wildtype mice. For all TEM experiments in this section, cochleae were split into a basal coil and an apical coil as indicated in the phalloidin stained cochlear culture in Figure 3.1.

3.1.1 Membrane bleb formation

The effects of neomycin treatment on the apical surfaces of cochlear cultures were studied at the ultrastructural level. Hair cells from cochlear cultures incubated in 0.1% DMSO for 15 minutes had a normal morphology with v-shaped hair bundles clearly visible (Figure 3.2**a,c**). Following 15 minutes of neomycin treatment, numerous membrane blebs were detected across the apical surface of hair cells on the hair bundle and around the hair-cell periphery (Figure 3.2**b,d**).

Cationic ferritin, a non-selective label which binds to the plasma membrane on the apical surface of hair cells, was used to investigate internalisation of membrane during recovery from neomycin treatment. Cochlear cultures were exposed to 1 mM neomycin for 15 minutes and pulse-labelled with cationic ferritin. After labelling, cultures were either fixed or allowed to recover for 10 minutes before preparation for TEM. After 10 minutes of recovery from

neomycin-induced damage, some membrane blebs were still present on the apical surface of hair cells. Serial sections of a single membrane bleb on the surface of an OHC (Figure 3.3**a-d**) were used to generate a 3-dimensional reconstruction (Figure 3.3**e**). The membrane bleb was located at the periphery of the apical surface of the hair cell, close to the tight junction separating the hair cell from the adjacent supporting cell. The majority of membrane blebs were found at this location. Cationic ferritin labeling was observed on the surface of the membrane bleb and labelled membrane was also seen within the cytoplasm-filled interior of the bleb (Figure 3.3). Although cationic ferritin labels the surface of membrane blebs formed following neomycin treatment (Figure 3.4**a-b**), some membrane blebs only had a proportion of their surface labelled with cationic ferritin (Figure 3.4**c**). Control cultures which were not treated with neomycin had cationic ferritin labelling across all hair cell apical plasma membrane (Figure 3.4**d**). This suggests the plasma membrane lacking cationic ferritin in neomycin treated cultures may have different properties to the labelled membrane.

3.1.2 Membrane bleb retrieval

Cultures treated with 1 mM neomycin for 15 minutes had a large number of membrane blebs across the apical surface of hair cells (Figure 3.5**a**). Following drug washout and incubation in RCM for 30 minutes, membrane blebs were no longer detected (Figure 3.5**b**). The removal of large amounts of damaged membrane is temperature dependent and appears to occur via endocytosis (Goodyear et al., 2008). To examine membrane bleb retrieval at an ultrastructural level, ultrathin sections were collected from cultures as described above. Images from ultrathin sections revealed large amounts of internalised cationic ferritin-labelled membrane. Internalised cationic ferritin labelling was observed within large membrane whorls in hair cells from multiple independent experiments. These were located beneath the apical surface of hair

cells at the periphery, close to the supporting cell and beneath the cuticular plate (Figure 3.6). A variety of other membrane features were also observed during the recovery period and are detailed below.

3.1.3 Clathrin-coated pits in recovering hair cells

Ultrathin sections from cultures fixed after 10 minutes recovery without cationic ferritin pulse labelling reveal the presence of numerous coated pits, a feature of clathrin-mediated endocytosis (Figure 3.7**a-d**). A dense coat was observed on the cytoplasmic face of plasma membrane invaginations at various stages of endocytosis. The pits were mostly located at the periphery of the apical surface of hair cells, adjacent to the cuticular plate in a region where membrane blebs typically form. Some clathrin-coated pits were also seen at the base of the stereocilia, but these were not as numerous. The surface-connected membrane invaginations were approximately 80 nm in diameter and were also observed in cultures which had not been treated with neomycin. These data suggest clathrin-mediated endocytosis may have a role in membrane retrieval during hair cell repair.

3.1.4 Caveolae-type invaginations during membrane repair

During the repair process, features associated with caveolae-dependent endocytosis were also observed. TEM images after 10 minutes of recovery contained membrane invaginations typical of caveolae. The caveolae were arranged in clusters and mostly located at the periphery of the apical surface of hair cells, adjacent to the cuticular plate (Figure 3.8**a-d**). Some networks of caveolae were also located at the base of the stereocilia (Figure 3.8**d**). Cationic ferritin labelling

was observed within caveolae beneath the apical surface of hair cells treated with ferritin (Figure 3.8**a,d**). The approximate size of individual caveolae was 80 nm and some clusters were associated with the apical plasma membrane (Figure 3.8**c,d**). Numerous membrane vesicles with an approximate size of 70 nm were located in the same region as the caveolae. Caveolae were also observed in cultures which had not been treated with neomycin (Figure 3.8**e**).

3.1.5 CLICs and GEECs observed during membrane repair

TEM images of samples fixed following 10 minutes of recovery from neomycin treatment indicate that the clathrin-independent carrier (CLIC) pathway may be involved in retrieval of neomycin-induced membrane damage. Long surface-connected tubular invaginations were observed at the periphery of hair cells, close to supporting cells (Figure 3.9**a-c**). These lacked a coat, had an approximate length of 800 nm and are a typical feature of the CLIC pathway of endocytosis. Cultures which had not been treated with neomycin did not appear to contain these tubules, suggesting invaginations labelled with cationic ferritin may have formed during the recovery period to remove damaged membrane from the apical surface of hair cells. Other features observed during recovery were ring-like structures beneath the hair-cell surface (Figure 3.10). These were labelled with cationic ferritin and resemble GPI-AP-enriched early endosomal compartments (GEECs).

3.1.6 Macropinocytosis as a repair mechanism

Large protrusions of plasma membrane which appear to be membrane blebs collapsing back onto the plasma membrane were observed in hair cells recovering from neomycin damage.

Serial sections collected from TEM samples were used to generate a 3-dimensional reconstruction of a portion of a single collapsing membrane projection. The serial sections showed a large bulk of cationic ferritin labelled membrane, collapsing and possibly fusing with the underlying plasma membrane (Figure 3.11**a-c**). The protruding membranes observed in recovering hair cells were large with an approximate diameter of 1 µm. A 3-dimensional reconstruction (Figure 3.11**d**) of one example was generated from serial sections (Figure 3.11**a-c**). Cationic ferritin labelled membrane appeared to be trapped between the collapsing membrane and the apical surface of the hair cell. The formation of large protrusions of membrane and their subsequent collapse and fusion with the apical plasma membrane is a typical feature of macropinocytotic mechanisms used to internalise large amounts of plasma membrane. Macropinocytosis may therefore be involved in hair cell repair from neomycin damage.

3.1.7 Autophagy during the repair process

The process of autophagy is characterised by the presence of double-membraned vesicles known as autophagosomes. Double-membraned vesicles were observed within hair cells recovering from neomycin damage. Following 10 minutes recovery, double membranes were seen within membrane blebs on the apical surface (Figure 3.12**a,c**) and just below the apical surface of hair cells (Fig. 3.12**b**). Some membrane blebs contained multiple double-membraned vesicles. Cultures which had been fixed immediately after neomycin damage did not contain double-membraned vesicles within the hair cells. These data suggest autophagy may aid in the removal of damaged membrane during recovery from neomycin treatment.

3.2 Inhibiting the damage repair process

Ultrastructural analysis of the repair process showed features typical of different pathways of endocytosis which could contribute towards the internalisation of membrane blebs. To probe the molecular mechanism(s) of endocytosis underlying hair cell repair, inhibitors of different endocytic pathways were used in an attempt to block or impede the repair process. A combination of live cell imaging and confocal microscopy were used to investigate the fate of damaged membrane following recovery from neomycin treatment. Scanning electron microscopy was also employed to study membrane bleb retrieval during the repair process. The effects of different compounds known to inhibit endocytosis, protein kinase activity and actin dynamics were tested for their potential to block repair. The different types of compounds used included inhibitors of dynamin-dependent endocytosis, clathrin-mediated endocytosis and caveolae-dependent endocytosis. Inhibitors of the CLIC/GEEC pathway, autophagy and macropinocytosis were also tested along with protein kinase inhibitors and an actin stabilising compound. The experiments performed, drug concentrations and numbers of cultures examined are listed in Table 2.1. Combinations of inhibitors were not used as when tested they were toxic to hair cells. In addition, antibodies to different proteins essential for clathrin-mediated and caveolae-dependent endocytosis were used to investigate colocalisation with internalised membrane during hair cell repair.

3.2.1 Myosin II is not essential for membrane repair

The formation and retraction of membrane blebs is seen with many different cell lines growing in vitro (Sato and Frank, 2014; Johnson, 1976; Laser-Azogui et al., 2014) and myosin motor

proteins are known to drive this process. Membrane blebs are formed when a local area of plasma membrane detaches from the actin cortex. This detachment is powered by myosin II ATPase causing a local contraction of the actin cortex which increases cytoplasmic pressure within the cell. This increased pressure drives cytoplasm into the growing bleb during a process known as nucleation (Charras et al., 2008a) (For more detail see section 1.4.2.1). The compound blebbistatin is a high affinity myosin II ATPase inhibitor, known to block formation of membrane blebs in various cell types (Charras et al., 2008b). Blebbistatin was tested first to see if it would inhibit formation of membrane blebs in neomycin-treated cultures and secondly to see if membrane repair could be inhibited as myosin II also powers bleb retraction. Annexin V-488 binds phosphatidylserine (PS), an aminophospholipid of the inner leaflet of the plasma membrane that is externalised in response to neomycin treatment (Goodyear et al., 2008). After neomycin exposure, numerous membrane blebs were observed on the apical surface of hair cells in the DMSO control cultures (Figure 3.13**a**). Annexin V-488 was also detected on the hair bundle and around the periphery of the hair cell apex (Figure 3.13**a'**). The blebbistatin pre-treated cultures formed membrane blebs in response to neomycin (Figure 3.13**b**) and also externalised PS, as detected by annexin V-488 labelling, on the surface of hair cells (Figure 3.13**b'**). These data show blebbistatin does not block neomycin-induced bleb formation. Following neomycin treatment, cultures were washed and allowed to recover for 30 minutes in RCM containing 0.1% DMSO or blebbistatin to investigate damage repair. The DMSO control and the blebbistatin treated cultures no longer had membrane blebs on the apical surface of hair cells (Figure 3.13**c,d**) and annexin V-488 had been internalised within the cytoplasm in distinct punctae (Figure 3.13**c'',d''**). These data show blebbistatin does not inhibit membrane bleb formation following neomycin treatment and myosin II is not essential for the repair of neomycin-induced membrane damage in cochlear cultures.

3.2.2 Repair does not require clathrin or caveolae

Caveolin 1 is the main component of caveolae and is required for caveolae-dependent endocytosis. Clathrin-mediated endocytosis is characterised by the formation of a clathrin lattice which is composed of clathrin heavy chains and light chains. Antibodies to caveolin 1 and clathrin heavy chains were used to see if they colocalise with internalised annexin V-488 during repair. Confocal microscopy revealed that following 10 minutes of recovery from neomycin treatment, most annexin V-488 was internalised within hair cells. Specifically, annexin V-488 labelling was distributed within cytoplasm of hair cells (Figure 3.14**a,c,d**). Clathrin heavy chain antibody staining following 10 minutes of recovery was localised to the apical surface of hair cells and very little was observed deep inside the cell (Figure 3.14**b,c,d**). There was no colocalisation between annexin V-488 labelling and antibodies to clathrin heavy chains (Figure 3.14**c,d**). Antibodies to caveolin 1 were located at the apical surface of hair cells and distributed throughout the cytoplasm, with two distinct areas of labelling in the kinocilial regions of OHCs (Figure 3.15**b**). There appeared to be no colocalisation between annexin V-488 and antibodies to caveolin 1 following 10 minutes of recovery from neomycin treatment (Figure 3.15**c,d**).

To further investigate whether clathrin-mediated or caveolae-dependent endocytosis may be involved in the repair process, inhibitors of these two mechanisms were tested for their potential to block or impede membrane internalisation. The suitability of the clathrin inhibitor chlorpromazine was first tested to see if it elicited PS externalisation in its own right. This test was conducted on all inhibitors used and any that caused PS externalisation or membrane bleb formation were excluded from the repair assay as this would confound results. After 10 minutes of DMSO treatment, control cultures had no annexin V-488 labelling on the surface of

hair cells (Figure 3.16**a**) and membrane blebs were not detected. Following 10 minutes of neomycin treatment, annexin V-488 labelling was detected on hair bundles, around the periphery of the hair-cell apical surface and on membrane blebs (Figure 3.16**b**). Chlorpromazine however, led to annexin V-488 labelling on hair bundles and around the hair-cell periphery, with no membrane bleb formation (Figure 3.16**c**). Not all hair cells labelled with annexin V-488 after chlorpromazine treatment, and labelling did not appear as bright as that seen in neomycin-treated cultures, but the concentration of chlorpromazine was much lower than the concentration of neomycin which would explain the difference in annexin V-488 labelling. These data suggest however, chlorpromazine was not a suitable compound to test as an inhibitor of repair from neomycin-induced damage.

Pitstop 2 inhibits clathrin terminal domain function and is a potent inhibitor of clathrin-mediated endocytosis (von Kleist et al., 2011). Clathrin-mediated endocytosis and caveolae-dependent endocytosis are both reliant on dynamin for scission of invaginations from the plasma membrane. The compounds dynasore and rhodadyn are both inhibitors of dynamin. As Pitstop 2, dynasore and rhodadyn did not cause the formation of blebs or elicit PS externalisation in their own right (data not shown), they were tested for their ability to block membrane repair following neomycin treatment. Cultures were treated with neomycin and allowed to recover as described previously. After 10 minutes of neomycin treatment, numerous membrane blebs (Figure 3.17**a-d**) and annexin V-488 (Figure 3.17**a'-d'**) labelling were seen around the perimeter of the apical surface of the hair cells.

After 30 minutes recovery in RCM, membrane blebs were no longer detected on the apical surface of hair cells in the DMSO control cultures (Figure 3.17**e**) and annexin V-488 was detected within the cytoplasm at a focal level between the apical surface of hair cells and the

nucleus (Figure 3.17**e''**). Annexin V-488 also appeared to be located within the cytoplasm of hair cells in Pitstop 2, dynasore and rhodadyn treated cultures (Figure 3.17**e''-h''**). There appeared to be slightly less annexin V-488 internalised within hair cells of rhodadyn treated cultures when compared to the other conditions. In addition, some membrane blebs were detected on the surface of Pitstop 2 treated hair cells after recovery. These data suggest Pitstop 2 and rhodadyn may impede, but not block membrane bleb retrieval.

To confirm these observations the cultures were fixed and double labelled with Texas Red phalloidin and examined by confocal microscopy. As expected, internalised annexin V-488 was seen in the cytoplasm of OHCs and inner hair cells (IHCs) from DMSO control cultures (Figure 3.18**a-a''**), cultures treated with Pitstop 2 (Figure 3.18**b-b''**), dynasore (Figure 3.18**c-c''**) and rhodadyn (Figure 3.18**d-d''**). There was however, less annexin V-488 internalised in the hair cells of rhodadyn treated cultures. These data suggest dynamin-dependent mechanisms of endocytosis may play a role, but are not essential, for internalisation of PS-annexin V-488 complexes.

3.2.3 Repair does not occur via macropinocytosis and is not CLIC/GEEC dependent

Cholera toxin B (CTxB) is used as a marker for studying endocytosis in various cell types. CTxB initially binds to GM1, a ganglioside located on the plasma membrane, and then becomes internalised within the cell. The underlying endocytic mechanism was initially thought to be caveolae-dependent, but more recently the CLIC/GEEC pathway has been suggested as the predominant mechanism of endocytosis (Kirkham and Parton, 2005). To visualise the

internalisation of CTxB, cultures were labelled with Alexa Fluor 488 CTxB for 10 minutes at 20°C. CTxB labelling was chiefly detected in the cytoplasm of supporting cells, including cells of the greater epithelial ridge, pillar cells and Deiters cells (Figure 3.19). A low level of fluorescent CTxB was also detected on the surface of OHCs, particularly in the third row. Internalisation of CTxB within hair cells could not be studied further as only a very low level of CTxB was bound to the plasma membrane.

The compound EIPA is a potent inhibitor of macropinocytosis and the CLIC/GEEC pathway of endocytosis (Nonnenmacher and Weber, 2011). EIPA did not elicit PS externalisation or cause membrane bleb formation in its own right (data not shown) and so the inhibitory effects of EIPA were tested. Cultures were treated with neomycin as described previously but after repair cultures were labelled with annexin V-594 to detect any PS present on the apical surface of hair cells. The 0.1% DMSO treated cultures developed membrane blebs in response to neomycin (Figure 3.20**a**) and had annexin V-488 labelling on the surface of hair cells (Figure 3.20**a'**). After recovery, membrane blebs were no longer detected (Figure 3.20**c**) and annexin V-594 labelling was not observed on the surface of hair cells (figure 3.20**c'**). The culture treated with 100 μM EIPA formed membrane blebs (figure 3.20**b**) and annexin V-488 was detected following neomycin treatment (Figure 3.20**b'**). After recovery some membrane blebs were still present on the surface of hair cells (Figure 3.20**d**) and a small amount of annexin V-594 labelling was detected in the same region (Figure 3.20**d'**) which appeared to be more than that observed in controls. The distribution of annexin V-594 labelling in the EIPA treated cultures was very different to the initial annexin V-488 labelling following neomycin treatment and it would appear most of the PS had been internalised during recovery. As EIPA failed to block recovery in most neomycin-treated hair cells, these data suggest macropinocytosis and the CLIC/GEEC pathway do not mediate damage repair.

3.2.4 Repair does not involve autophagy

Autophagy is a degradation process used for the sequestration of various cellular components into autophagosomes. PI3K inhibitors are specific blockers of this pathway (Blommaart et al., 1997). As the two PI3K inhibitors, LY294002 and wortmannin, did not cause bleb formation or PS externalisation in their own right (data not shown), they were tested for their potential to prevent membrane repair. Experiments similar to those described earlier were performed. Following neomycin treatment, membrane blebs were present on the apical surface of hair cells in cultures that had been exposed to 0.1 % DMSO, 10 µM LY294002 or 10 µM wortmannin (Figure 3.21**a-c**). Annexin V-488 was also detected on the surface of hair cells in cultures from all three conditions following neomycin exposure (Figure 3.21**a'-c'**). After 30 minutes recovery, membrane blebs were no longer detected on the apical surface of hair cells in all three conditions (Figure 3.21**d-f**). Annexin V-488 was also internalised within the cytoplasm of hair cells and was located between the cuticular plate and the nucleus in all three conditions (Figure 3.21**d''-f''**).

Confocal images of cultures that had been fixed and double labelled with Texas Red phalloidin after recovery showed that internalised annexin V-488 was located between the apical surface of the hair cells and the hair-cell nucleus in all three conditions (Figure 3.22**a-c''**). These data show LY294002 and wortmannin do not block internalisation of damaged membrane and that autophagy is therefore unlikely to be involved in internalisation of damaged membrane.

3.2.5 Repair is actin dependent

The actin cytoskeleton is required for endocytosis and transcytosis at the apical surface of polarised epithelial cells (Apodaca, 2001). Virus entry can be inhibited in polarised cells by stabilising actin filaments using the compound jasplakinolide (Sun and Whittaker, 2007). Jasplakinolide promotes actin polymerisation by binding to the sides of actin filaments and inducing actin nucleation (Bubb et al., 2000). As jasplakinolide alone did not elicit PS externalisation or bleb formation (data not shown), it was first tested to see if membrane bleb formation was disrupted in response to neomycin. Following neomycin treatment, small blebs formed on the apical surface of hair cells along the length of the cochlea in DMSO treated control cultures (Figure 3.23**a,c**). In cultures treated with jasplakinolide, slightly larger blebs formed in the basal coils and much larger blebs formed in the apical coils in response to neomycin when compared to those seen in DMSO-treated cultures (Figure 3.23**b,d**). To obtain a quantitative measure of bleb formation under different conditions, bleb volume was calculated in jasplakinolide and control cultures. For membrane bleb quantification, it was assumed blebs were spherical in shape. The bleb located at the kinocilial region was the most prominent in both DMSO control cultures and jasplakinolide-treated cultures; therefore the diameter of this bleb was measured from each OHC in a field of view of a captured DIC image. Membrane bleb measurements were made from images of the mid-basal cochlear region 10 minutes after neomycin treatment and the mid-apical region 12 minutes after neomycin treatment in each condition. Membrane bleb volume was significantly larger in cultures treated with jasplakinolide (33.27 μm^3 ± 1.82, n=213 OHCs), when compared to DMSO control cultures following neomycin treatment (6.29 μm^3 ± 0.82, n=98 OHCs) (Figure 3.24). By stabilising actin filaments, membrane bleb size in response to neomycin was greatly increased.

Jasplakinolide was also tested for its ability to block internalisation of annexin V-488 and retrieval of membrane blebs during recovery from neomycin-induced damage. Experiments similar to those described previously were performed. Membrane blebs and annexin V-488 labelling was detected on the apical surface of hair cells following neomycin treatment in 0.1 % DMSO control cultures (Figure 3.25**a,a'**) and 5 µM jasplakinolide treated cultures (Figure 3.25**b,b'**). Following 30 minutes recovery, membrane blebs were no longer present on the surface of hair cells in DMSO treated cultures (Figure 3.25**c**). Numerous membrane blebs were, however, detected on the surface of hair cells from cultures treated with jasplakinolide (Figure 3.25**d**). Annexin V-488 was internalised in hair cells from DMSO control cultures after recovery (Figure 3.25**c''**) but annexin V-488 was not detected in the cytoplasm of hair cells from jasplakinolide treated cultures (Figure 3.25**d''**). As jasplakinolide appeared to block internalisation of membrane blebs and annexin V-488, cultures from both conditions were fixed, double labelled with Texas Red phalloidin and imaged using confocal microscopy (Figure 3.26). In the DMSO control cultures, confocal images revealed internalised annexin V-488 was localised between the apical surface of the hair cell and the hair-cell nucleus (Figure 3.26 **a-a''**). As jasplakinolide competitively binds to F-actin, Texas Red phalloidin staining was not detected in jasplakinolide treated cultures. It is clear however that annexin V-488 was not distributed throughout the hair cells as seen in DMSO control cultures (Figure 3.26**b-b''**). These data show jasplakinolide restricts annexin V-488 to the apical surface during the recovery period.

To investigate the effects of jasplakinolide on membrane bleb retrieval, experiments similar to those described above were analysed by SEM. Membrane blebs were not observed on the apical surface of DMSO treated control cultures (Figure 3.27**a**), but were numerous on the surface of neomycin treated hair cells (Figure 3.27**c**). Cultures treated with both neomycin and jasplakinolide formed membrane blebs, which were larger than those in cultures that were

only treated with neomycin (Figure 3.27**e**). Following recovery, the DMSO control and neomycin-treated cultures had no membrane blebs on the apical surfaces (Figure 3.27**b,d**). Cultures treated with both neomycin and jasplakinolide still had numerous membrane blebs across the apical surface of hair cells following 30 minutes (Figure 3.27**f**). These data, together with those obtained with confocal microscopy, show jasplakinolide blocks internalisation of membrane blebs and membrane-bound annexin V-488. Fully functional actin dynamics are therefore required for the damage repair process.

3.2.6 Repair is PKA dependent

Receptor-mediated endocytosis in polarised epithelial cells is regulated by protein kinase activity (Fallon and Danaher, 1992) and the non-selective protein kinase inhibitor staurosporine reduces endocytosis in epithelial cells (Fallon and Danaher, 1992). Staurosporine alone did not cause bleb formation or PS externalisation (data not shown) and was tested for its ability to block the damage repair process. Cultures were treated with neomycin and allowed to recover as described previously. The control cultures exposed to 0.1% DMSO formed membrane blebs in response to neomycin treatment (Figure 3.28**a**), this also occurred to the same extent in 50 nM staurosporine-treated cultures (Figure 3.28**b**). Cultures from both conditions had annexin V-488 labelling on the hair bundle and around the periphery of the hair cell (Figure 3.28**a',b'**). After 30 minutes recovery, blebs were no longer detected in DMSO control cultures (Figure 3.28**c**) and annexin V-488 was present within the cytoplasm of hair cells (Figure 3.28**c''**). Following recovery, the staurosporine-treated culture still had some blebs left on the apical surface and only a small proportion of annexin V-488 was internalised (Figure 3.28**d-d''**). As the repair process was partially blocked by staurosporine, it is likely protein kinases are involved in the damage repair process.

Protein kinase A (PKA) is directly anchored to the actin cytoskeleton (Rivard et al., 2009) and regulates actin dynamics (Howe, 2004). To further investigate the role of protein kinases in membrane repair, the PKA inhibitors KT5720 and H-89 were also tested as described above at concentrations of 10 µM and 20 µM respectively. After neomycin treatment, membrane blebs were detected on the apical surface of hair cells in DMSO control cultures, KT5920-treated cultures and H-89-treated cultures (Figure 3.29**a-c**). Hair cells from all 3 conditions also had annexin V-488 labelling on the apical surface (Figure 3.29**a'-c'**). Following 30 minutes recovery, membrane blebs were no longer detected on the surface of hair cells from DMSO control cultures (Figure 3.29**d**). Membrane blebs were no longer detected in KT5720 treated cultures and appeared to have been internalised (Figure 3.29**e**). The H-89 treated cultures however, had numerous membrane blebs on the surface of hair cells following recovery (Figure 3.29**f**). After recovery, annexin V-488 was distributed within the cytoplasm of hair cells from DMSO treated cultures (Figure 3.29**d''**). In KT5720-treated cultures, annexin V-488 was not distributed deeply within the hair cells and appeared to be restricted towards the apical surface (Figure 3.29**e''**). In H-89 treated cultures, annexin V-488 was not detected within the cytoplasm of hair cells and the distribution was similar to that observed in KT5720-treated cultures (Figure 3.29**f''**).

To further investigate the effects of H-89 on annexin V-488 internalisation, the DMSO control cultures and H-89-treated cultures were imaged using confocal microscopy (Figure 3.30). KT5720 treated cultures were not imaged using confocal microscopy as similar results with more repetition were obtained using the inhibitor H-89. Images revealed DMSO control cultures had internalised annexin V-488 following 30 minutes recovery with labelling distributed between the apical surface of hair cells and the nucleus (Figure 3.30**a-a''**). Cultures

treated with H-89 had annexin V-488 labelling restricted to the apical surface of hair cells (Figure 3.30**b-b''**).

To investigate the effects of H-89 on membrane bleb retrieval, SEM was used to analyse experiments similar to those described above. The 0.1% DMSO control cultures did not develop membrane blebs (Figure 3.31**a**), and as expected numerous membrane blebs formed across the apical surface of OHCs and IHCs in neomycin-treated cultures (Figure 3.31**c**). Cultures treated with both neomycin and 20 µM H-89 also developed numerous membrane blebs on the surface of hair cells (Figure 3.31**e**). DMSO control and neomycin-treated cultures had no membrane blebs on the apical surface of hair cells following recovery (Figure 3.31**b,d**). Cultures treated with neomycin and H-89 still had numerous membrane blebs across the apical surface of hair cells following recovery (Figure 3.31**f**) but there were slightly fewer blebs than before recovery (Figure 3.31**e**) although this was not quantified. These data show PKA is involved in the internalisation of membrane blebs and annexin V-488 bound membrane during the damage repair process.

As repair is PKA-dependent, two other protein kinase inhibitors were also tested to investigate the specificity of PKA in the repair process. The p21 activated kinase (PAK1) inhibitor IPA 3 and the protein kinase C (PKC) inhibitor BIM I were tested for their ability to block membrane repair. Actin cytoskeletal dynamics are regulated by the PAK family of proteins (Garcia et al., 2014; Bokoch, 2003) and PKC (Yang et al., 2013). Cultures were treated with neomycin and allowed to recover as described previously. Following neomycin treatment, membrane blebs were observed on the apical surface of hair cells in DMSO treated control cultures and in cultures that had been treated with 5 µM BIM I and 10 µM IPA 3 (Figure 3.32**a-c**). Annexin V-488 was also detected on the surface of hair cells from all three conditions (Figure 3.32 **a'-c'**).

After 30 minutes recovery, membrane blebs were no longer observed in the three different conditions (Figure 3.32**d-f**) and annexin V-488 was distributed between the apical surface and nucleus (Figure 3.32**d''-f''**).

3.3 Mice with mutations in Atpb81, Ptprq, TRPC and Eps8 are able to repair neomycin-induced membrane damage

3.3.1 Atp8b1 mutant mice

Atp8b1 is a P4 P-type ATPase which functions as a phospholipid flippase and maintains membrane lipid asymmetry by translocating aminophospholipids from the outer leaflet of the plasmalemma to the inner leaflet (van der Mark et al., 2013). Mice with a mutation in the gene encoding Atp8b1 exhibit a significant hearing loss, detected by measuring auditory brainstem responses (ABRs) (Stapelbroek et al., 2009). A hair bundle phenotype has been previously reported at P16 in Atp8b1 deficient mice, with normal bundle development observed at P4 (Stapelbroek et al., 2009). Mice with a mutation in Atp8b1 were examined to see if a bundle phenotype is detected at an earlier age than previously reported and hair cells from these mice were tested for their ability to recover from neomycin induced damage. Hair cells from these mice were also tested to see if they spontaneously externalise PS when maintained in vitro.

3.3.1.1 Atp8b1 deficient mice have hair bundle abnormalities

To investigate if a phenotype was detectable in hair bundles from Atp8b1 deficient mice prior to P16, confocal microscopy was performed on phalloidin stained cochlear preparations from early postnatal Atp8b1$^{G308V/G308V}$ mutant mice and age-matched heterozygous littermate controls. Hair bundle morphology was compared in heterozygous and Atp8b1$^{G308V/G308V}$ mice at ages P0, P3 and P7 (Figure 3.33). Confocal images of hair cells from P0 heterozygous cochleae reveal v-shaped hair bundles typical of normal mice (Figure 3.33**a**). An abnormal hair bundle morphology was observed at P0 in Atp8b1$^{G308V/G308V}$ mice (Figure 3.33**b**). Hair bundles of OHCs in P0 Atp8b1$^{G308V/G308V}$ mice also had a degeneration of some stereocilia. At P3, Atp8b1$^{G308V/G308V}$ mice have a hair bundle phenotype (Figure 3.33**d**) which does not appear any worse when compared to Atp8b1$^{G308V/G308V}$ P0 mice. By P7 there is further loss of stereocilia and a bundle phenotype in the OHCs and IHCs of Atp8b1$^{G308V/G308V}$ mice is more severe than that observed at P3. The stereocilia of IHCs from P7 mutant mice appear slightly disorganised with some stereocilia missing. The OHCs also look more abnormal with further degeneration of stereocilia and a deviation from the V-shaped bundles seen in age-matched controls. These data show a distinct hair bundle phenotype is evident in Atp8b1 deficient mice that is apparent by P0 and gets worse by P7.

3.3.1.2 Atp8b1 deficient mice do not spontaneously externalise PS

The possibility of spontaneous PS accumulation in the outer leaflet of the plasma membrane was studied in cochlear cultures. Cochlear cultures from age P2 Atp8b1$^{G308V/G308V}$ mice and heterozygous controls were maintained in vitro for 2 (+2), 3 (+3) or 4 (+4) days, labelled with annexin V-488, fixed and double labelled with Texas Red phalloidin. Photomontages were

generated from fluorescence images of each culture. PS externalisation was not detected in any hair cells in P2+2 heterozygous control cultures or Atp8b1$^{G308V/G308V}$ cultures. By P2+3, a small number of hair cells were annexin V-488 positive in both the control cultures and Atp8b1$^{G308V/G308V}$ cultures. At P2+4 a greater number of annexin V-488 positive hair cells were detected in control and mutant cultures (Figure 3.34**a,b**). At P2+3, no significant difference in spontaneous PS externalisation was detected between heterozygous controls (1.8% ± 1, n=4 cochleae) and Atp8b1$^{G308V/G308V}$ mutants (2% ± 1.9, n=5 cochleae) (Figure 3.34**c**). Although there was less spontaneous PS externalization in heterozygous controls (2.6% ± 0.8%, n=6 cochleae) at P2+4 when compared to Atp8b1$^{G308V/G308V}$ mutants (4.1% ± 1.4, n=10 cochleae), this difference was also not significant (Figure 3.34**c**). These data show that a mutation in the protein encoding the phospholipid flippase Atp8b1 does not lead to increased spontaneous PS externalisation in hair cells from cultures maintained for 2, 3 and 4 days in vitro.

3.3.1.3 Atp8b1 deficient mice recover from aminoglycoside induced membrane damage

Loss of Atp8b1 function may prevent the restoration of membrane phospholipid asymmetry in hair cells following neomycin exposure. Cultures from Atp8b1$^{G308V/G308V}$ mice and heterozygous littermates were therefore treated with neomycin and allowed to recover as described previously. Following neomycin treatment, membrane blebs and annexin V-488 labelling were detected on the apical surface of hair cells in cultures from heterozygous controls (Figure 3.35**a,a'**) and Atp8b1$^{G308V/G308V}$ mutants (Figure 3.35**b,b'**). After 30 minutes recovery, membrane blebs were no longer detected on the apical surface and annexin V-488 was internalised inside hair cells from heterozygous controls (Figure 3.35**c-c''**) and Atp8b1$^{G308V/G308V}$ mutants (Figure 3.35**d-d''**).

To study annexin V-488 internalisation in more detail, the cultures were fixed, double labelled with Texas Red phalloidin and imaged in the mid-basal region using confocal microscopy (Figure 3.36). Confocal images showed annexin V-488 was internalised within hair cells of heterozygous controls (Figure 3.36**a-a''**) and Atp8b1$^{G308V/G308V}$ mutants (Figure 3.36**b-b''**) between the apical surface and the nucleus. These data show Atp8b1 deficient mice are able to repair neomycin-induced membrane damage.

3.3.2 Ptprq deficient mice recover from aminoglycoside-induced membrane damage

A role for Ptprq in apical endocytosis has been suggested as the intracellular domain interacts with eps 15 homology domain 3 (EHD3), a protein involved in endocytosis (Nayak, 2010). Mice with a mutation in Ptprq were tested for their ability to endocytose neomycin-induced damaged membrane during repair.

Cultures from Ptprq$^{CAT/CAT}$ and heterozygous controls were treated as described above but annexin V-594 was added after recovery to detect any PS still present in the outer leaflet of the apical membrane. During neomycin treatment membrane blebs and annexin V-488 were detected on the surface of hair cells in both the heterozygous control and Ptprq$^{CAT/CAT}$ cultures (Figure 3.37**a-b'**). After 30 minutes recovery, membrane blebs (Figure 3.37**c,d**) and annexin V-594 were no longer observed on the surface of hair cells in either controls or Ptprq$^{CAT/CAT}$ cultures (Figure 3.37**c',d'**). These data show mice with a mutation in Ptprq are able to repair the membrane damage caused by exposure to neomycin.

3.3.3 Eps8 deficient mice recover from aminoglycoside-induced membrane damage

Disruption of actin filaments by pharmacological methods impairs endocytosis (see section 3.2.5). Actin dynamics are regulated by various actin capping proteins such as Eps8 (Welsch et al., 2007). Hair cells from the cochleae of mice deficient in Eps8 were therefore tested for their ability to repair neomycin-induced membrane damage.

After neomycin treatment, membrane blebs and annexin V-488 labelling was present on the surface of IHCs and OHCs of cultures from Eps8$^{tm1Ppdf/tm1Ppdf}$ mutants and heterozygous controls (Figure 3.38**a-b'**). Following 30 minutes recovery, membrane blebs were no longer detected on the surface of hair cells from either heterozygous controls or cultures from Eps8$^{tm1Ppdf/tm1Ppdf}$ mice (Figure 3.38**c,d**). Annexin V-488 was located in the cytoplasm of hair cells from both heterozygous controls and Eps8$^{tm1Ppdf/tm1Ppdf}$ cultures (Figure 3.38**c'',d''**). These data show Eps8 is not necessary for removal of damaged membrane from the apical surface of hair cells recovering from neomycin-induced damage.

3.3.4 TRPC3/TRPC6 deficient mice recover from aminoglycoside-induced membrane damage

An application of extracellular Ca^{2+} can trigger PS externalisation in hair cells from cochlear cultures (Goodyear et al., 2008). Externalisation of PS can also be triggered by elevated cytosolic Ca^{2+} in platelets (Mahaut-Smith, 2013). Entry of Ca^{2+} via the non-selective cation channels TRPC3 and TRPC6 activates PS externalisation (Mahaut-Smith, 2013). Externalisation

of PS in response to neomycin treatment was therefore studied in TRPC3 and TRPC6 double knockout mice as hair cells from these mice may have a weaker response to neomycin-induced PS externalisation and ability to repair neomycin-induced membrane damage.

Cultures from TRPC3/TRPC6 double KO and heterozygous control mice were treated with neomycin and allowed to recover as described above. During neomycin treatment, membrane blebs and annexin V-488 labelling were present on the apical surface of hair cells in both the heterozygous control and the TRPC3/TRPC6 DKO cultures (Figure 3.39**a-b'**). Following 30 minutes recovery, membrane blebs and annexin V-594 were not detected on the surface of hair cells in either heterozygous controls (Figure 3.39**c,c'**) or TRPC3/TRPC6 DKO cultures (Figure 3.39**d,d'**). These data show mice lacking both TRPC3 and TRPC6 are able to repair the membrane damage caused by neomycin exposure.

3.4 EIPA blocks entry of neomycin into hair cells

One potent inhibitor of the CLIC pathway is the amiloride derivative EIPA (Nonnenmacher and Weber, 2011). As amiloride is known to block the MET channel (Rusch et al., 1994), it was important to first check if EIPA blocks neomycin entry into hair cells. Cochlear cultures from P2 wildtype mice were used for all experiments investigating the MET blocking effects of EIPA.

3.4.1 EIPA blocks FM1-43 loading

FM1-43 is a positively charged styryl dye which is able to enter hair cells via the MET channel (Gale et al., 2001). To test whether EIPA blocks entry of FM1-43 into hair cells, cultures were treated with 0.1% DMSO as a control or 100 µM EIPA in HBHBSS for 5 minutes, labelled with 0.3 µM FM1-43 for 10 seconds, washed and imaged to assess levels of FM1-43 fluorescence in the hair cells. Images were captured from basal-coil cultures 5 minutes after FM1-43 dye application (Figure 3.40**a**), whilst images from apical-coil cultures were captured 7 minutes after dye application (Figure 3.40**c**). The focal level of imaging was between the cuticular plate and the nucleus of the OHCs. In both DMSO control cultures and EIPA treated cultures, loading of FM1-43 was specific to OHCs and IHCs with no labelling detected in supporting cells. A gradient of FM1-43 loading could be seen, with higher levels of FM1-43 observed in the basal end of basal-coil cochlear cultures, matching a gradient of hair cell maturation (also number of stereocilia and the size of unit channel conductance). Arbitrary fluorescence levels of FM1-43 in OHCs of DMSO treated cultures (79.15 ± 2.34, n=40 OHCs) were significantly higher than in OHCs from EIPA treated cultures (27.59 ± 1.47, n=40 OHCs) (Figure 3.41). These data suggest EIPA could be inhibiting FM1-43 entry into hair cells by blocking the MET channel.

3.4.2 EIPA blocks uptake of neomycin and dihydrostreptomycin

As FM1-43 uptake is blocked by EIPA, and as aminoglycosides are thought to enter hair cells via the same route, EIPA was tested for its ability to block aminoglycoside entry into hair cells. Two different aminoglycosides, both conjugated to Texas Red were used to test this hypothesis. Cultures were treated with 0.5 mM neomycin Texas Red or 0.5 mM dihydrostreptomycin Texas Red in the presence of 200 µM EIPA or 0.1% DMSO for 15 minutes.

Cultures were fixed and imaged, enabling arbitrary fluorescence levels of Texas Red conjugates to be measured. In DMSO control cultures treated with dihydrostreptomycin Texas Red, the vast majority of hair cells were labelled with dihydrostreptomycin (Figure 3.42**a,c**) with a gradient running from the basal end of the basal coil to the apical end of the apical coil. Cultures treated with dihydrostreptomycin Texas Red in the presence of EIPA, had virtually no hair cell labelling in either basal or apical-coil cultures (Figure 3.42**b,d**). A significant difference in fluorescence levels was detected when comparing DMSO control cultures (71.16 ± 5.92, n=20 OHCs) and EIPA treated cultures (9.14 ± 1.04, n=20 OHCs) (Figure 3.43).

In control cultures treated with neomycin Texas Red in the presence of 0.1% DMSO the majority of hair cells in the basal coil were labelled and the intensity of labelling decreased towards the apical end of the apical coil (Figure 3.44**a,c**). In cultures treated with 200 µM EIPA there was virtually no neomycin Texas Red loading at any point along the length of the cochlea (Figure 3.44**b,d**). A significant difference was found in fluorescence levels with the DMSO control culture (57.05 ± 6.74, n=20 OHCs) being significantly brighter than the EIPA treated culture (6.69 ± 0.77, n=20 OHCs) (Figure 3.45).

3.4.3 EIPA protects hair cells from short term neomycin damage

As EIPA was shown to reduce aminoglycoside entry into hair cells, it was tested for its ability to block neomycin-induced membrane damage. Cultures were pre-treated with 100 µM EIPA or 0.1% DMSO in HBHBSS as a control for 5 minutes before 1 mM neomycin was added for 15 minutes in the presence of annexin V-488. Control cultures started to develop membrane blebs and label with annexin V-488 on the apical surface of OHCs within 5 minutes of

neomycin treatment in the mid-basal region (Figure 3.46**a,a'**) with more severe blebbing and annexin V-488 labelling detected after 10 minutes (Figure 3.46**c,c'**). Cultures pre-treated with EIPA had no membrane blebbing and annexin V-488 labelling following neomycin treatment (Figure 3.46**b,b',d,d'**). EIPA therefore appears to block neomycin-induced membrane bleb formation and PS externalisation in cochlear cultures.

To test whether the MET blocking effects of EIPA were reversible at physiological temperature, cultures were pre-treated with 100 µM EIPA or DMSO for 5 minutes before the addition of 1 mM neomycin in the presence of annexin V-488. After 15 minutes neomycin treatment, the EIPA pre-treated cultures were washed, incubated in RCM, washed again and then rechallenged with 1 mM neomycin in the presence of annexin V-488. Extensive annexin V-488 labelling was detected basally in the control cultures after 5 minutes (Figure 3.47**a**) and apically after 7 minutes (Figure 3.47**d**). Annexin V-488 labelling included the OHC bundle and punctae around the periphery of the apical surface of hair cells, which became more apparent after 10 minutes basally (Figure 3.47**g**) and 12 minutes apically (Figure 3.47**j**). The mid-basal and mid-apical region in the EIPA treated cultures did not label with annexin V-488 basally (Figure 3.47**b,h**) or apically (Figure 3.47**e,k**), even after 15 minutes of neomycin treatment. Following EIPA washout and a rechallenge with neomycin, annexin V-488 was detected on the majority of hair cells after 5 minutes rechallenge in the mid-basal region (Figure 3.47**c**). Labelling was detected on the hair bundle of some hair cells in the mid-apical region after 7 minutes (Figure 3.47**f**). More intense labelling was detected 10 minutes after rechallenge basally (Figure 3.47**i**) and 12 minutes after rechallenge apically (Figure 3.47**l**). The annexin V-488 labelling was not quite as intense for the rechallenge when compared to the control culture but this may not be significant. These data show the block of neomycin entry by 200 µM EIPA is almost entirely reversible at physiological temperature.

3.4.4 EIPA protects hair cells from long term neomycin damage

EIPA was tested for its ability to block neomycin damage over a longer time period and to assess whether it causes any damage to hair cells during long term treatment. Cultures were incubated in RCM containing either 0.1% DMSO, 50 µM EIPA, 250 µM neomycin or a mixture of 250 µM neomycin and 50 µM EIPA. After 24 hours, cultures were washed, fixed and labelled with Texas Red phalloidin. Hair-cell structural damage was assessed by checking phalloidin staining of hair bundles. The hair bundles in the apical and basal-coil cultures incubated in 0.1% DMSO had no damage after 24 hours incubation. High magnification images of hair bundles from the mid-basal and mid-apical regions show typical healthy hair cells with intact hair bundles (Figure 3.48**a,b**). Following incubation in RCM containing 50 µM EIPA, phalloidin staining indicates hair bundles remain undamaged in both basal (Figure 3.48**c**) and apical coils (Figure 3.48**d**). Incubation in RCM containing 250 µM neomycin caused extensive hair-cell damage along the entire length of the cochlea. High magnification images show hair-bundle damage in both basal-coil (Figure 3.48**e**) and apical-coil cultures (Figure 3.48**f**). Cultures incubated in RCM containing neomycin and EIPA appear to have damage to hair cells in basal but not in the apical-coil cultures (Figure 3.48**h,g**). These data suggest EIPA is able to protect hair bundles from neomycin damage in the apical coil but not in the basal coil over a 24 hour period.

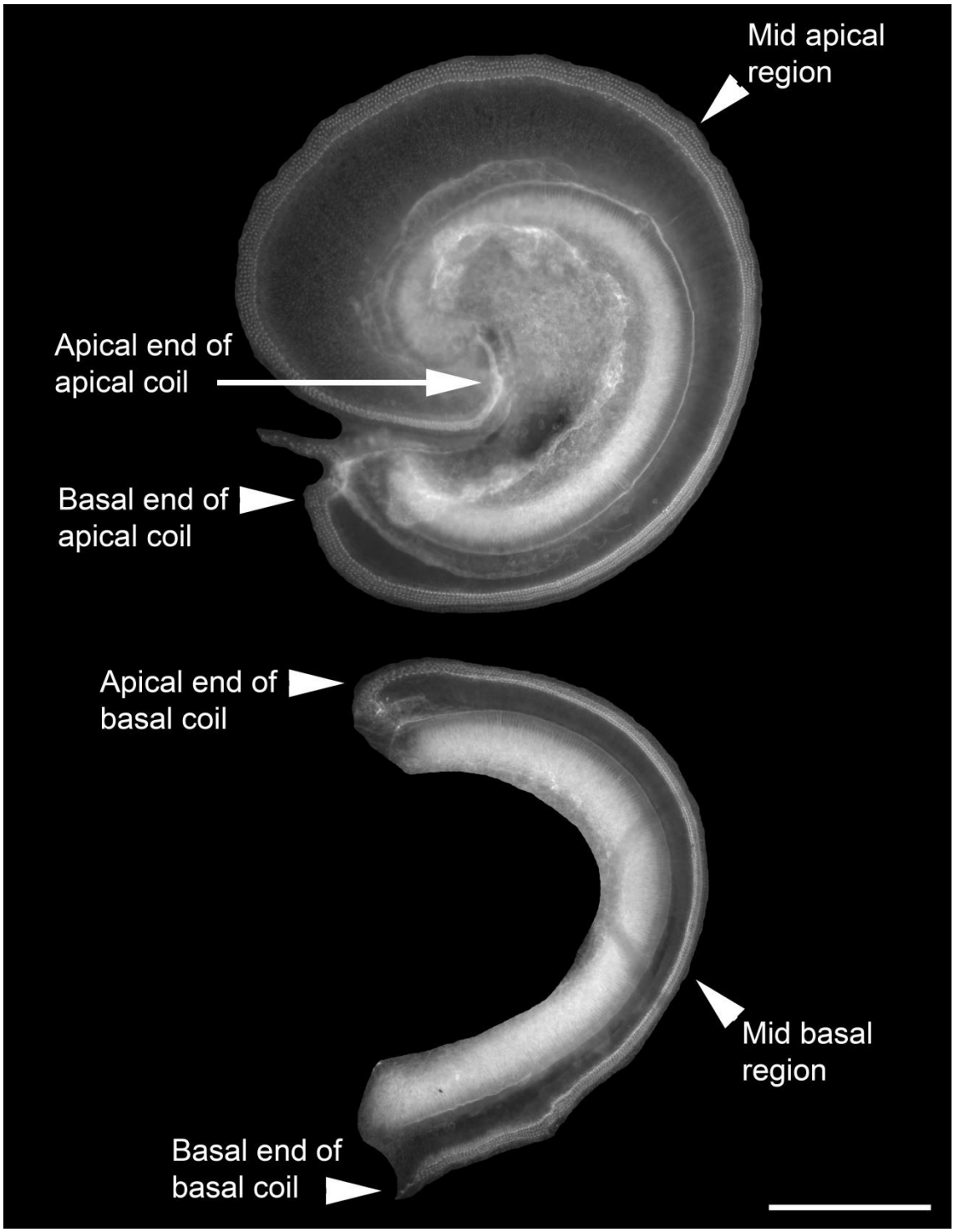

Figure 3.1. The different regions of a cochlear culture. Scale bar = 200 µm.

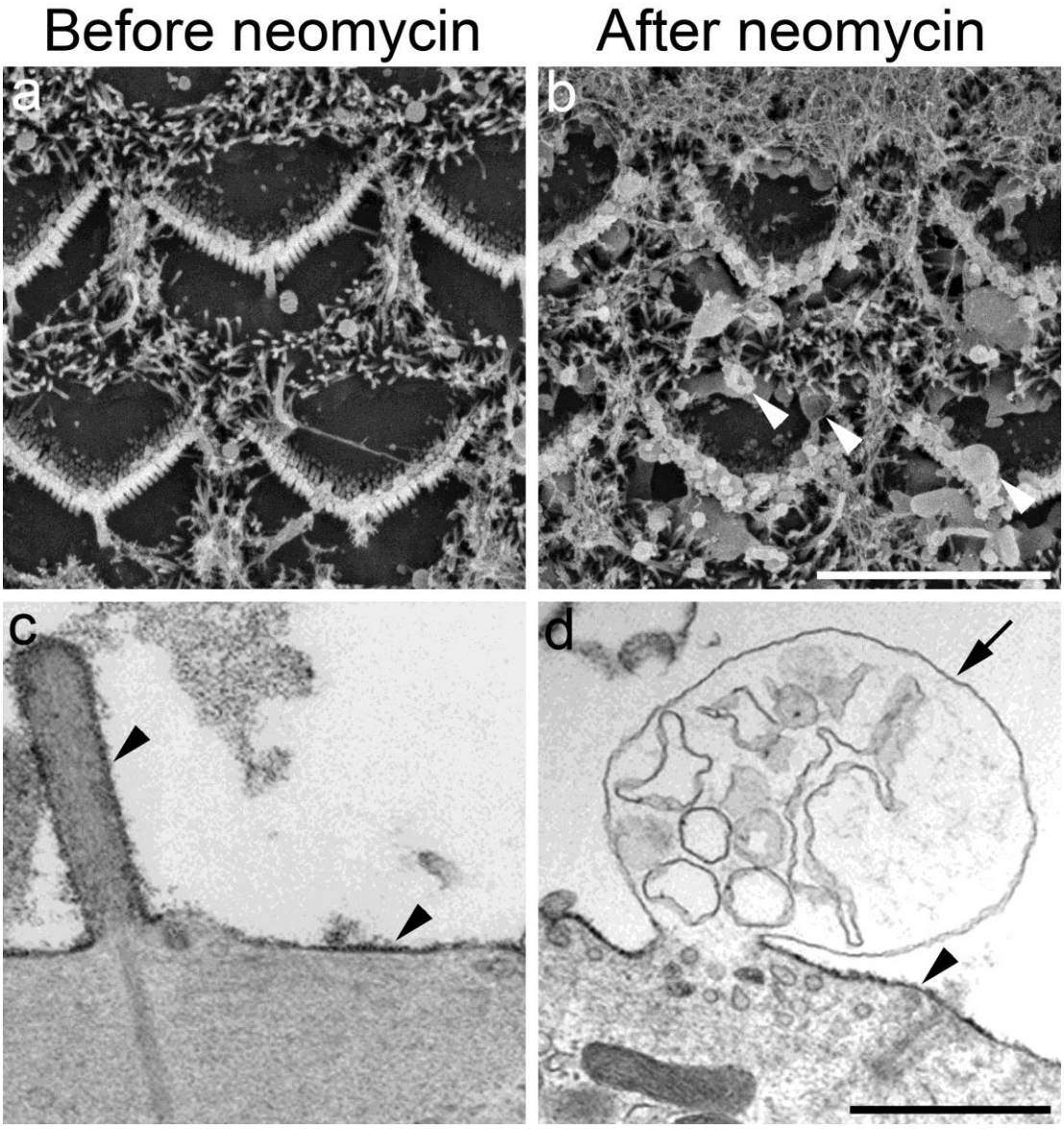

Figure 3.2. SEM (**a,b**) and TEM (**c,d**) images of hair cells in the middle of basal-coil cochlear cultures before (**a,c**) and after 15 minutes of 1 mM neomycin treatment at 20°C (**b,d**). White arrowheads indicate membrane blebs on the apical surface of OHCs. Black arrow indicates a single membrane bleb. Black arrowheads indicate cationic ferritin labelling. White scale bar = 5 µm. Black scale bar = 800 nm.

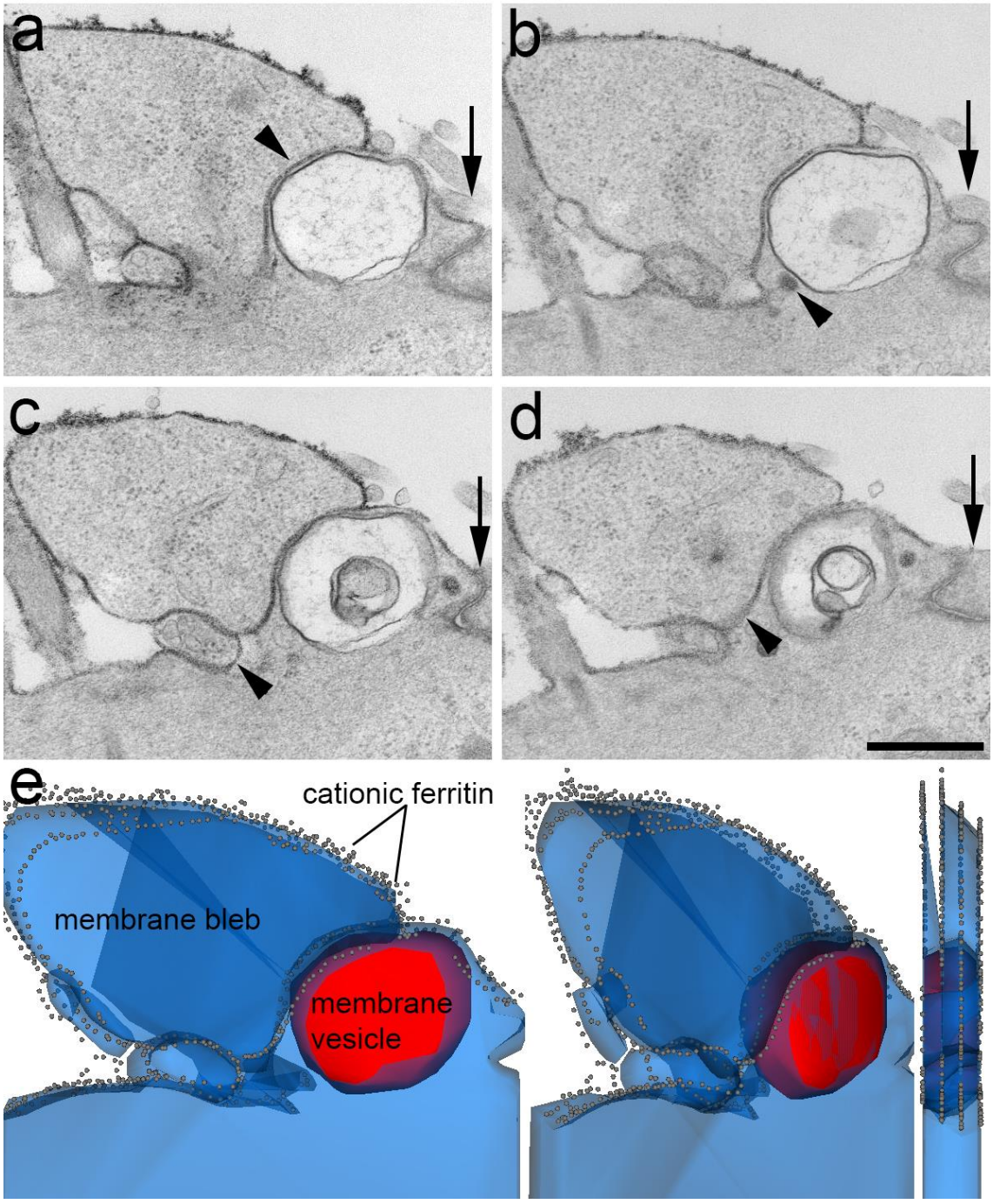

Figure 3.3. Four 100 nm ultrathin serial sections (**a-d**) were collected from cultures which had been treated with 1 mM neomycin, labelled with cationic ferritin and allowed to recover for 10 minutes. The four serial sections were used to generate a 3-dimensional reconstruction (**e**) using the computer program Reconstruct. The grey dots and arrowheads represent cationic ferritin, the red sphere represents a large vesicle and arrows indicate the supporting cell. Scale bar = 600 nm.

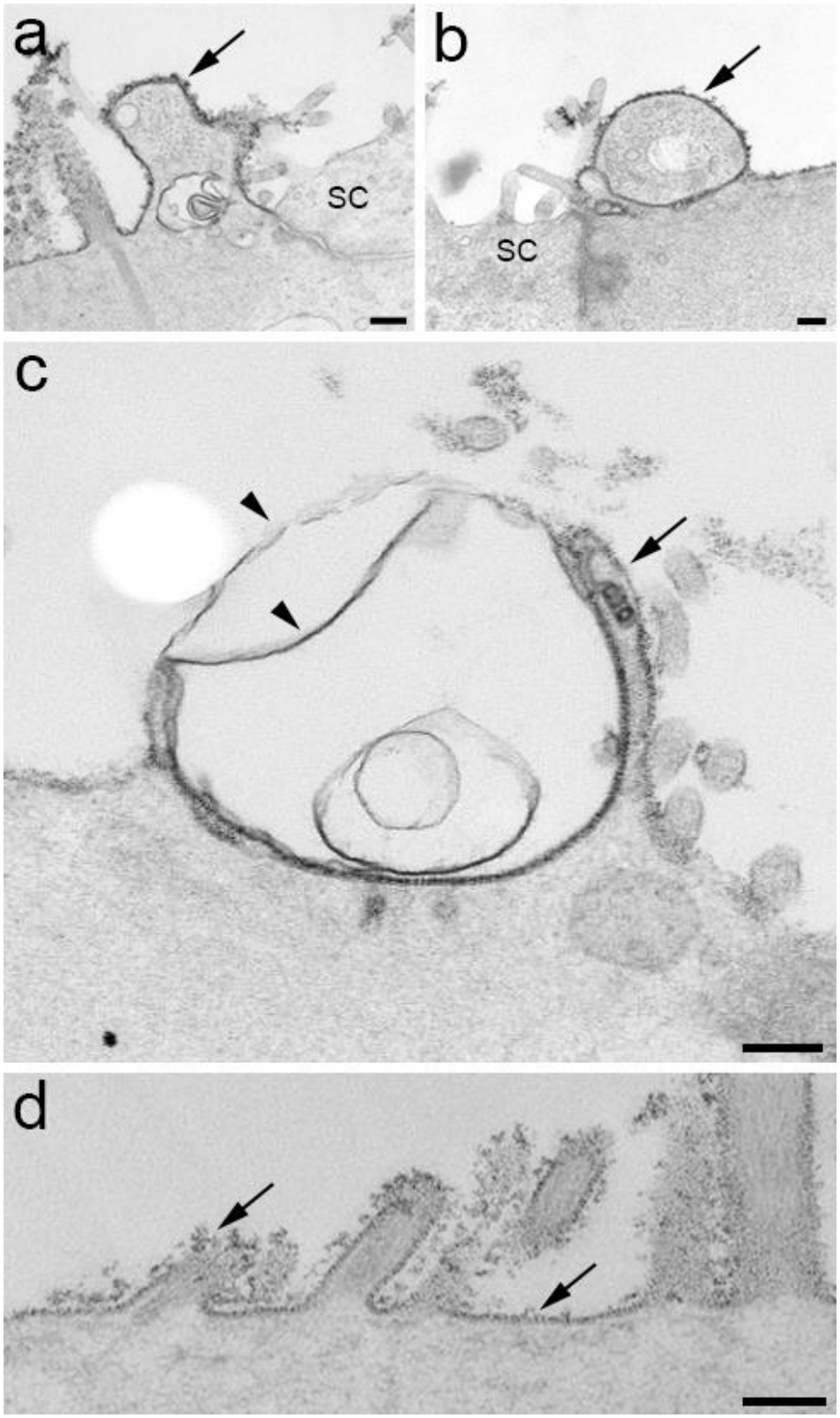

Figure 3.4. Blebs observed following 10 minutes of recovery from 1 mM neomycin (**a-c**). The surfaces of some membrane blebs were entirely labelled with cationic ferritin (**a-b**) whilst the surface of others were only partially labelled (**c**). Cationic ferritin labelling was seen across the entire apical surface of hair cells not exposed to neomycin (**d**). Arrowheads indicate membrane that does not contain cationic ferritin labelling and arrows indicate cationic ferritin labelled membrane. SC = supporting cell. Scale bar = 200 nm.

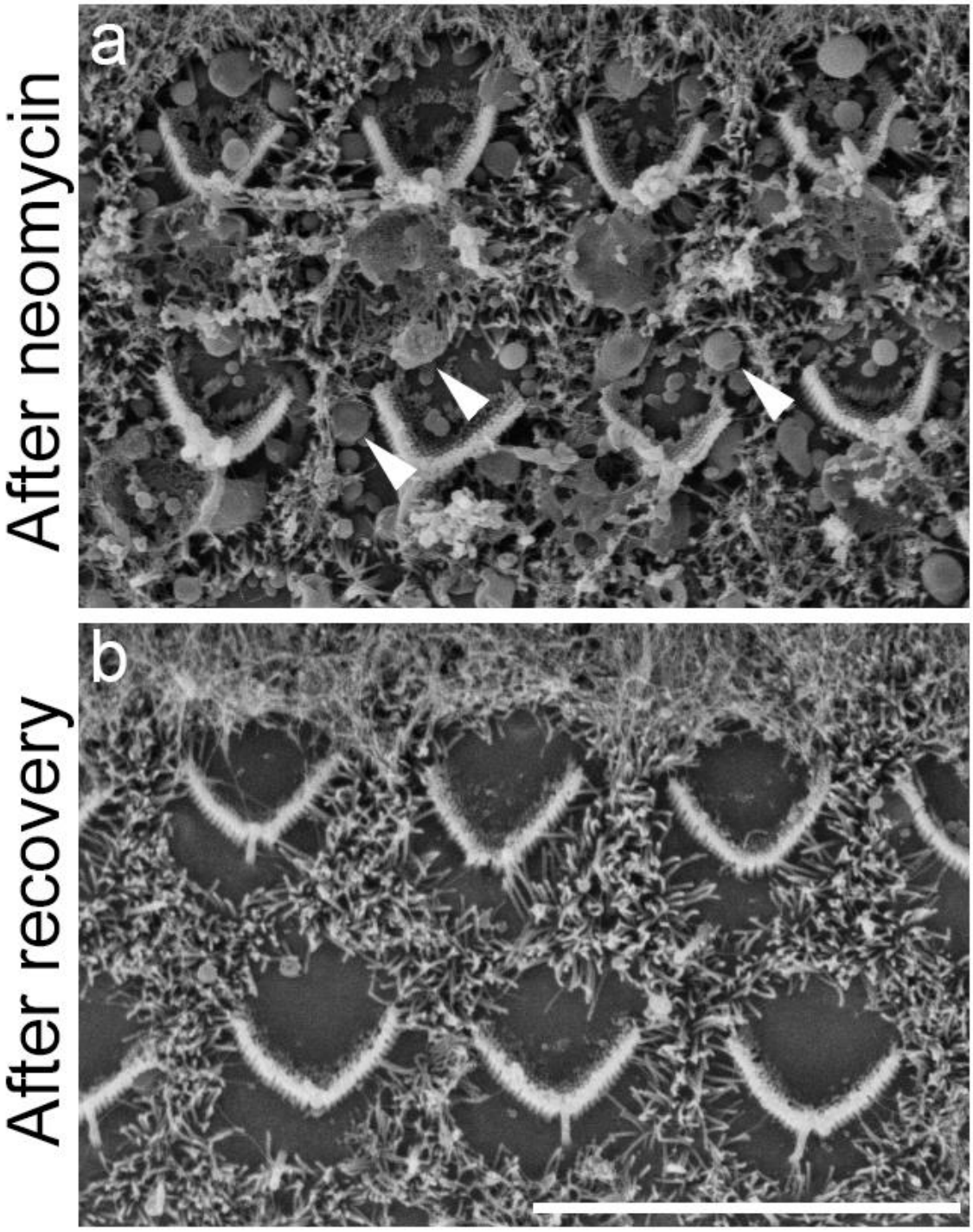

Figure 3.5. SEM images of hair cells in the middle of basal-coil cochlear cultures that were treated with 1 mM neomycin for 15 minutes at 20°C and then fixed (**a**) or treated, washed and allowed to recover for 30 minutes at 37°C before fixation (**b**). Arrowheads indicate membrane blebs on the apical surface of OHCs. Scale bar = 10 µm.

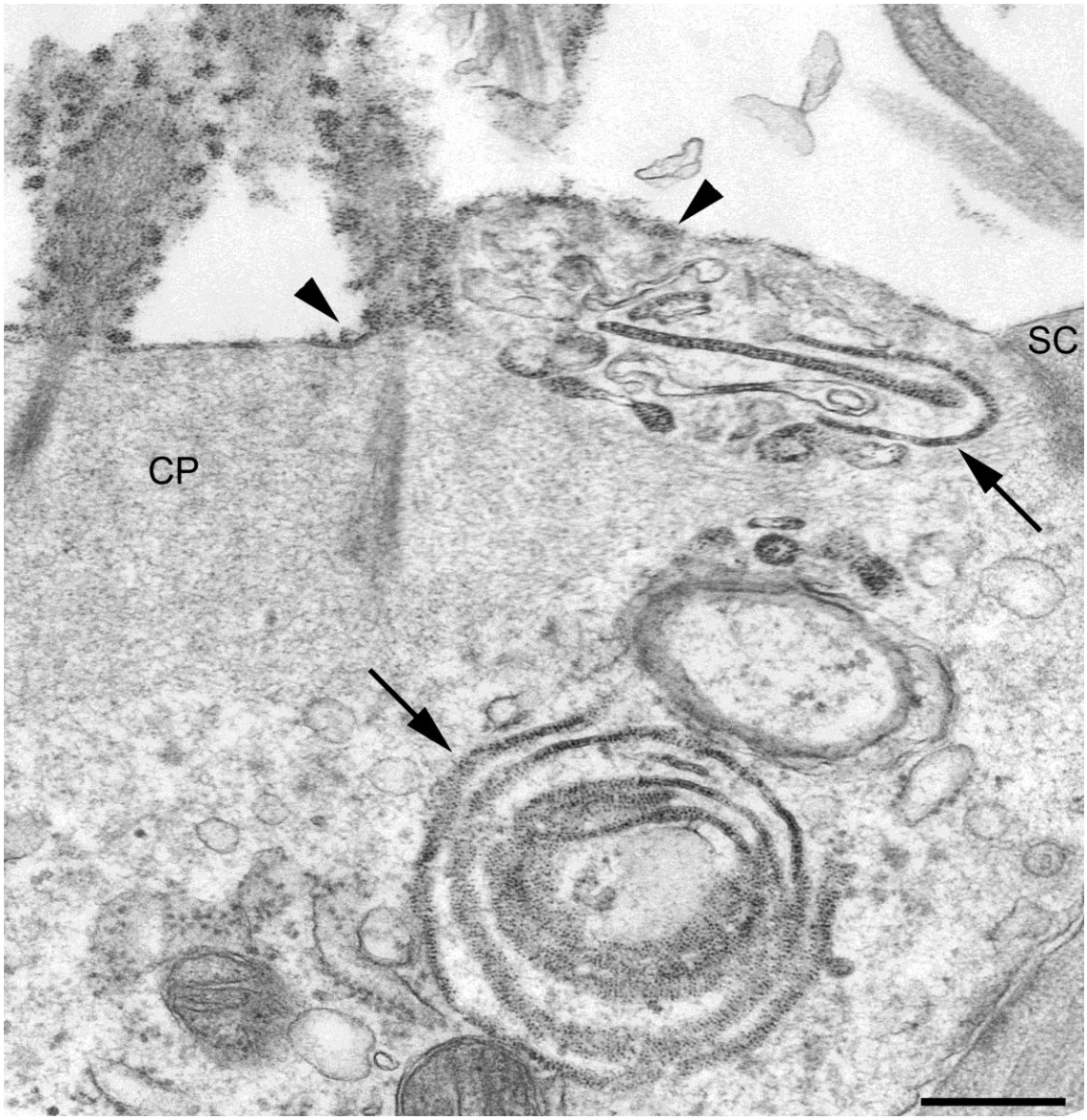

Figure 3.6. TEM image from a hair cell that was labelled with cationic ferritin following treatment with 1 mM neomycin and allowed to recover for 10 minutes. Arrowheads indicate cationic ferritin labelling on the hair cell apical surface and arrows indicate internalised cationic ferritin. SC = supporting cell. CP = cuticular plate. Scale bar = 400 nm.

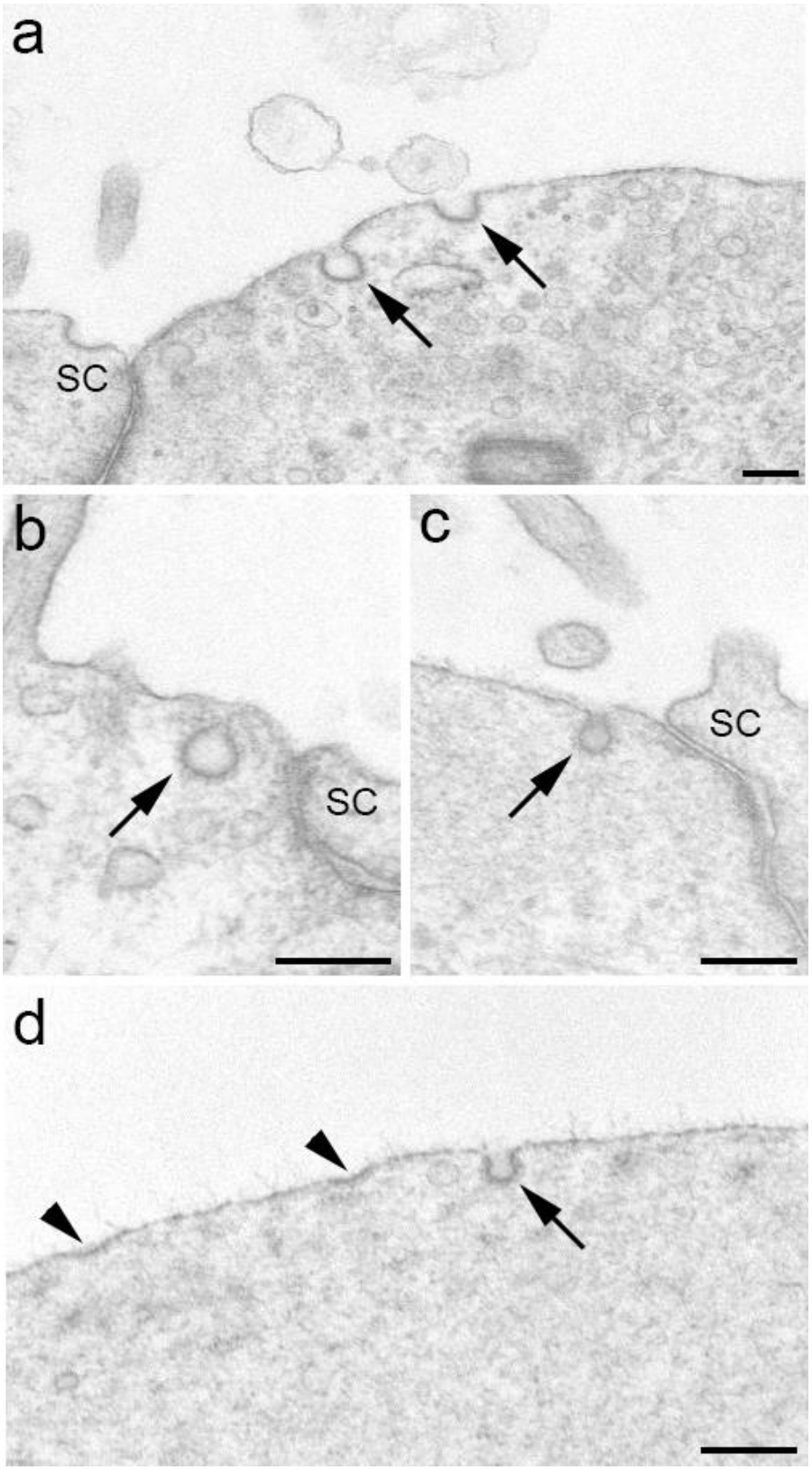

Figure 3.7. TEM images from hair cells treated with 1 mM neomycin and allowed to recover for 10 minutes reveal clathrin-coated pits on the apical surface of OHCs. Arrows indicate coated pits and arrowheads highlight patches of curved coated membrane starting to invaginate. SC = supporting cell. Scale bar = 100 nm (**a**) 200 nm (**b-d**).

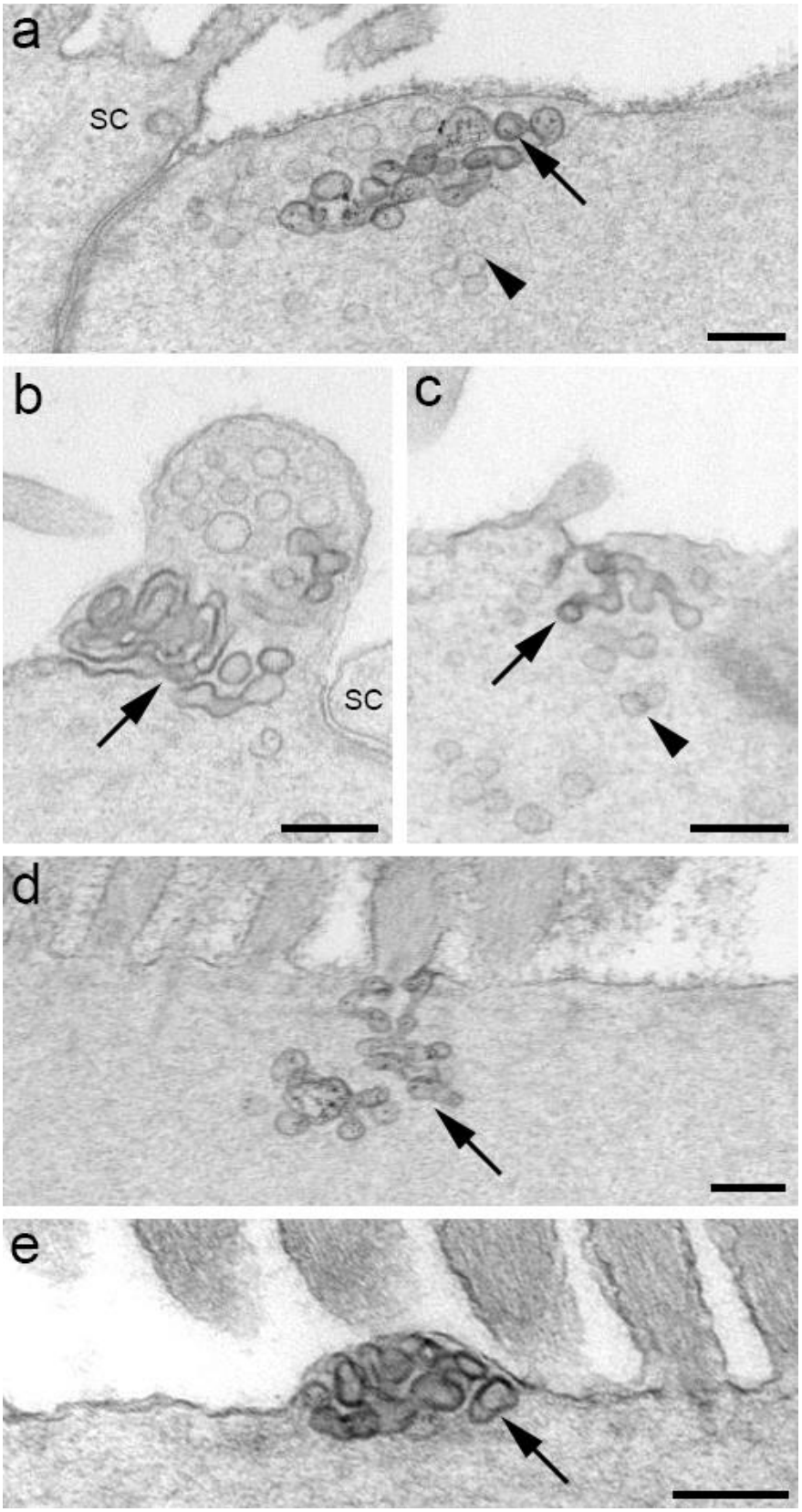

Figure 3.8. Caveolae were seen in TEM images from hair cells labelled with cationic ferritin (**a,d**) or without (**b,c**) following neomycin treatment and allowed to recover for 10 minutes. Caveolae were also observed in cultures not treated with neomycin (**e**). Arrows indicate invaginations, arrowheads show internalised vesicles. SC = supporting cell. Scale bar = 200 nm.

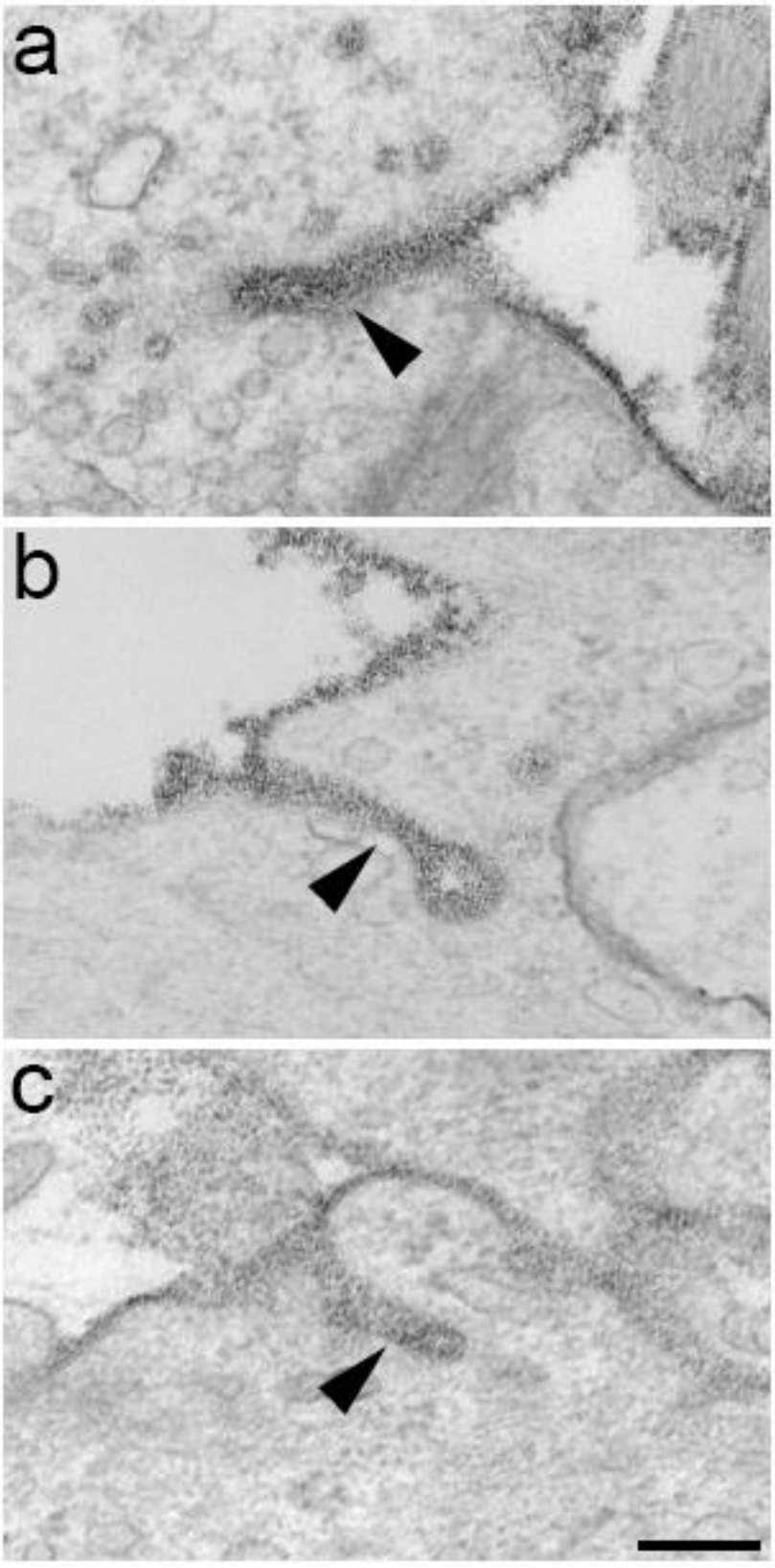

Figure 3.9. TEM images obtained from cultures treated with 1 mM neomycin and labelled with cationic ferritin prior to 10 minutes recovery. Long tubular invaginations typical of the CLIC pathway contained cationic ferritin and were located at the apical pole of OHCs (**a-c**) indicated by arrowheads. Scale bar = 400 nm.

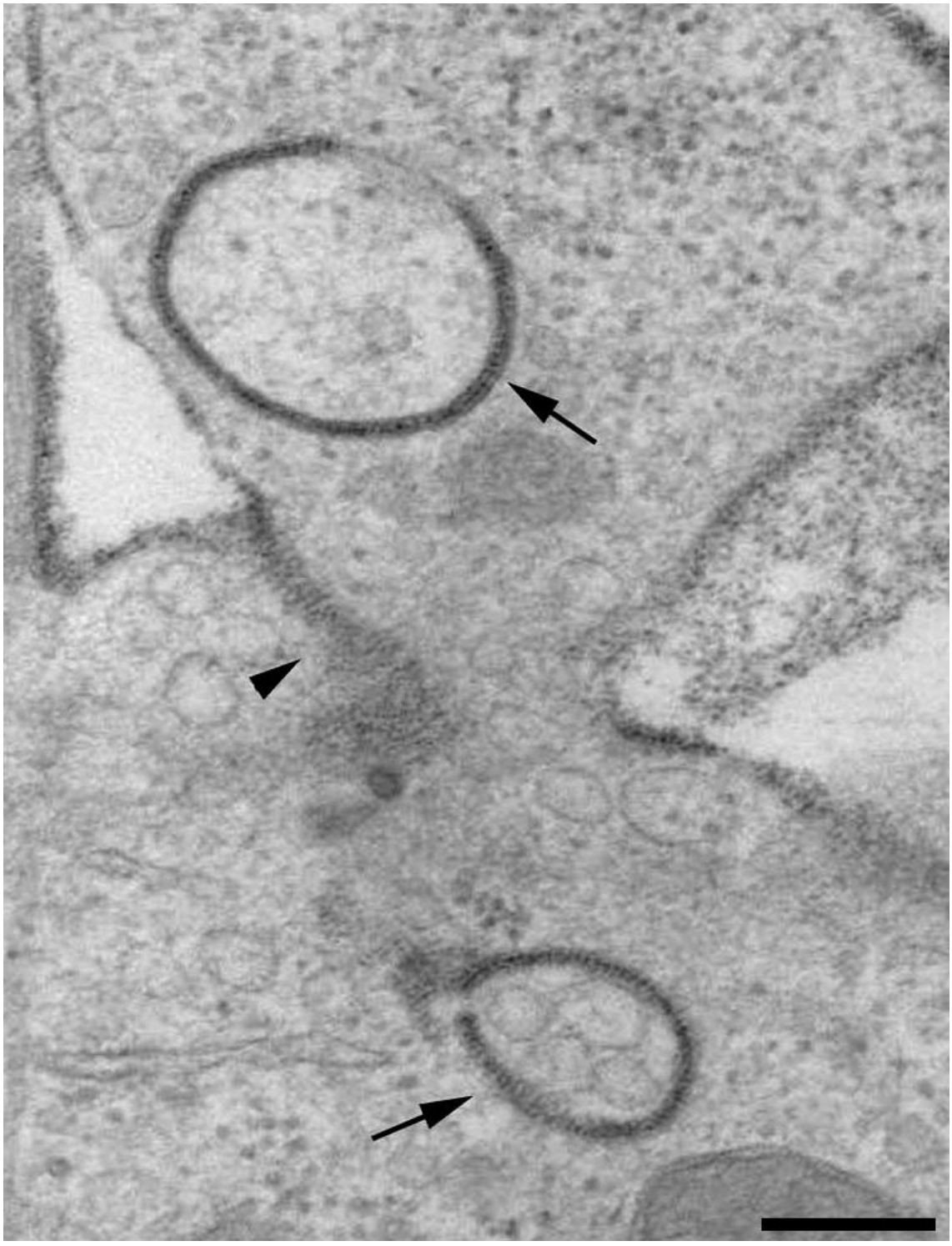

Figure 3.10. TEM image obtained from cultures treated with 1 mM neomycin and labelled with cationic ferritin prior to 10 minutes recovery. Ring-like structures containing cationic ferritin were observed within membrane blebs and beneath the apical surface of hair cells. Arrows highlight ring-like structures, arrowhead indicates a tubular invagination. Scale bar = 200 nm.

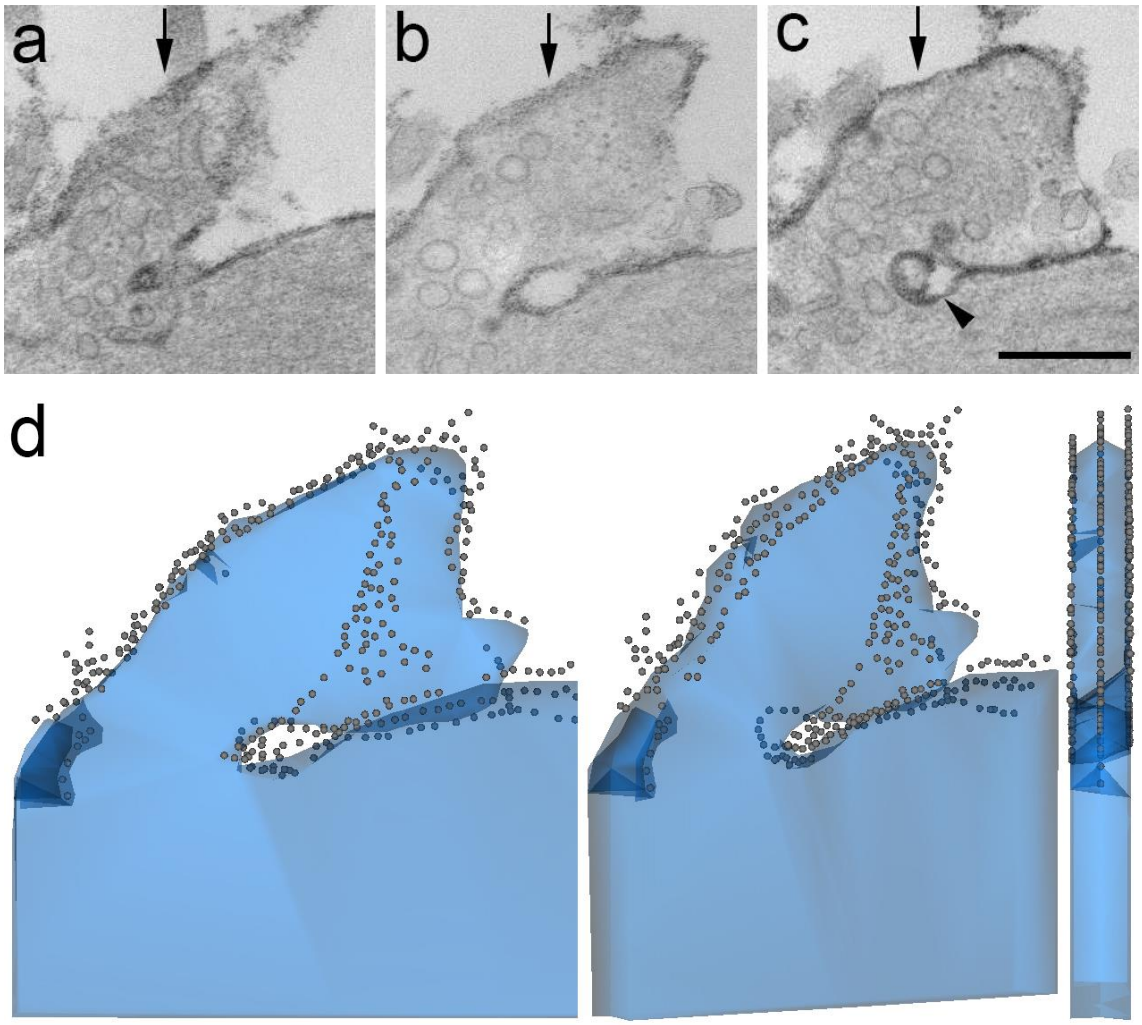

Figure 3.11. Three 100 nm ultrathin serial sections (**a-c**) were collected from cultures that had been treated with 1 mM neomycin, labelled with cationic ferritin and allowed to recover for 10 minutes at 37°C. The three serial sections were used to generate a 3-dimensional reconstruction (**d**). The grey dots represent general localisation of cationic ferritin. The large collapsing membrane protrusion is typical of macropinocytosis. Arrows show the collapsing membrane bleb, arrowhead indicates cationic ferritin trapped between the apical surface of the hair cell and the collapsing bleb. Scale bar = 400 nm.

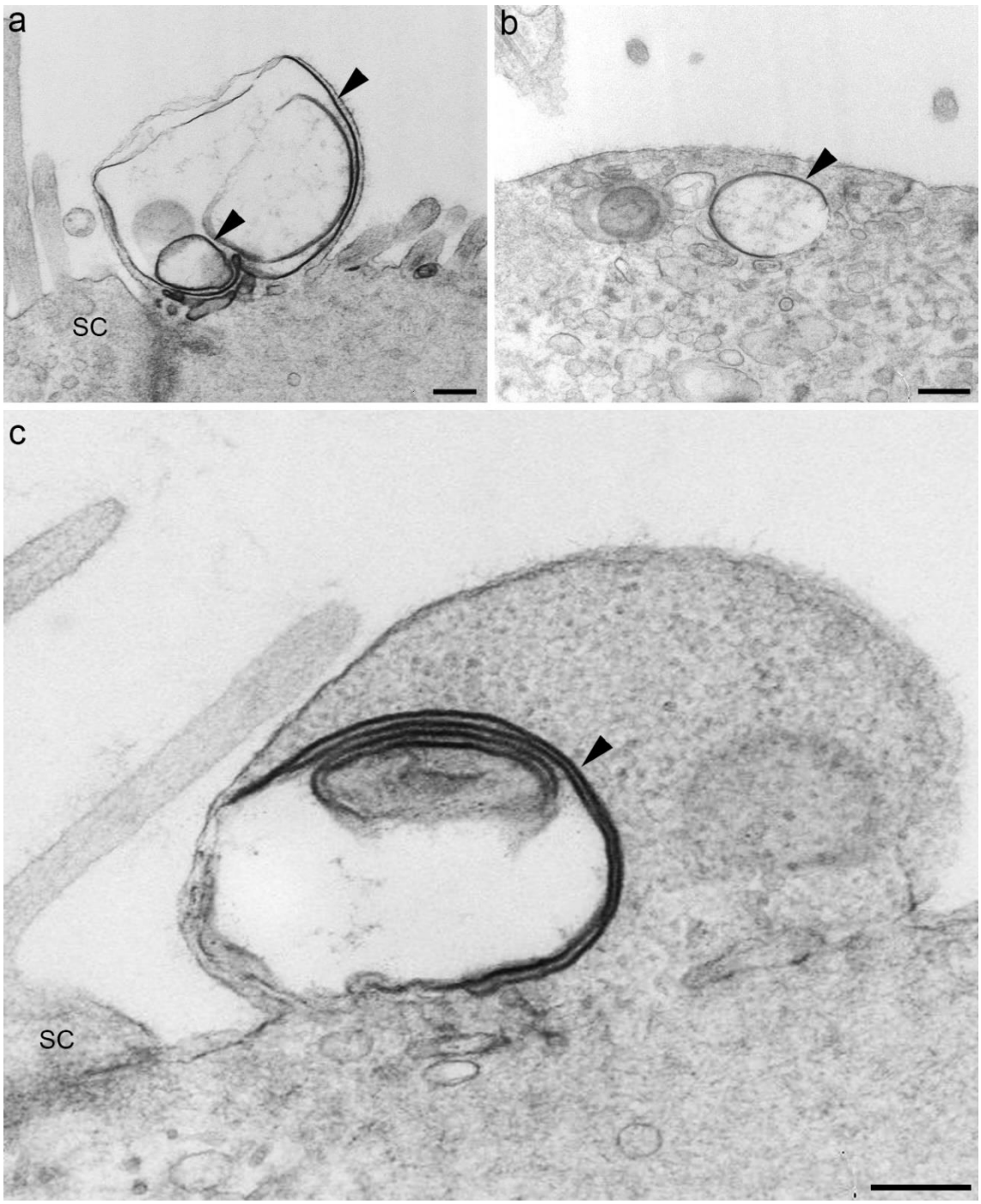

Figure 3.12. TEM images obtained from ultrathin sections of cultures that were treated with 1 mM neomycin for 15 minutes and allowed to recover for 10 minutes. All images (**a-c**) show double membranes (arrowheads) that are within blebs (**a,c**) or just below the apical surface of OHCs (**b**). SC = supporting cell. Scale bars = 200 nm.

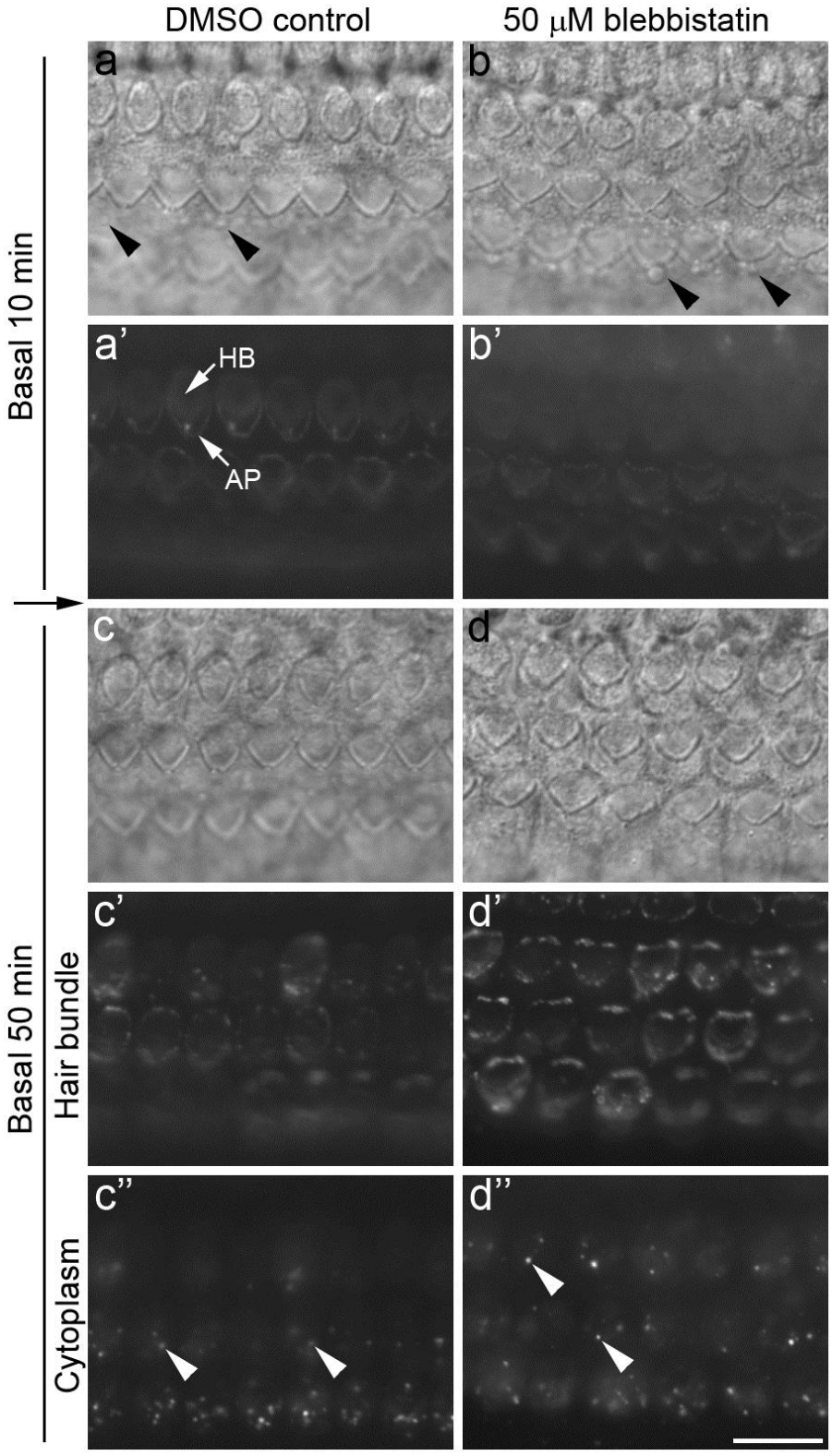

Figure 3.13. Live imaging of hair cells in the middle of basal-coil cochlear cultures that were pre-incubated in RCM containing DMSO as a control or 50 μM blebbistatin for 1 hour, washed, and treated with 1 mM neomycin for 15 minutes in the presence of annexin V-488 (**a-b**), washed again and allowed to recover for 30 minutes in RCM containing DMSO as a control (**c-c''**) or 5 μM blebbistatin (**d-d''**). Black arrow represents 30 minutes recovery, black arrowheads indicate membrane blebs, and white arrowheads indicate internalised annexin V-488 punctae. HB = hair bundle, AP = apical perimeter. Scale bar = 10 μm.

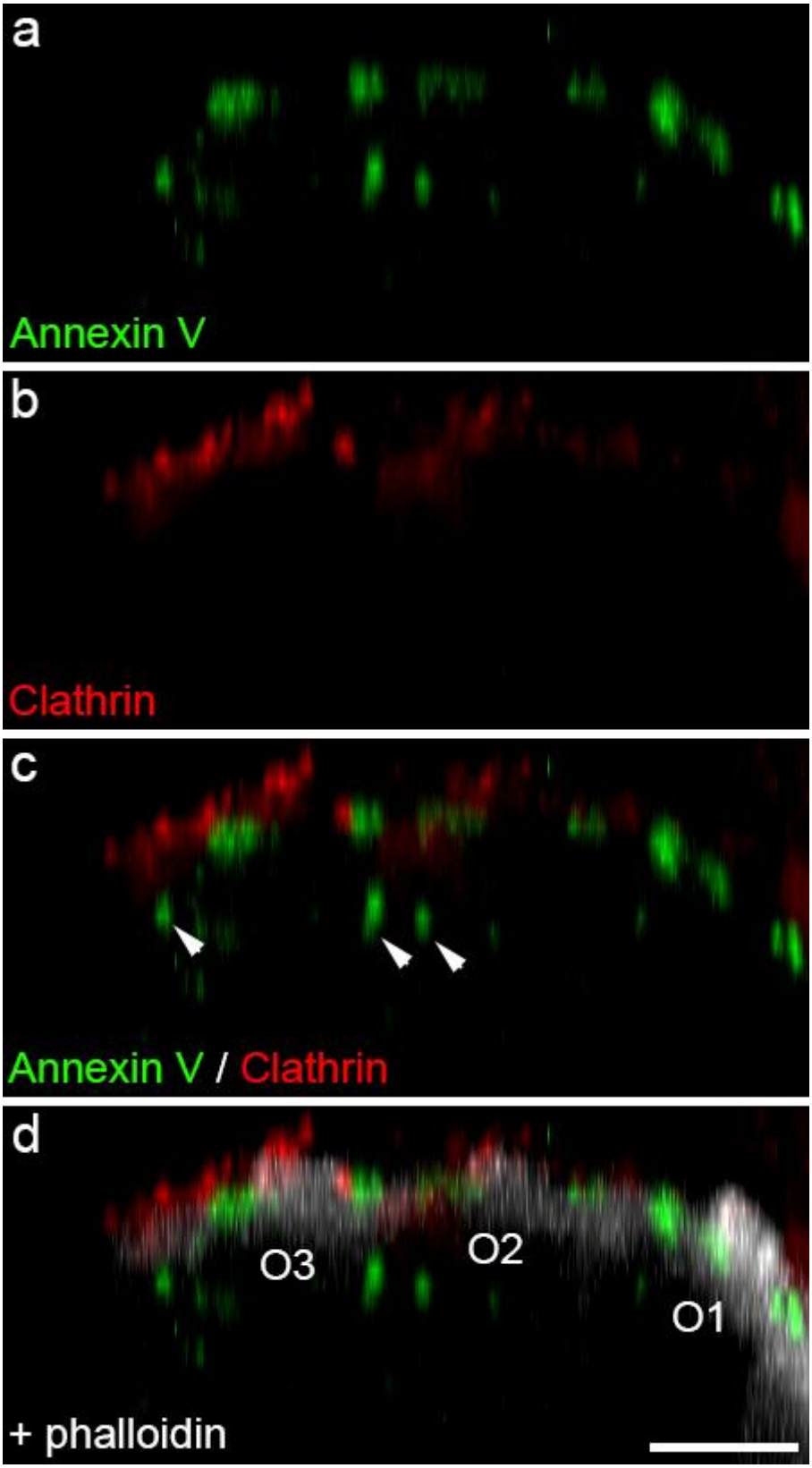

Figure 3.14. Orthogonal z-projections from confocal stacks obtained from hair cells in the middle of basal-coil cochlear cultures that were treated with 1 mM neomycin in the presence of annexin V-488 for 15 minutes, washed and allowed to recover for 10 minutes. After fixation cultures were labelled with antibodies to clathrin and Texas Red phalloidin. Arrowheads indicate internalised annexin V-488. Scale bar = 5 µm.

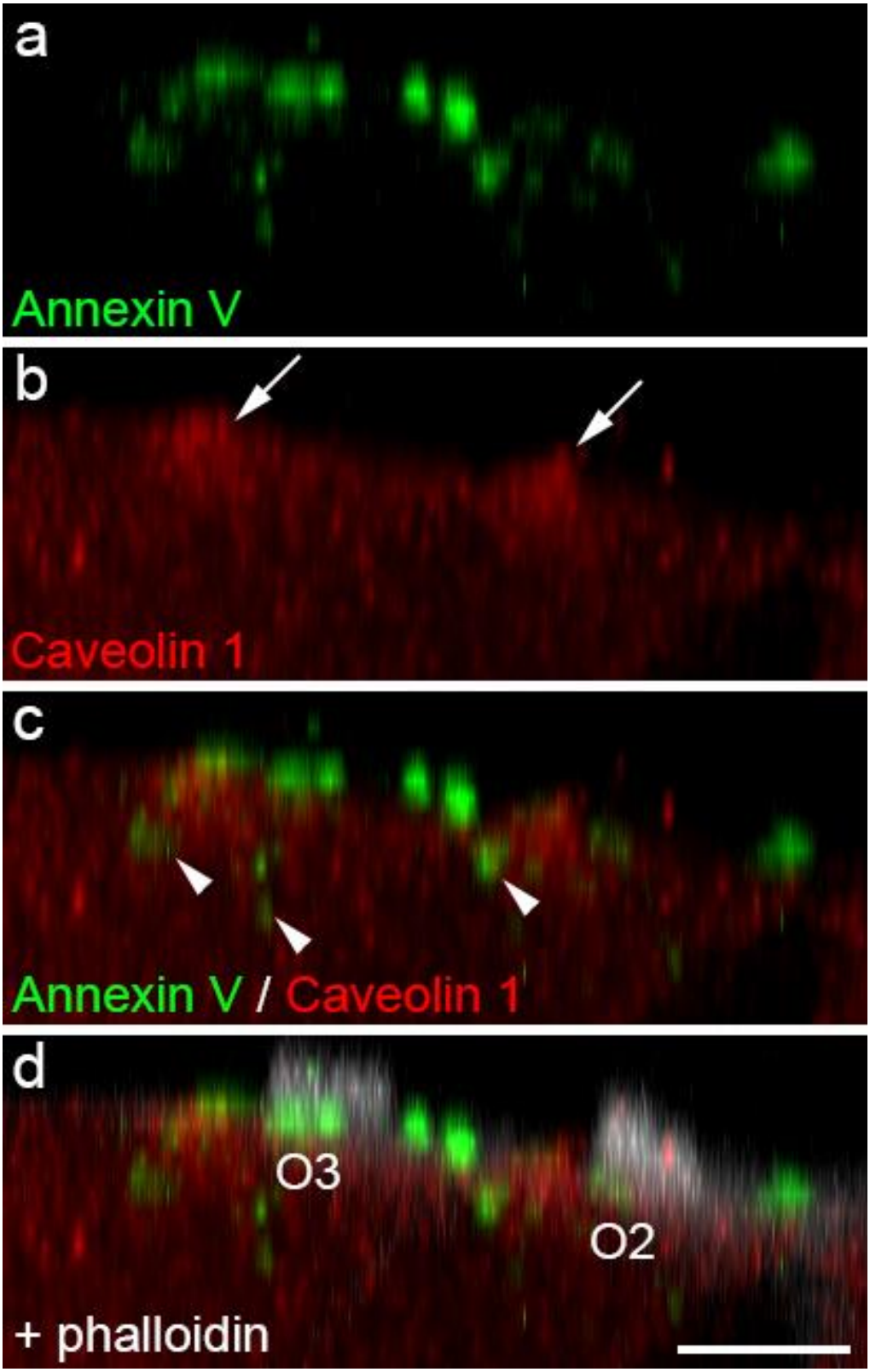

Figure 3.15. Orthogonal z-projections from confocal stacks obtained from hair cells in the middle of basal-coil cochlear cultures that were treated with 1 mM neomycin for 15 minutes in the presence of annexin V-488, washed and allowed to recover for 10 minutes. After fixation cultures were labelled with antibodies to caveolin 1 and Texas Red phalloidin. Arrowheads indicate internalised annexin V-488 and white arrows highlight condensed areas of caveolin 1 antibody labelling. Scale bar = 5 µm.

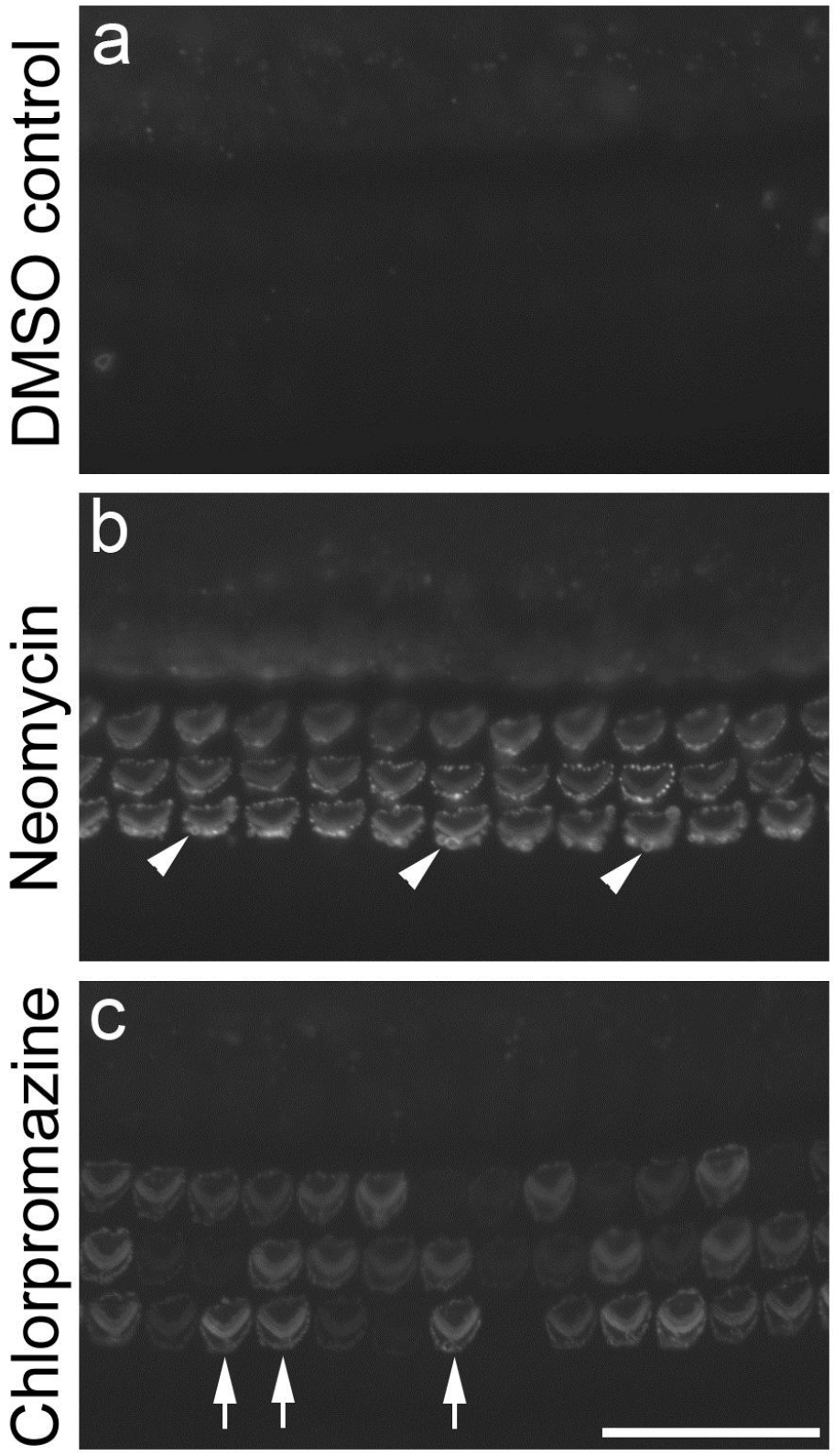

Figure 3.16. Live cell imaging of hair cells in the middle of basal-coil cochlear cultures that were labelled with annexin V-488 and treated with DMSO as a control (**a**), 1 mM neomycin (**b**) or 12.5 µm CPZ (**c**) in RCM at 37°C for 15 minutes. Images were taken 10 minutes after the addition of DMSO, neomycin or chlorpromazine. Arrowheads indicate annexin V-488 positive blebs, arrows indicate annexin V-488 labelling in response to chlorpromazine. Scale bar = 20 µm.

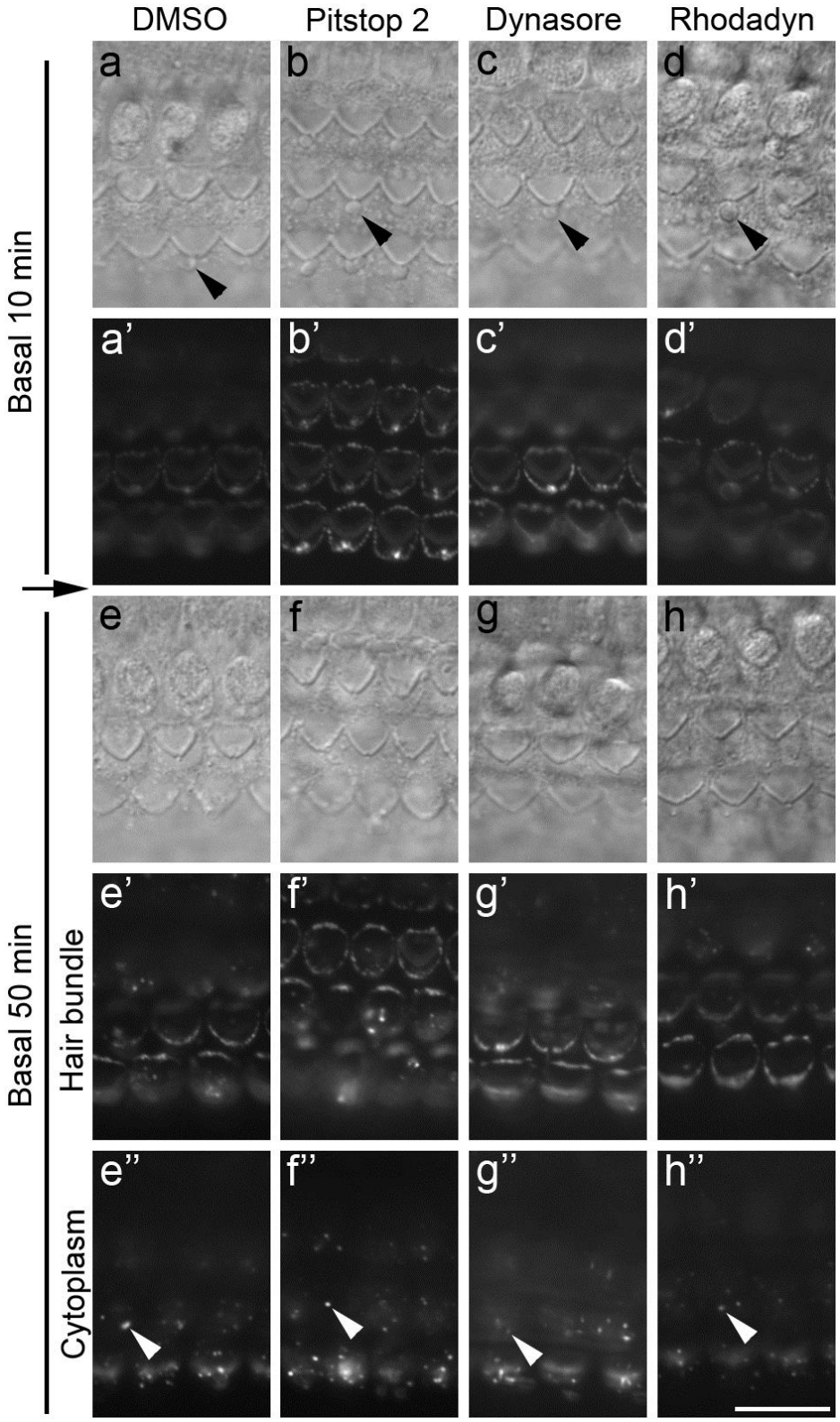

Figure 3.17. Live imaging of hair cells in the middle of basal-coil cochlear cultures that were treated with 1 mM neomycin for 15 minutes in the presence of annexin V-488 (**a-d**), washed and allowed to recover for 30 minutes in RCM containing DMSO as a control (**e-e''**), 60 µM Pitstop 2 (**f-f''**), 100 µM dynasore (**g-g''**) or 70 µM rhodadyn (**h-h''**). Black arrow represents 30 minutes recovery, black arrowheads indicate membrane blebs, and white arrowheads indicate internalised annexin V-488 punctae. Scale bar = 10 µm.

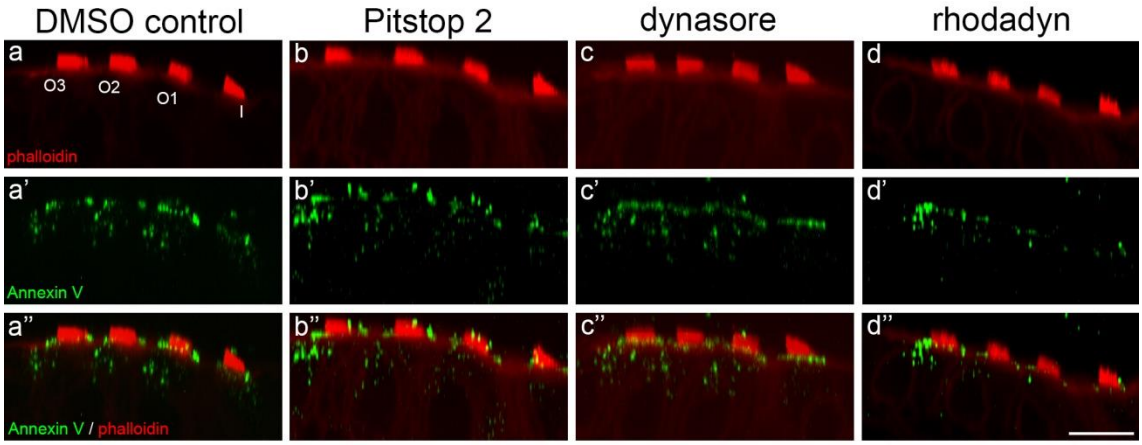

Figure 3.18. Orthogonal z-projections from confocal stacks obtained from hair cells in the middle of basal-coil cochlear cultures that were treated with 1 mM neomycin in the presence of annexin V-488 for 15 minutes, washed and allowed to recover for 30 minutes in RCM containing DMSO as a control (**a-a''**), 60 µM Pitstop 2 (**b-b''**), 100 µM dynasore (**c-c''**) or 70 µM rhodadyn (**d-d''**). After fixation cultures were double labelled with Texas Red phalloidin. Scale bar = 10 µm.

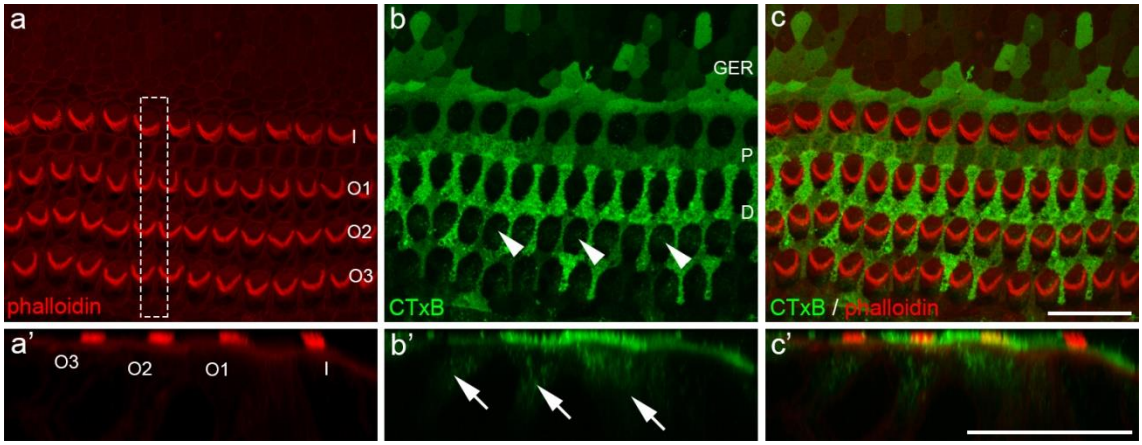

Figure 3.19. Confocal images from confocal stacks obtained from hair cells in the middle of apical-coil cochlear cultures that were labelled with CTxB 488 for 10 minutes at 20°C, fixed and double labelled with Texas Red phalloidin. CTxB 488 labels cells of the greater epithelial ridge, pillar cells and Deiters cells (**b,c**). A small amount of CTxB labelled the apical surface of OHCs, indicated by arrowheads (**b,c**). CTxB labelling was seen within the cytoplasm of supporting cells indicated by arrows (**b'**). I= IHCs, O1, O2 and O3= OHCs, GER= greater epithelial ridge, P= pillar cells, D= Deiters cells. Scale bar = 20 µm.

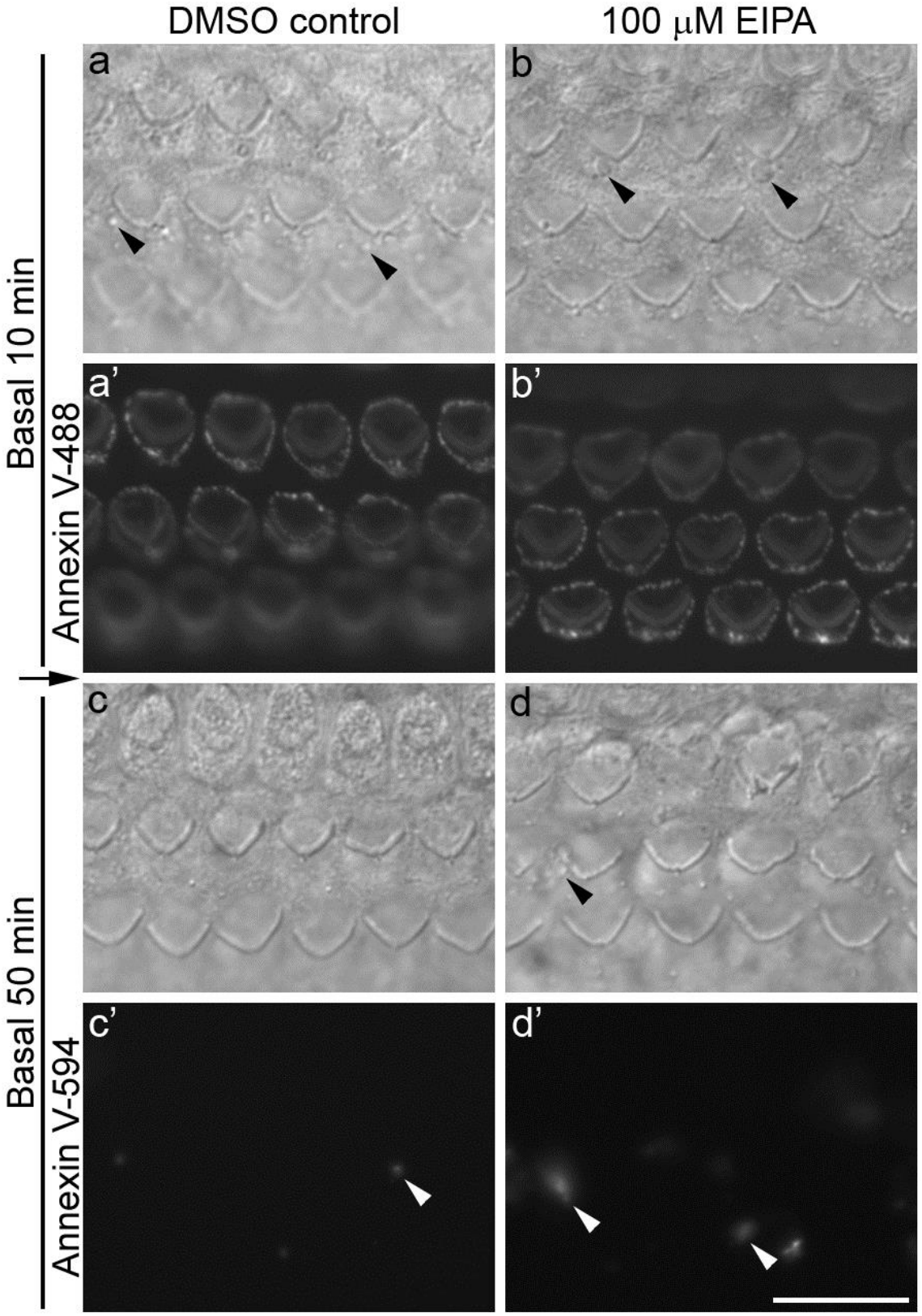

Figure 3.20. Live imaging from hair cells in the middle of basal-coil cochlear cultures treated with 1 mM neomycin for 15 minutes in the presence of annexin V-488 (**a-b'**), washed and allowed to recover for 30 minutes in RCM containing DMSO as a control or 100 μM EIPA (**c-d'**). Cultures were washed again and labelled with annexin V-594. Black arrow represents 30 minutes recovery, black arrowheads indicate membrane blebs and white arrowheads indicate annexin V-594 labelling. Scale bar = 10 μm.

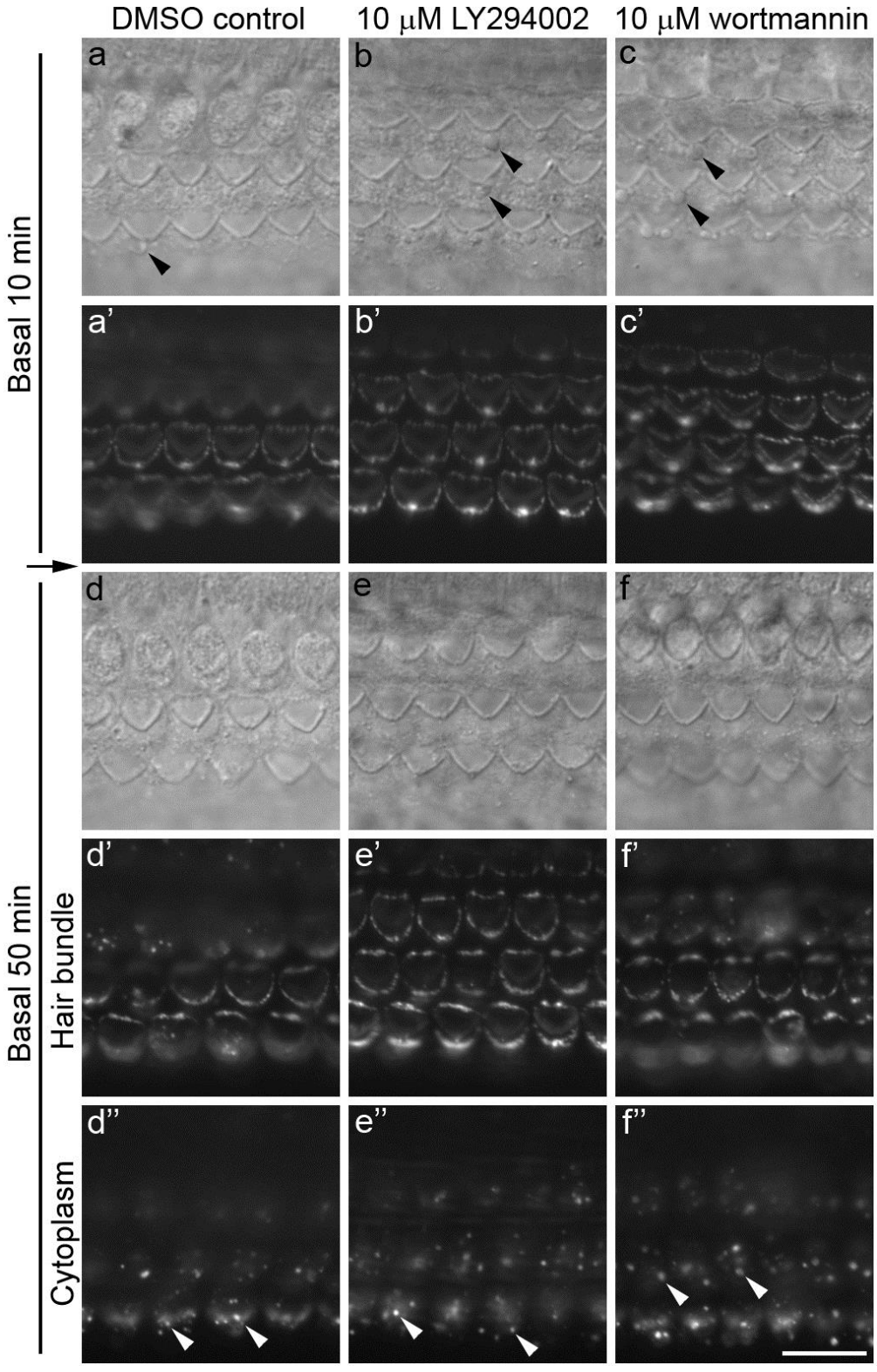

Figure 3.21. Live imaging of hair cells in the middle of basal-coil cochlear cultures that were pre-incubated in RCM with DMSO, 10 μM LY294002 or 10 μM wortmannin for 1 hour, washed and treated with 1 mM neomycin for 15 minutes in the presence of annexin V-488 (**a-c'**), washed and allowed to recover for 30 minutes in RCM containing DMSO as a control (**d-d''**), LY294002 (**e-e'**) or wortmannin (**f-f'**). Black arrow represents 30 minutes recovery, black arrowheads indicate blebs and white arrowheads indicate internalised annexin V-488 punctae. Scale bar = 10 μm.

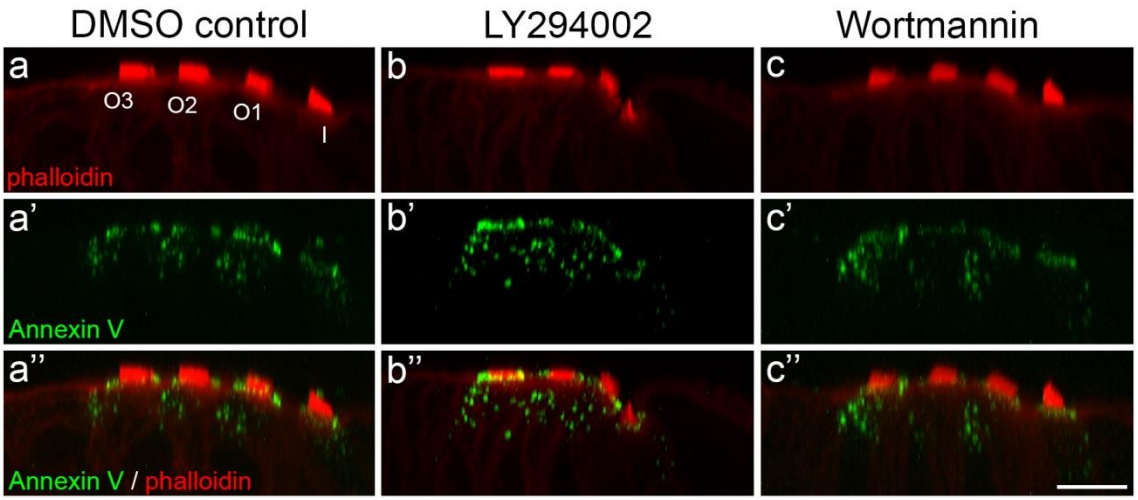

Figure 3.22. Orthogonal z-projections from confocal stacks obtained from hair cells in the middle of basal-coil cochlear cultures that were pre-incubated in RCM containing DMSO, 10 µM LY294002 or 10 µM wortmannin for 1 hour, washed and treated with neomycin for 15 minutes in the presence of annexin V-488, washed again and allowed to recover for 30 minutes in RCM containing DMSO as a control (**a-a''**), LY294002 (**b-b''**) or wortmannin (**c-c''**). After fixation cultures were double labelled with Texas Red phalloidin. Scale bar = 10 µm.

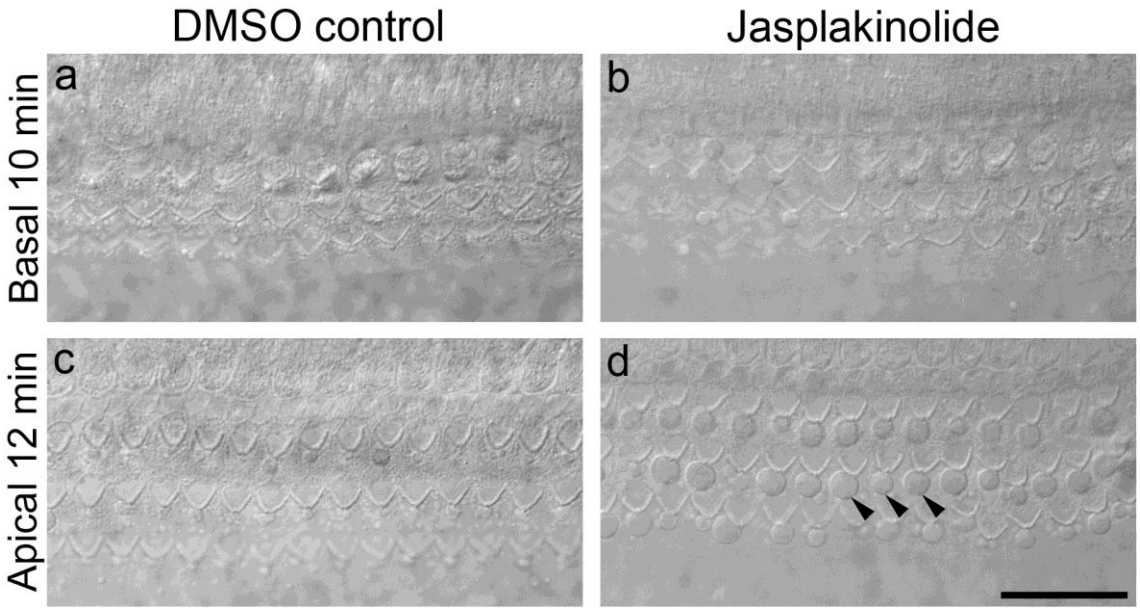

Figure 3.23. Live imaging of hair cells in the middle of basal-coil and apical-coil cochlear cultures that were pre-incubated in RCM containing DMSO or 5 µM jasplakinolide for 1 hour, washed and treated with 1 mM neomycin in the presence of DMSO or jasplakinolide (**a-d**). Membrane blebs were larger in cultures treated with jasplakinolide when compared to controls. Arrowheads indicate large membrane blebs present in the kinocilial region. Scale bar = 20 µm.

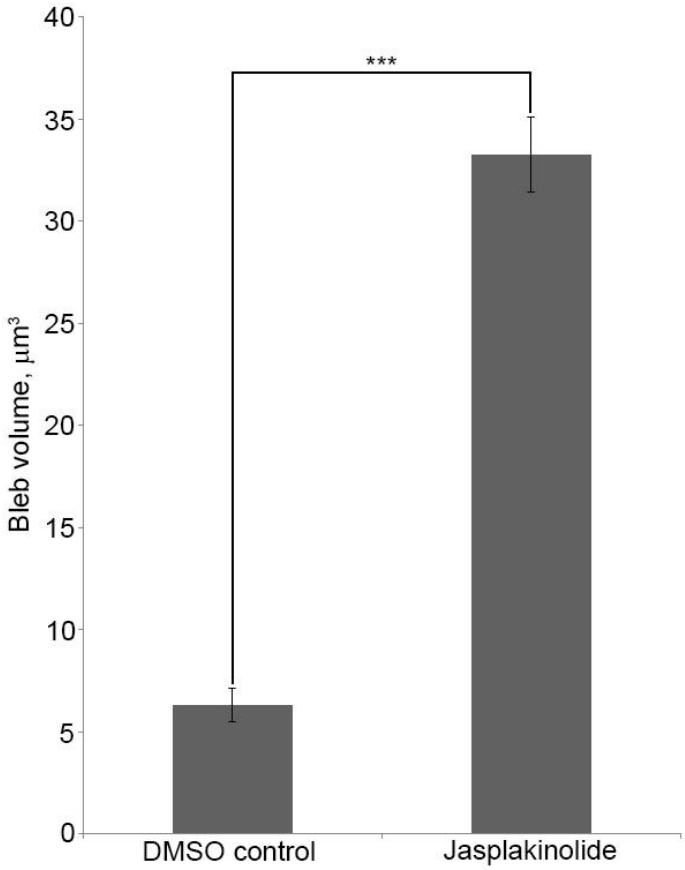

Figure 3.24. Quantification of membrane bleb volume from hair cells in cochlear cultures pre-incubated for 1 hour in RCM containing DMSO or 5 µM jasplakinolide, washed and treated with 1 mM neomycin in the presence of DMSO or jasplakinolide. Membrane blebs were significantly larger in the jasplakinolide treated cultures when compared to controls. *** Indicates a significant difference of $p < 0.001$. The statistical test used was an unpaired t test. Error bars represent SEM.

Number of OHCs measured:

DMSO control n = 98 OHCs (mean = 6.29 μm^3, SEM ± 0.82).

5 µM Jasplakinolide n = 213 OHCs (mean = 33.27 μm^3, SEM ± 1.82).

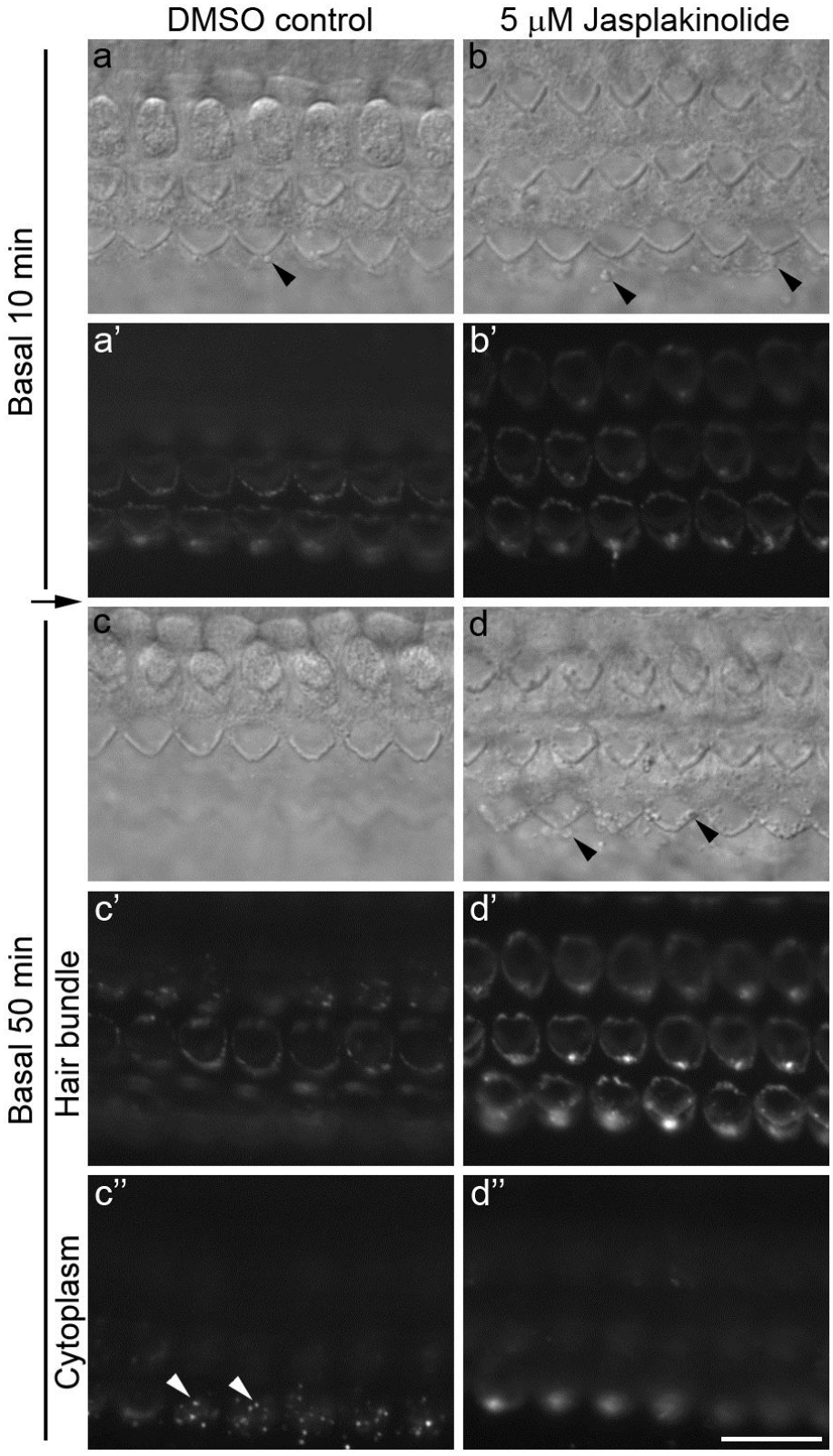

Figure 3.25. Live imaging of hair cells in the middle of basal-coil cochlear cultures that were pre-incubated in RCM containing DMSO or 5 μM jasplakinolide, washed and treated with 1 mM neomycin for 15 minutes in the presence of annexin V-488 (**a-b'**), washed again and allowed to recover for 30 minutes in RCM containing DMSO (**c'-c''**) or jasplakinolide (**d'-d''**). Black arrow represents 30 minutes recovery, black arrowheads indicate blebs and white arrowheads indicate internalised annexin V-488 punctae. Scale bar = 10 μm.

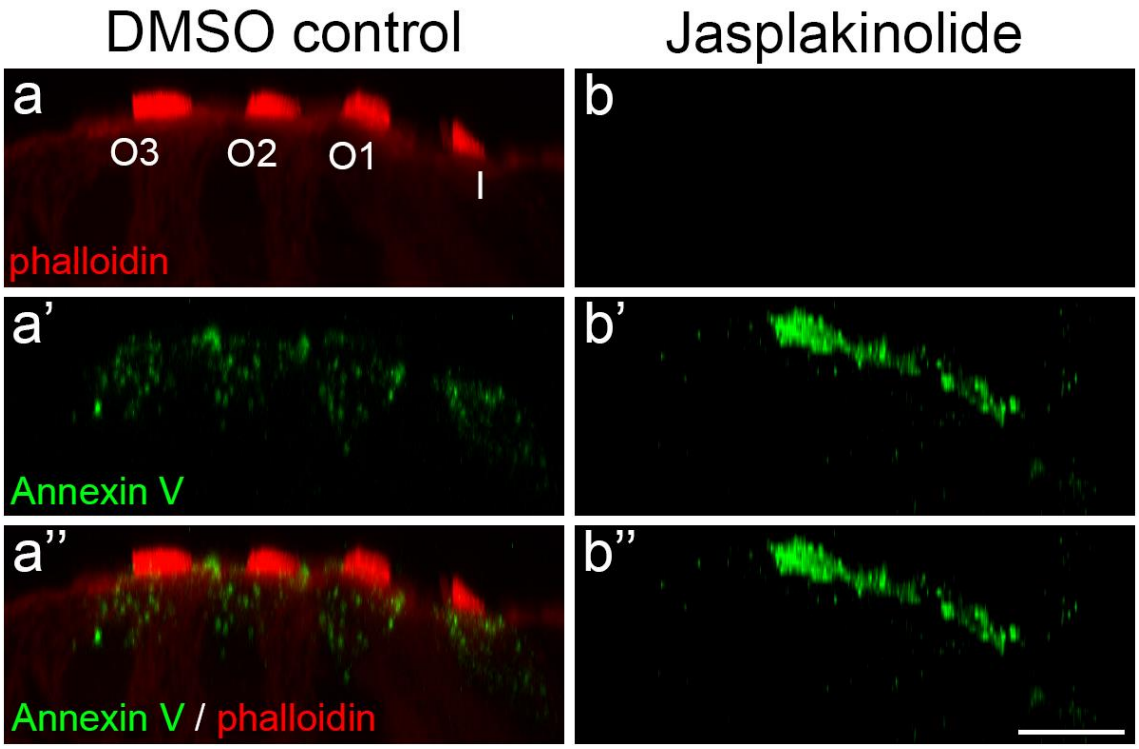

Figure 3.26. Orthogonal z-projections from confocal stacks obtained from the hair cells in the middle of basal-coil cochlear cultures that were pre-incubated in RCM containing DMSO or 5 µM jasplakinolide, washed and treated with 1 mM neomycin for 15 minutes in the presence of annexin V-488, washed again and allowed to recover for 30 minutes in RCM containing DMSO (**a-a''**) or jasplakinolide (**b-b''**). After fixation cultures were double labelled with Texas Red phalloidin. Scale bar = 10 µm.

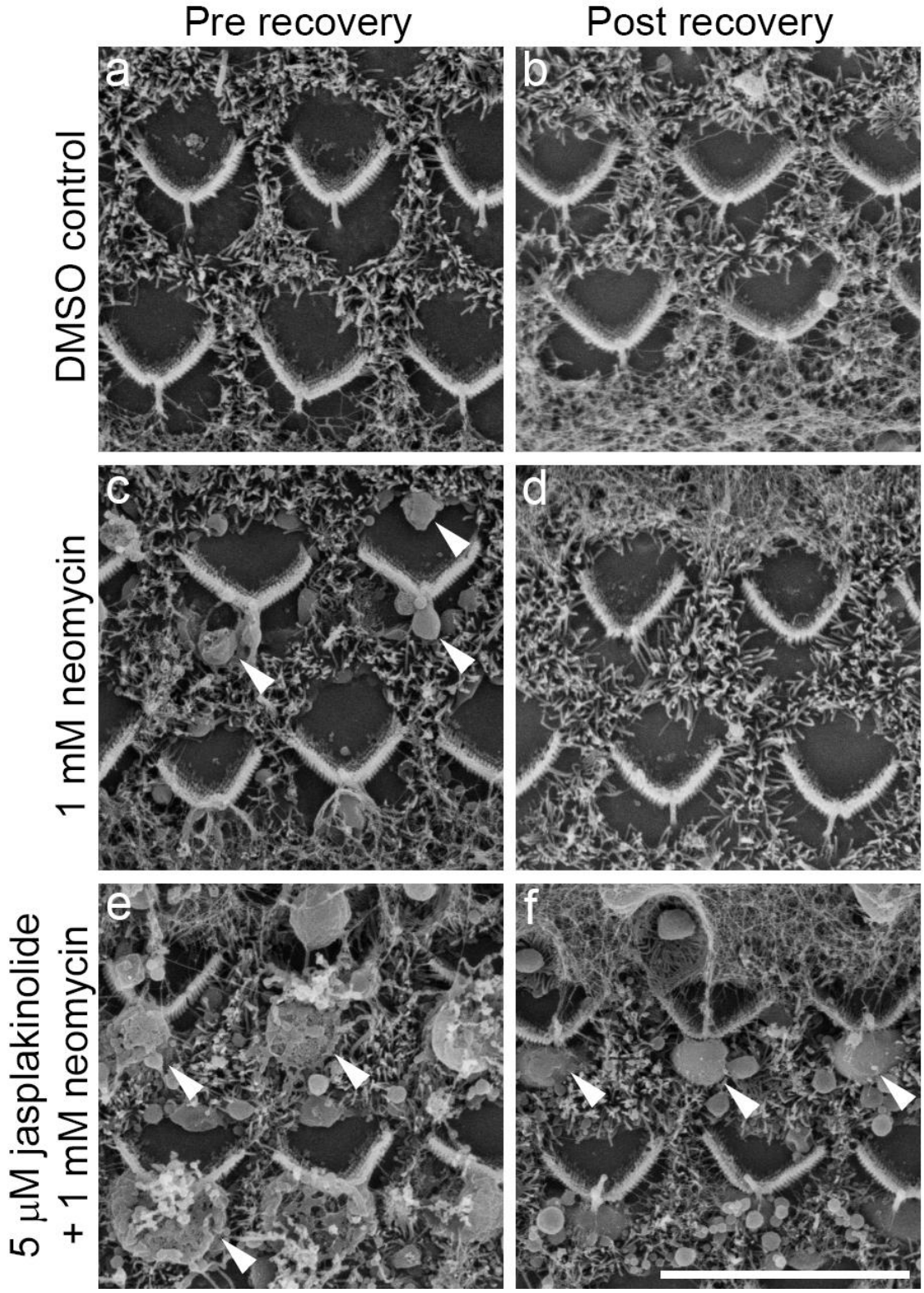

Figure 3.27. SEM images of hair cells in the middle of basal-coil cochlear cultures that were treated with DMSO as a control (**a**), 1 mM neomycin (**c**) or 1 mM neomycin and 5 µM jasplakinolide (**e**) for 15 minutes, washed and allowed to recover for 30 minutes in RCM containing DMSO (**b,d**) or jasplakinolide (**f**). White arrowheads indicate membrane blebs. Scale bar = 10 µm.

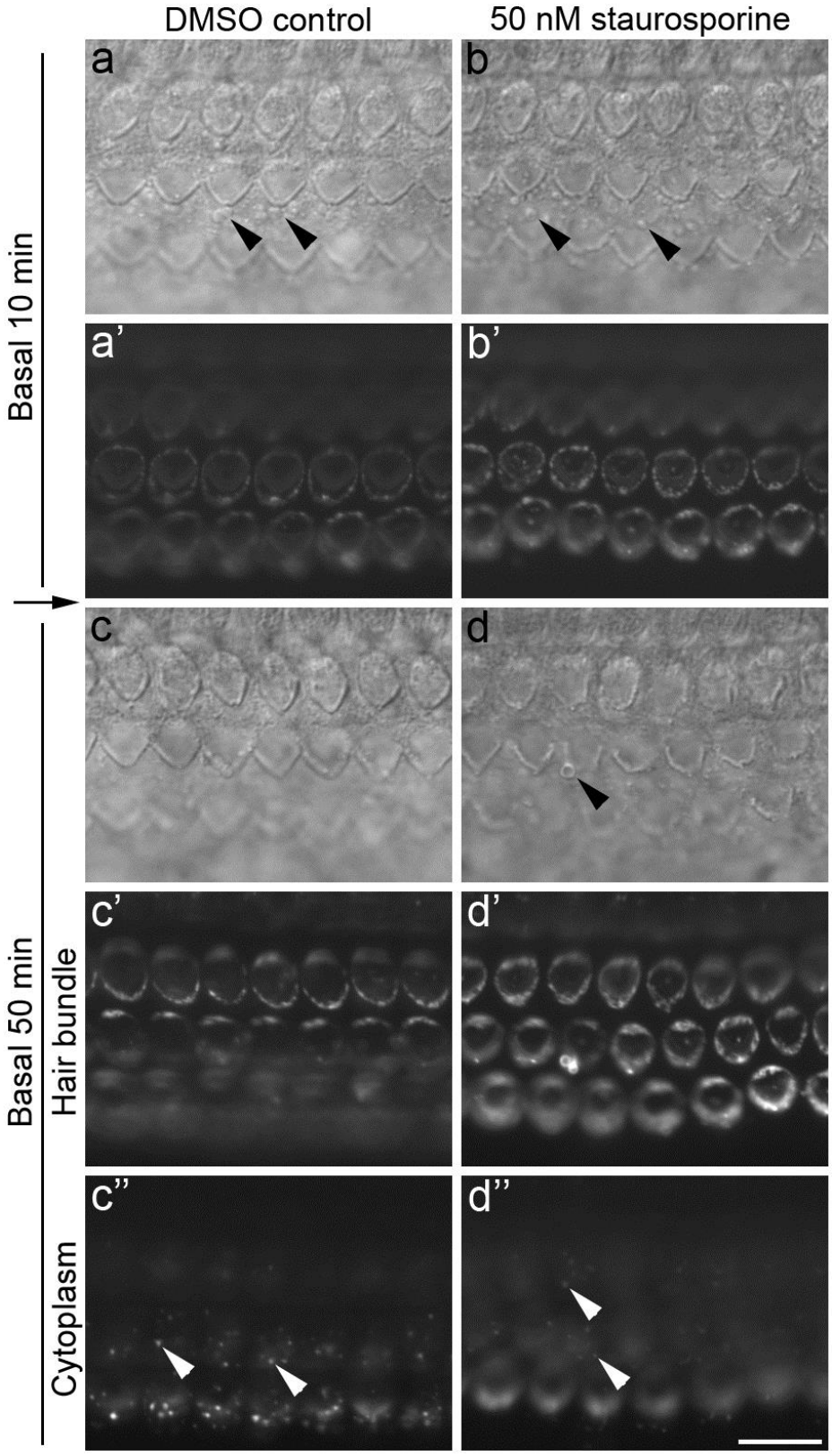

Figure 3.28. Live imaging of hair cells in the middle of basal-coil cochlear cultures that were pre-incubated in RCM containing DMSO or 50 nM staurosporine, washed and treated with 1 mM neomycin for 15 minutes in the presence of annexin V-488 (**a-b'**), washed again and allowed to recover for 30 minutes in RCM containing DMSO (**c'-c''**) or 50 nM staurosporine (**d'-d''**). Black arrow represents 30 minutes recovery, black arrowheads indicate blebs and white arrowheads indicate internalised annexin V-488 punctae. Scale bar = 10 µm.

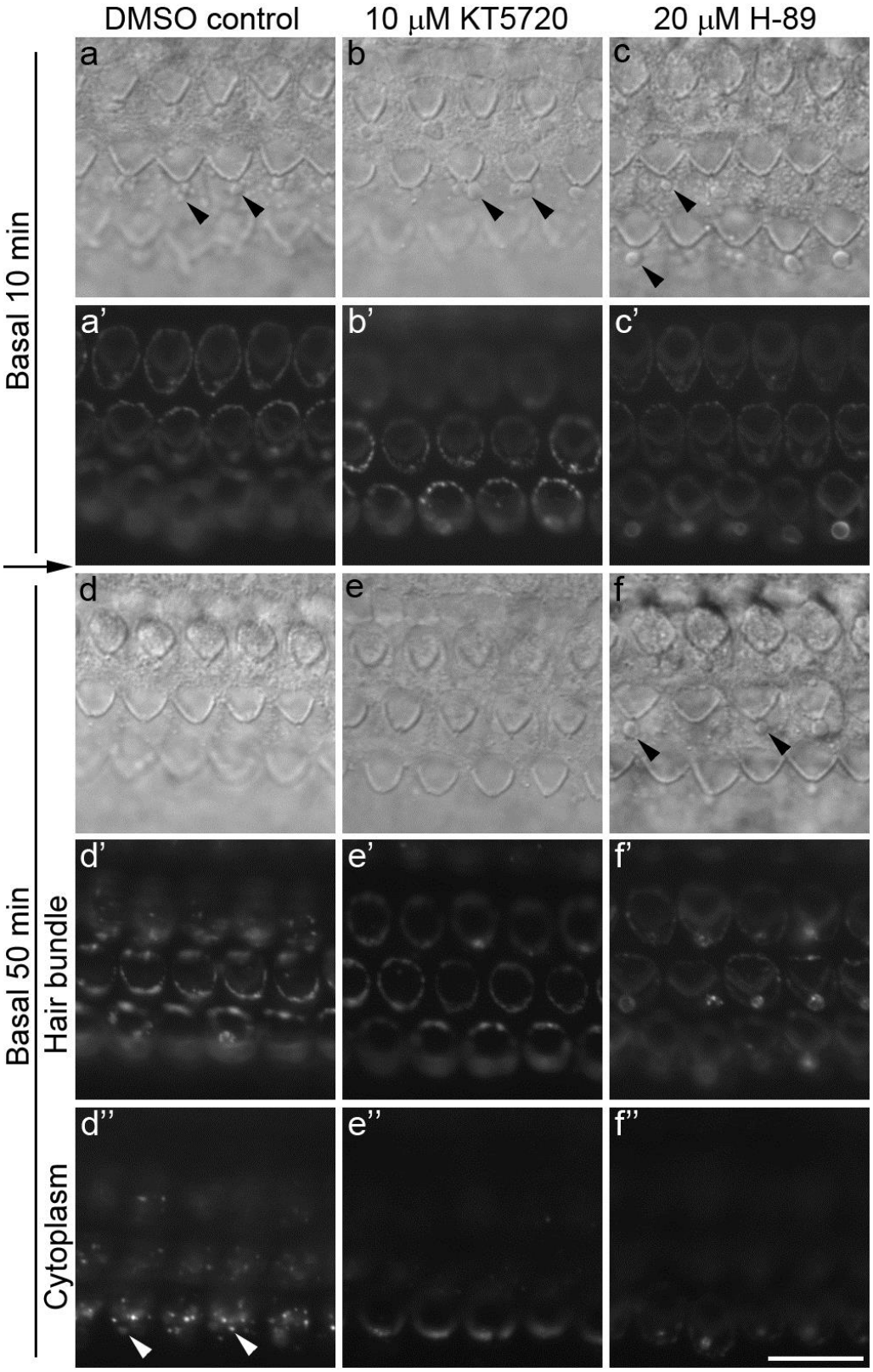

Figure 3.29. Live imaging of hair cells in the middle of basal-coil cochlear cultures that were pre-incubated in RCM containing DMSO, 10 μM KT5720 or 20 μM H-89, washed and treated with 1 mM neomycin for 15 minutes in the presence of annexin V-488 (**a-c'**), washed again and allowed to recover for 30 minutes in RCM containing DMSO as a control (**d-d''**), KT5720 (**e-e''**) or H-89 (**f-f''**). Black arrow represents 30 minutes recovery, black arrowheads indicate blebs and white arrowheads indicate internalised annexin V-488 punctae. Scale bar = 10 μm.

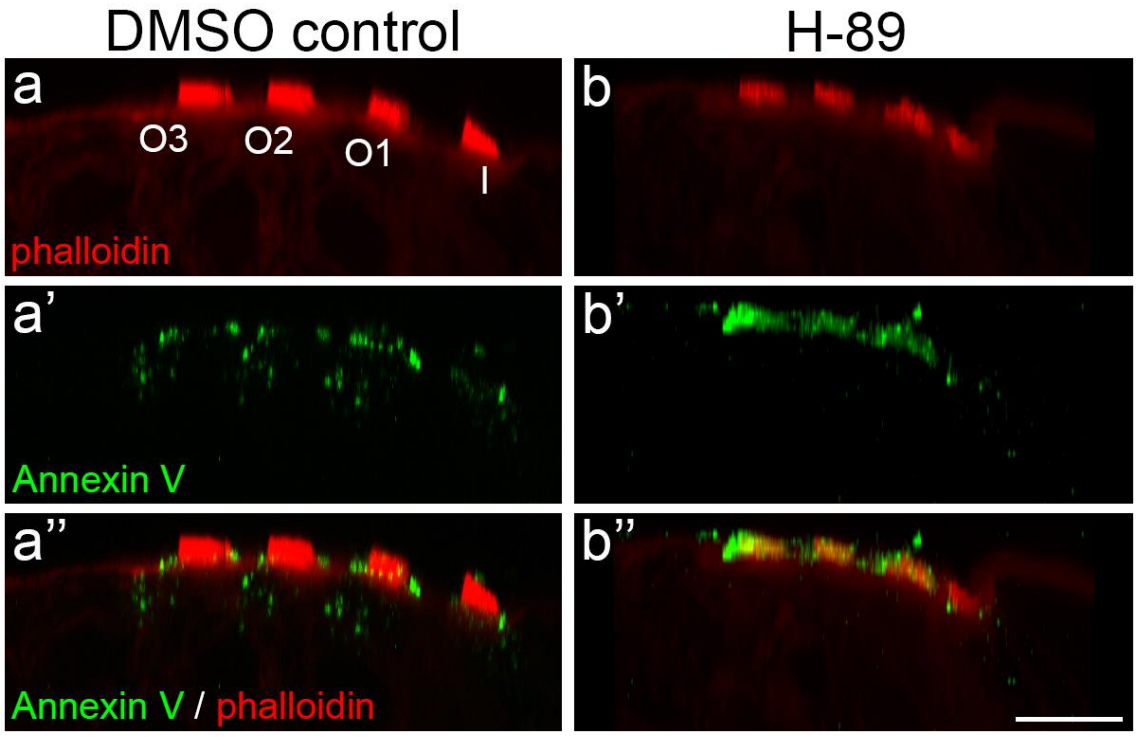

Figure 3.30. Orthogonal z-projections from confocal stacks obtained from hair cells in the middle of basal-coil cochlear cultures that were pre-incubated in RCM containing DMSO or 20 µM H-89, washed and treated with 1 mM neomycin for 15 minutes in the presence of annexin V-488, washed again and allowed to recover for 30 minutes in RCM containing DMSO (**a-a''**) or H-89 (**b-b''**). After fixation cultures were double labelled with Texas Red phalloidin. Scale bar = 10 µm.

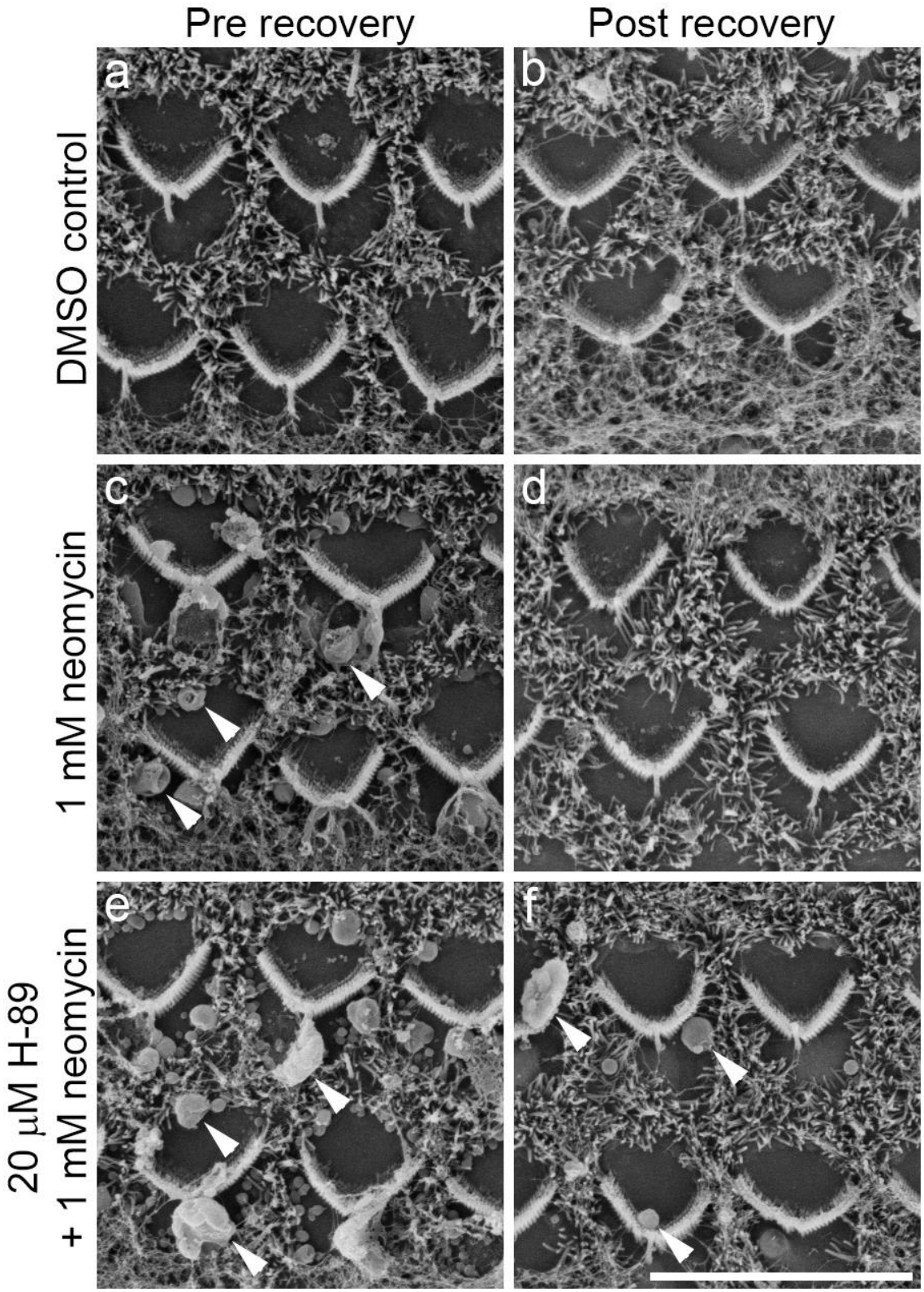

Figure 3.31. SEM images of hair cells in the middle of basal-coil cochlear cultures treated with DMSO as a control (**a**), 1 mM neomycin (**c**) or 1 mM neomycin and 20 μM H-89 (**e**) for 15 minutes, washed and allowed to recover for 30 minutes in RCM containing DMSO (**b,d**) or H-89 (**f**). White arrowheads indicate membrane blebs. Scale bar = 10 μm.

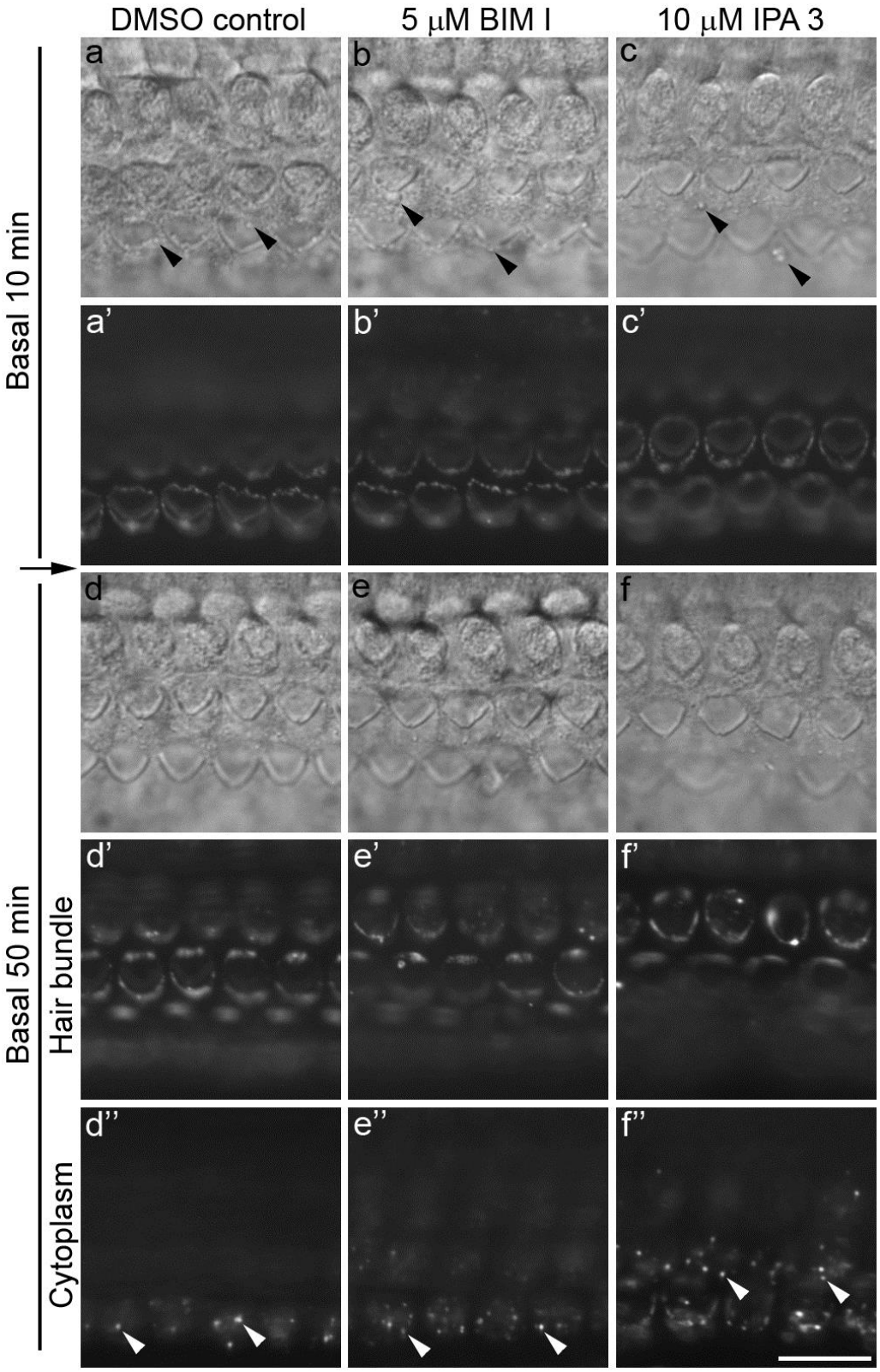

Figure 3.32. Live imaging of hair cells in the middle of basal-coil cochlear cultures that were pre-incubated in RCM containing DMSO, 5 μM BIM I or 10 μM IPA 3, washed and treated with 1 mM neomycin for 15 minutes in the presence of annexin V-488 (**a-c'**), washed again and allowed to recover for 30 minutes in RCM containing DMSO as a control (**d-d''**), BIM I (**e-e''**) or IPA 3 (**f-f''**). Black arrow represents 30 minutes recovery, black arrowheads indicate blebs and white arrowheads indicate internalised annexin V-488 punctae. Scale bar = 10 μm.

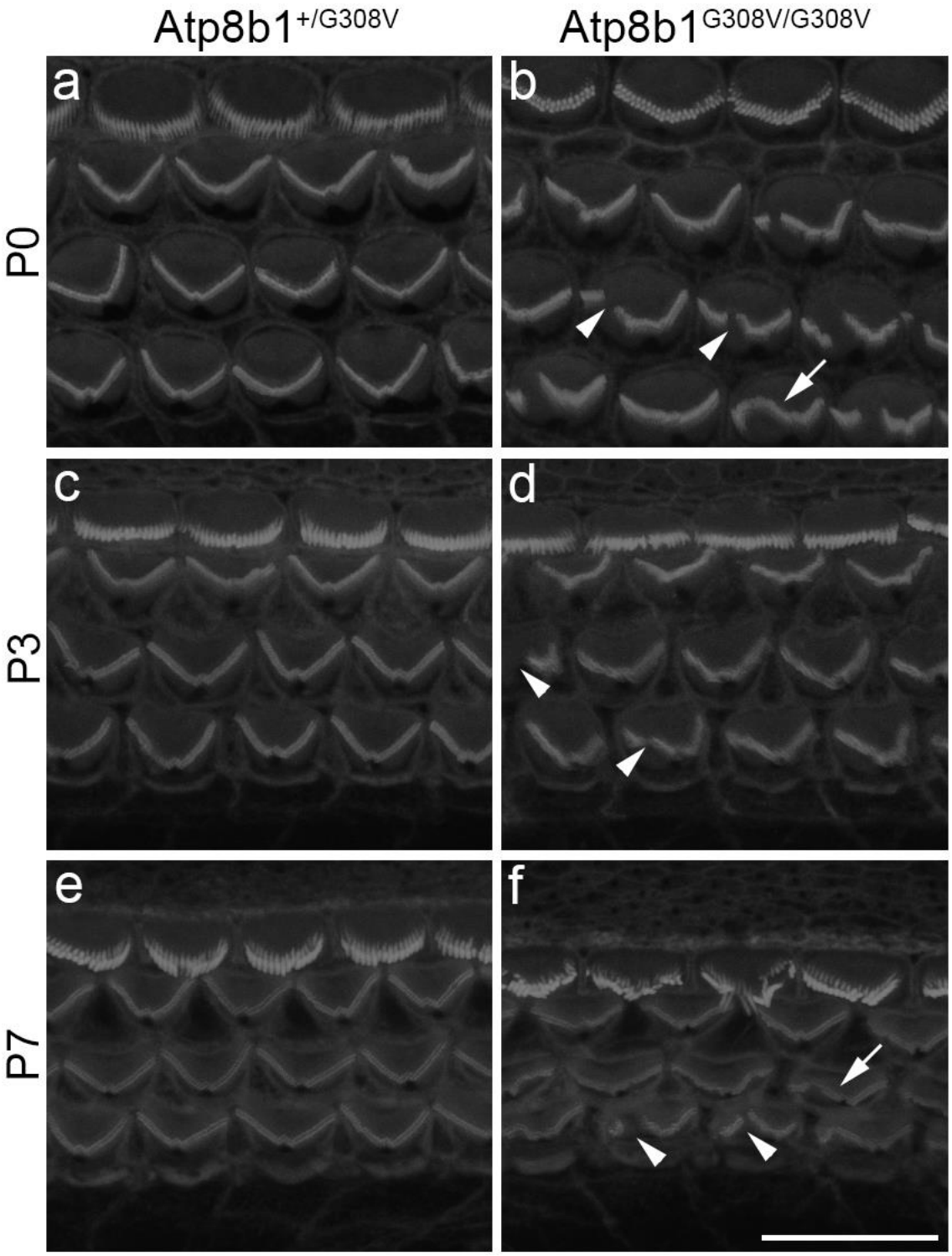

Figure 3.33. Confocal stacks of phalloidin stained P0, P3 and P7 cochlear preparations. Images of hair cells in the middle of basal-coil cochleae from heterozygous control mice (**a,c,e**) and Atp8b1$^{G308V/G308V}$ mice (**b,d,f**). White arrows indicate abnormal hair bundle shape, white arrowheads indicate missing stereocilia. Scale bar = 10 µm.

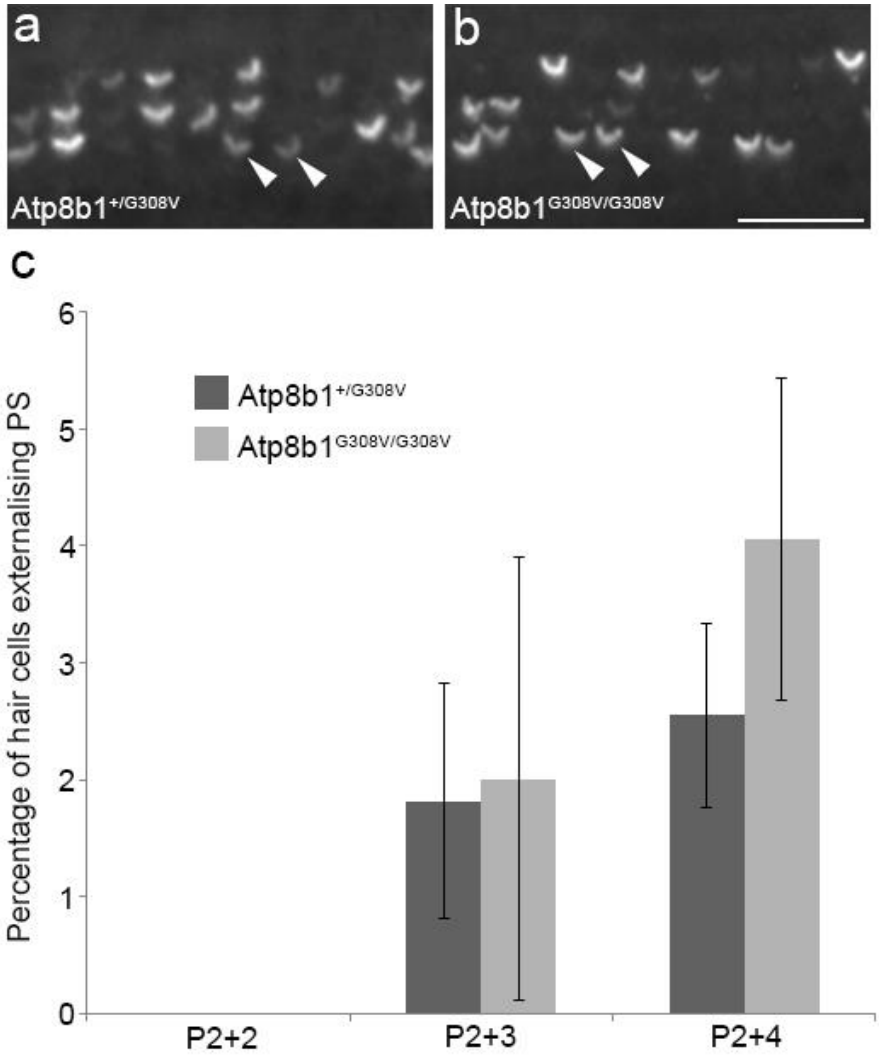

Figure 3.34. Quantification of spontaneous PS flopping as detected by annexin V-488 labelling. Cochlear cultures from Atp8b1 mutant mice and heterozygous littermates were maintained in vitro for 2 days (P2+2), 3 days (P2+3) or 4 days (P2+4) before the addition of annexin V-488 for 15 minutes. Annexin V-488 positive OHCs were counted and percentage of OHCs that were labelled were calculated. Annexin V-488 labelling of spontaneous flopping from P2+4 cultures (**a,b**). There was no significant difference in spontaneous PS flopping between mutants and heterozygous controls at P2+2, P2+3 and P2+4. A value of $p > 0.05$ was taken to be non significant. The statistical test used was an unpaired t test. Error bars represent SEM.

Number of P2+2 cochleae used:

Atp8b1^{+G308V} n = 2 cochleae (mean = 0%, SEM ± 0). Atp8b1$^{G308V/G308V}$ n = 4 cochleae (mean = 0% SEM ± 0).

Number of P2+3 cochleae used:

Atp8b1^{+G308V} n = 4 cochleae (mean = 1.8%, SEM ± 1%). Atp8b1$^{G308V/G308V}$ n = 5 cochleae (mean = 2%, SEM ± 1.9%).

Number of P2+4 cochleae used:

Atp8b1^{+G308V} n = 6 cochleae (mean = 2.6% , SEM ± 0.8%). Atp8b1$^{G308V/G308V}$ n = 10 cochleae (mean = 4.1%, SEM ± 1.4%).

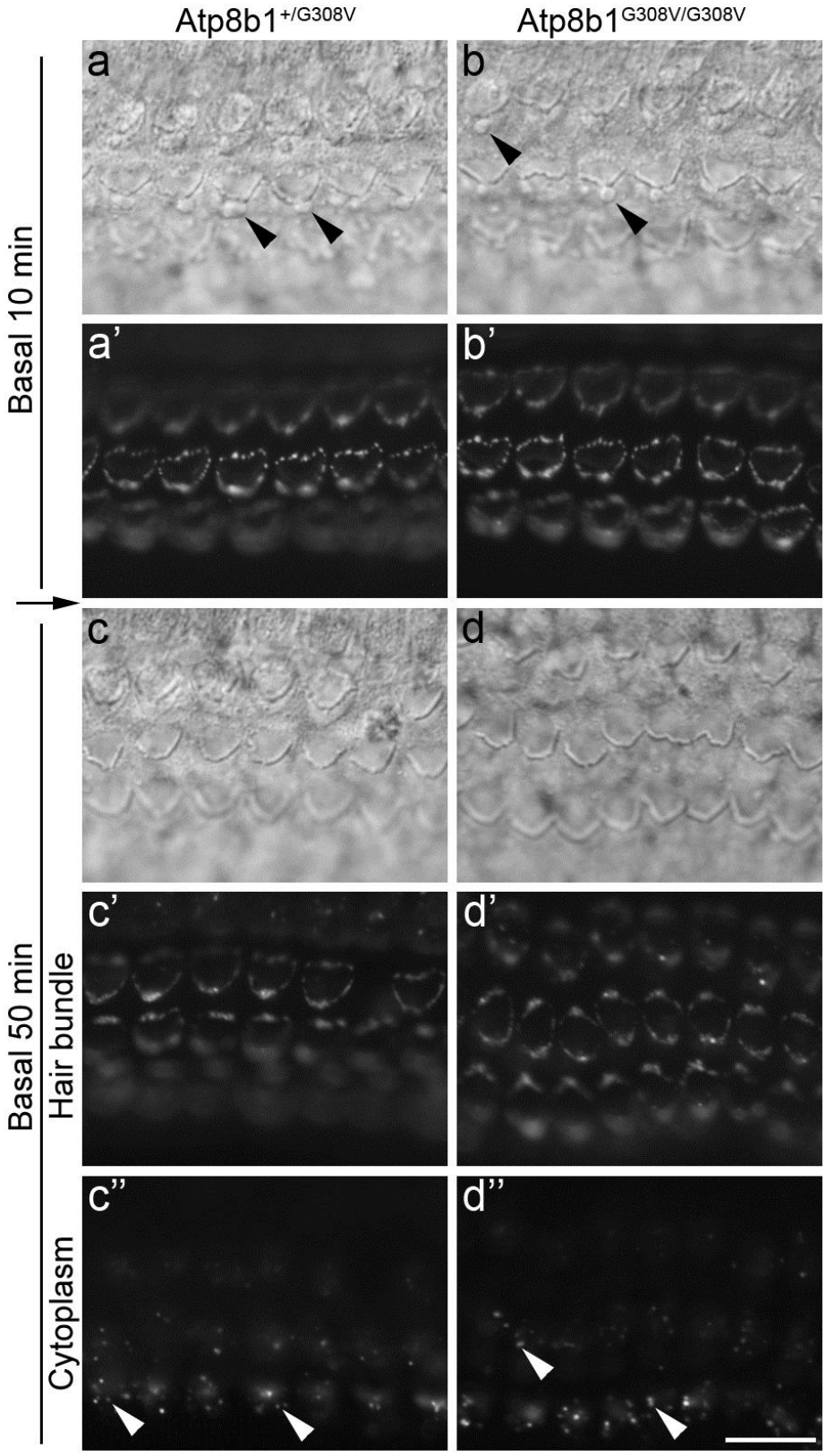

Figure 3.35. Live imaging of hair cells in the middle of basal-coil cochlear cultures that were generated from Atp8b1$^{G308V/G308V}$ and heterozygous control mice. Cultures were treated with 1 mM neomycin for 15 minutes in the presence of annexin V-488 (**a-b'**), washed and allowed to recover for 30 minutes in RCM (**c-d''**). Black arrow represents 30 minutes recovery, black arrowheads indicate blebs and white arrowheads indicate internalised annexin V-488 punctae. Scale bar = 10 µm.

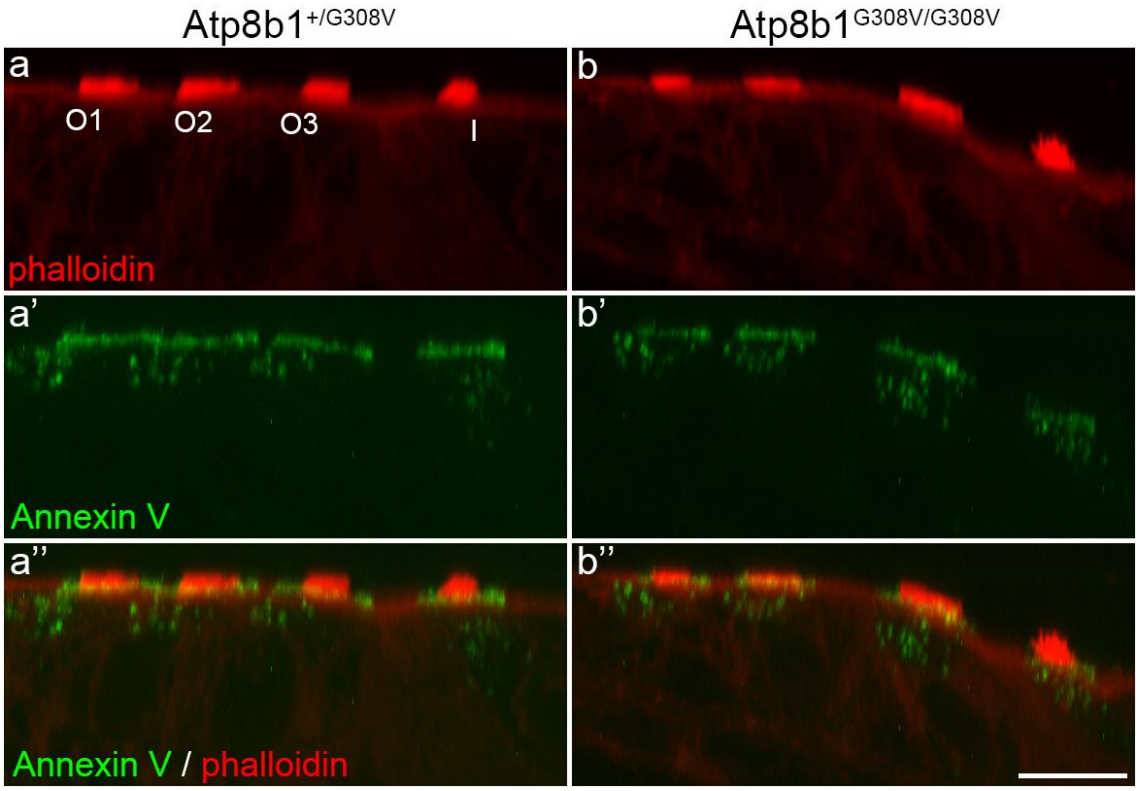

Figure 3.36. Orthogonal z-projections from confocal stacks obtained from hair cells in the middle of basal-coil cochlear cultures generated from Atp8b1$^{G308V/G308V}$ and heterozygous control mice. Cultures were treated with 1 mM neomycin for 15 minutes in the presence of annexin V-488, washed and allowed to recover for 30 minutes in RCM. After fixation cultures were double labelled with Texas Red phalloidin. Scale bar = 10 µm.

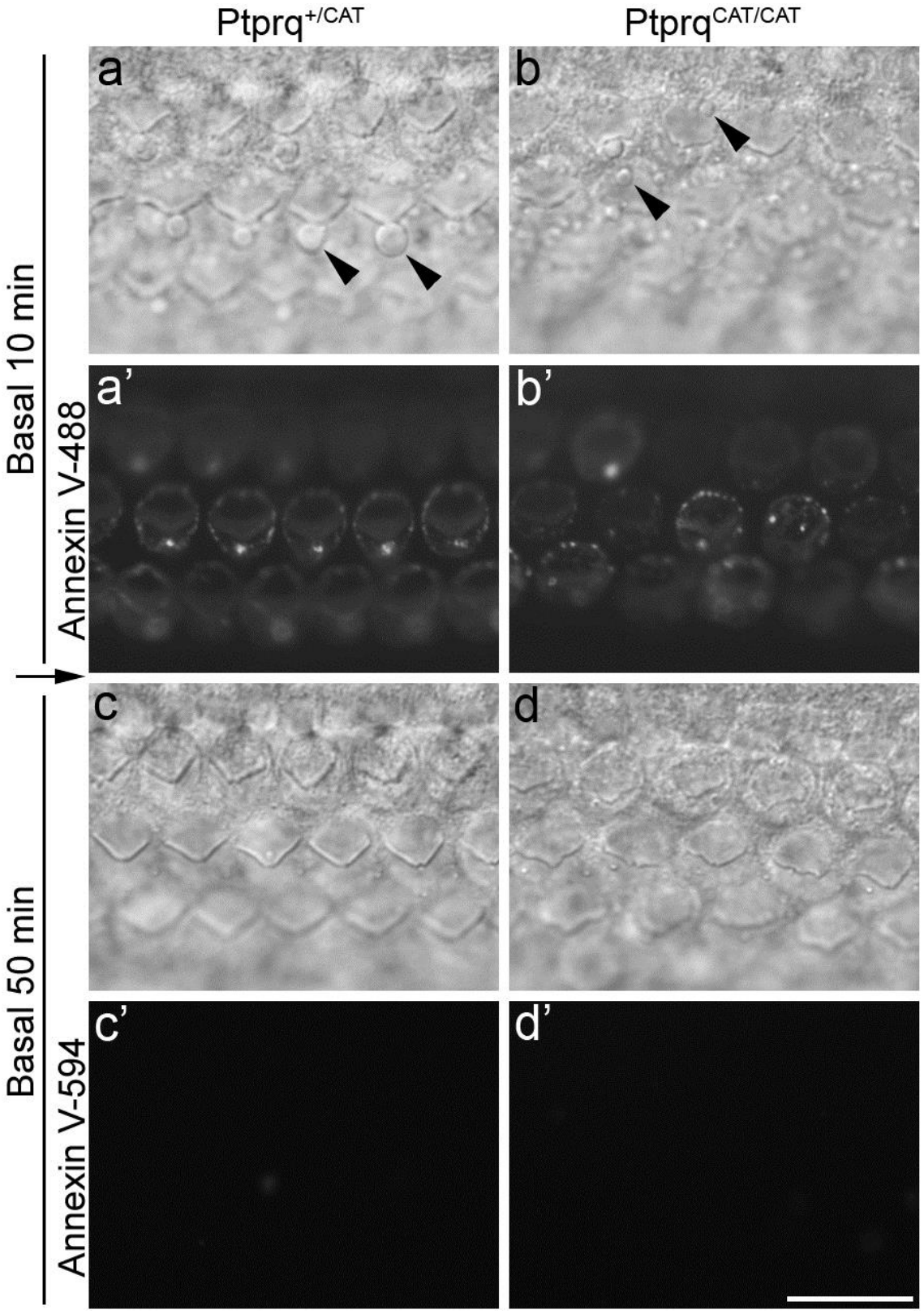

Figure 3.37. Live imaging of hair cells in the middle of basal-coil cochlear cultures that were generated from Ptprq$^{CAT/CAT}$ and heterozygous control mice. Cultures were treated with 1 mM neomycin for 15 minutes in the presence of annexin V-488 (**a-b'**), washed and allowed to recover for 30 minutes in RCM. Cultures were washed again and labelled with annexin V-594 (**c-d'**) to detect PS which had not been internalised. Black arrow represents 30 minutes recovery and black arrowheads indicate blebs. Scale bar = 10 µm.

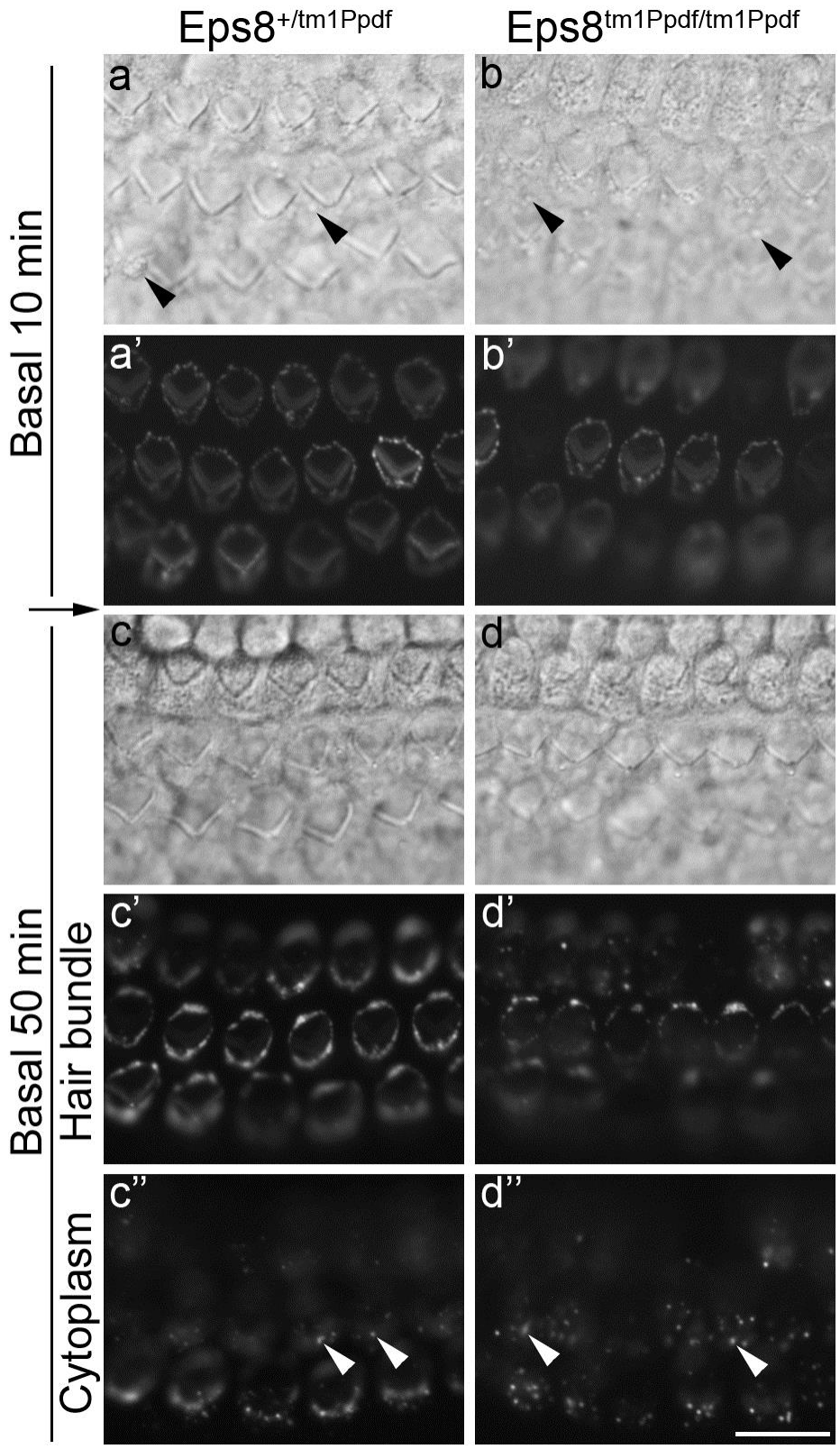

Figure 3.38. Live imaging of hair cells in the middle of basal-coil cochlear cultures that were generated from Eps8$^{tm1Ppdf/tm1Ppdf}$ and heterozygous control mice. Cultures were treated with 1 mM neomycin for 15 minutes in the presence of annexin V-488 (**a-b'**), washed and allowed to recover for 30 minutes in RCM (**c-d''**). Black arrow represents 30 minutes recovery, black arrowheads indicate blebs and white arrowheads indicate internalised annexin V-488 punctae. Scale bar = 10 µm.

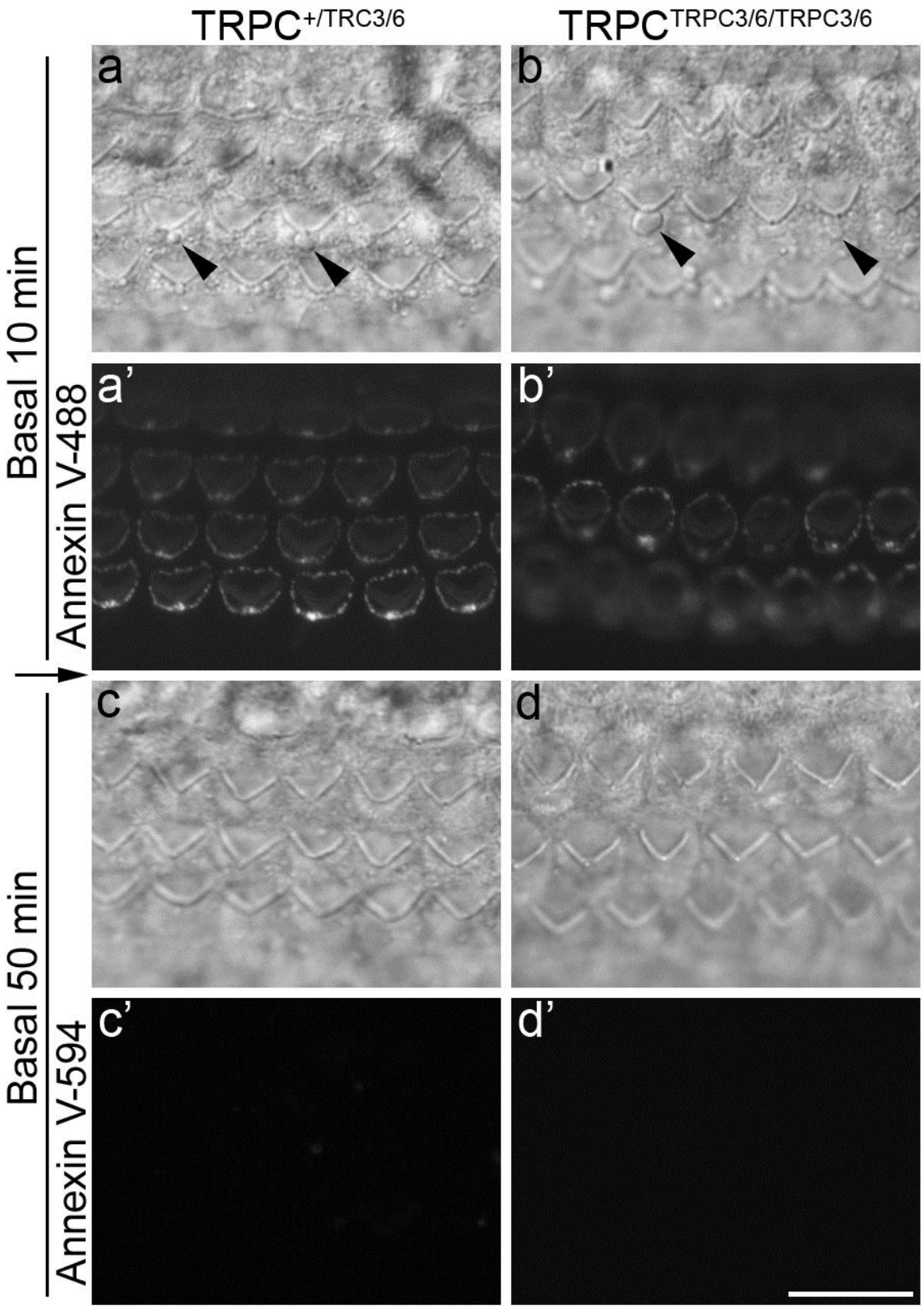

Figure 3.39. Live imaging of hair cells in the middle of basal-coil cochlear cultures that were generated from TRPC3/TRPC6 DKO and heterozygous control mice. Cultures were treated with 1 mM neomycin for 15 minutes in the presence of annexin V-488 (**a-b'**), washed and allowed to recover for 30 minutes in RCM. Cultures were washed again and labelled with annexin V-594 (**c-d'**) to detect PS which had not been internalised. Black arrow represents 30 minutes recovery and black arrowheads indicate blebs. Scale bar = 10 µm.

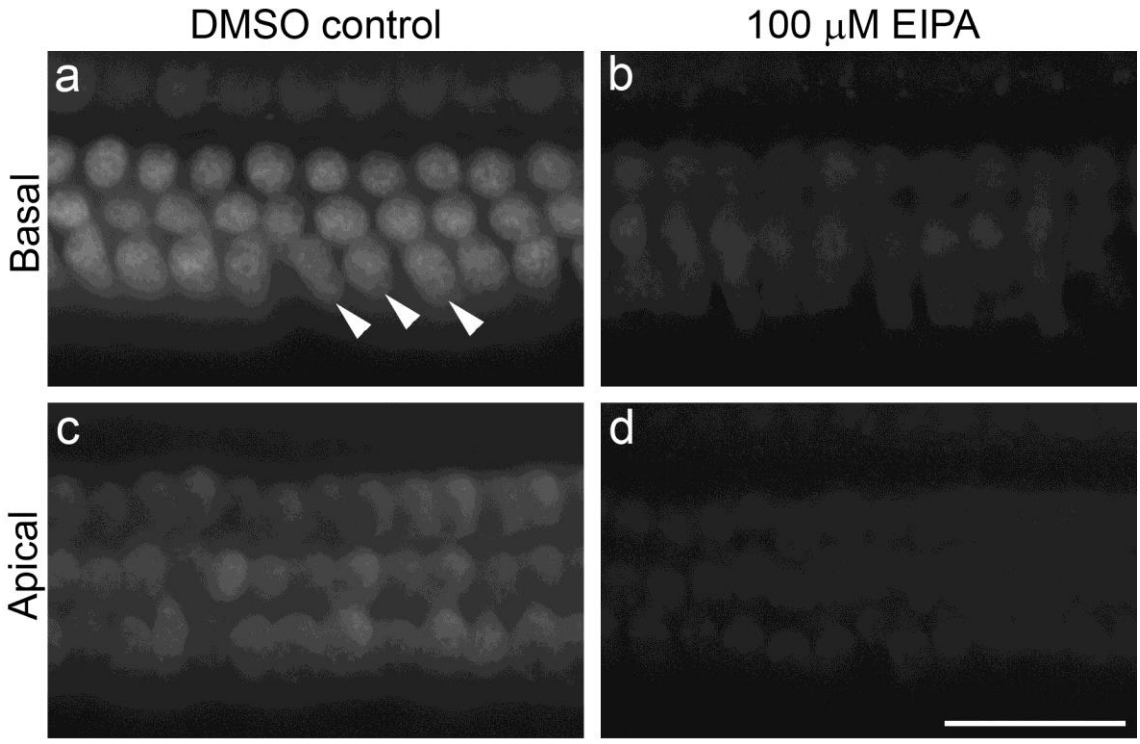

Figure 3.40. Live imaging of FM1-43 loading in hair cells in the middle of basal-coil (**a,b**) and the middle of apical-coil (**c,d**) cochlear cultures treated with 100 μM EIPA (**b,d**) or DMSO as a control (**a,c**). FM1-43 loading was reduced in hair cells treated with EIPA. Images captured from the mid-basal and mid-apical regions 5 and 7 minutes respectively after the addition of FM1-43. White arrowheads indicate hair cells loaded with FM1-43. Scale bar = 20 μm.

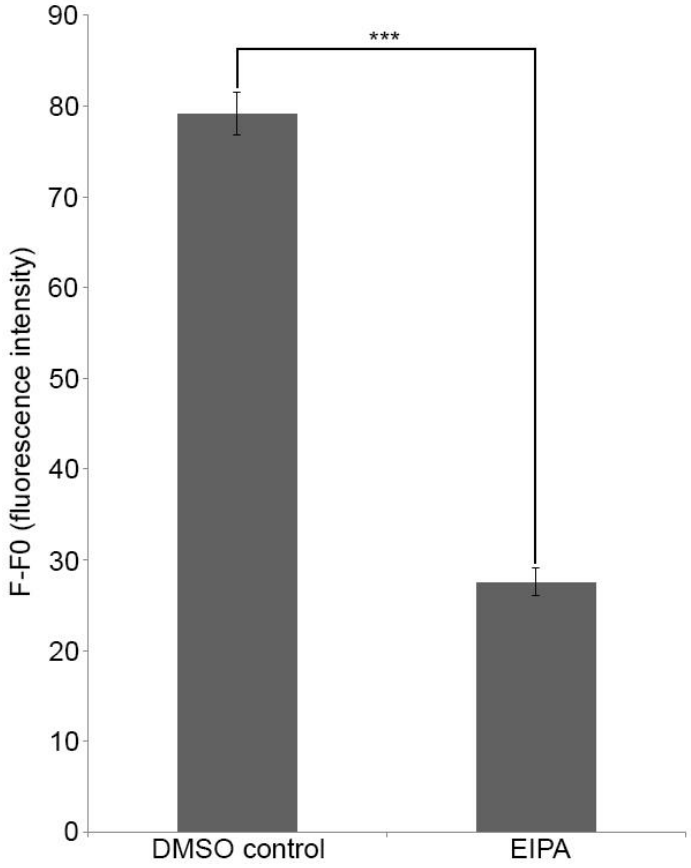

Figure 3.41. Quantification of FM1-43 fluorescence intensity from OHCs pre-treated with DMSO as a control or 100 µM EIPA. FM1-43 fluorescence was significantly more intense in OHCs treated with DMSO when compared to EIPA treated cultures. *** Indicates a significance level of $p < 0.001$. The statistical test used was an unpaired t test. Error bars represent SEM.

Number of OHCs measured:

DMSO control n = 40 OHCs (mean = 79.15, SEM ± 2.342).

100 µM EIPA n = 40 OHCs (mean = 27.59, SEM ± 1.47).

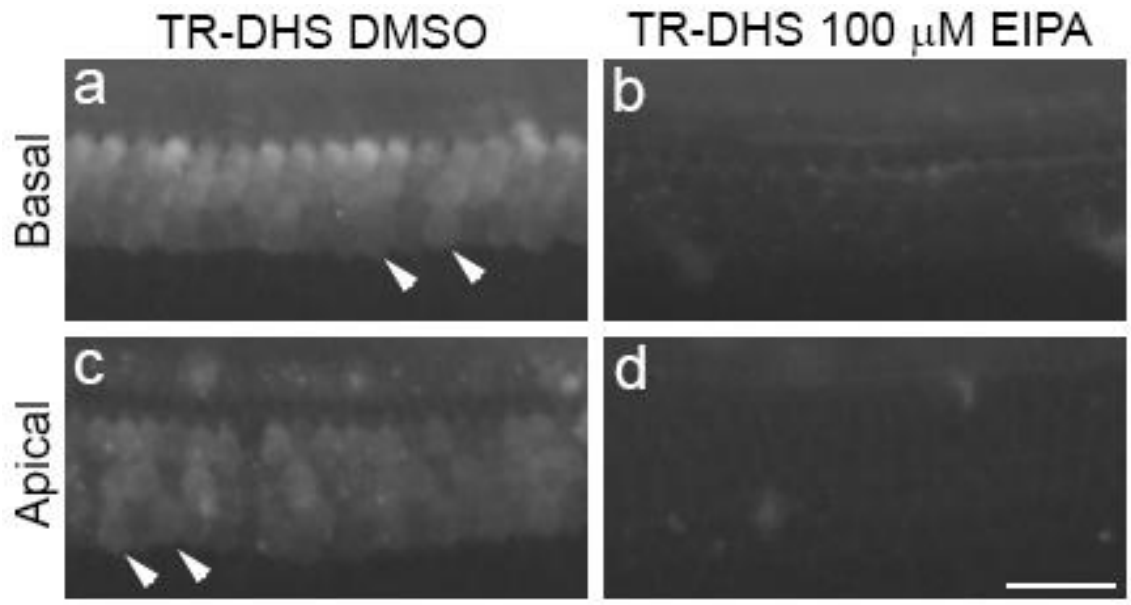

Figure 3.42. High magnification images of hair cells in the middle of basal-coil (**a,b**) and middle of apical-coil (**c,d**) cochlear cultures treated with Texas Red dihydrostreptomycin in the presence of DMSO (**a,c**) or 100 μM EIPA (**b,d**). EIPA greatly reduced Texas Red dihydrostreptomycin loading into hair cells in both the basal and apical coils. The culture treated with DMSO loaded dihydrostreptomycin in the majority of hair cells with a gradient running from the basal end of the basal coil to the apical end of the apical coil. White arrowheads indicate hair cells loaded with Texas Red dihydrostreptomycin. Scale bar = 20 μm.

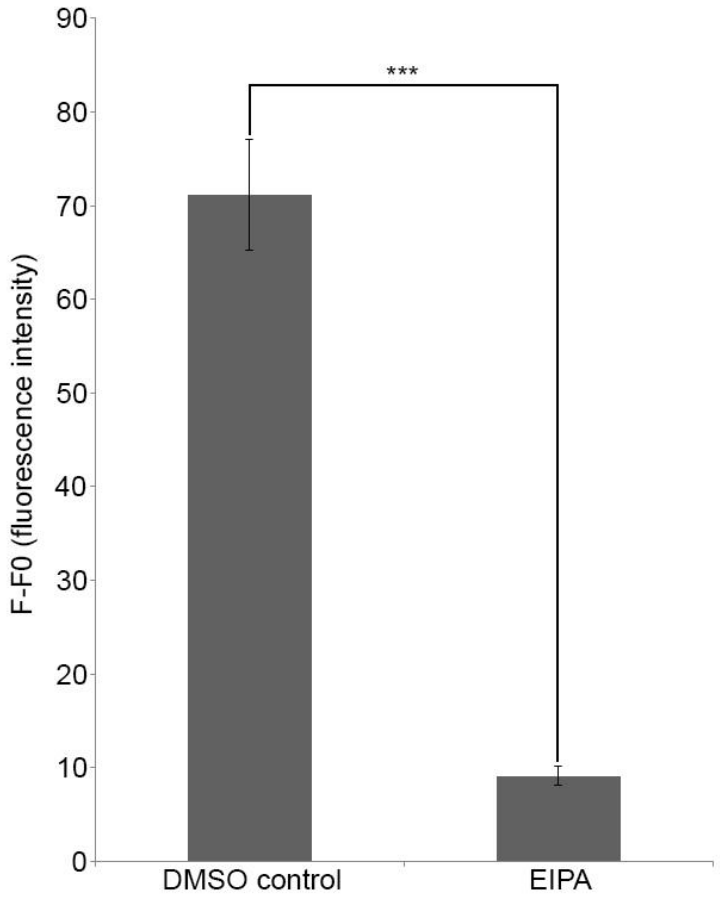

Figure 3.43. Quantification of Texas Red dihydrostreptomycin fluorescence intensity from OHCs pre-treated with DMSO as a control or 100 µM EIPA. Texas Red dihydrostreptomycin fluorescence was significantly more intense in OHCs treated with DMSO when compared to EIPA treated cultures. *** Indicates a significance level of $p < 0.001$. The statistical test used was an unpaired t test. Error bars represent SEM.

Number of OHCs measured:

DMSO control n = 20 OHCs (mean = 71.16, SEM ± 5.923).

100 µM EIPA n = 20 OHCs (mean = 9.14, SEM ± 1.04).

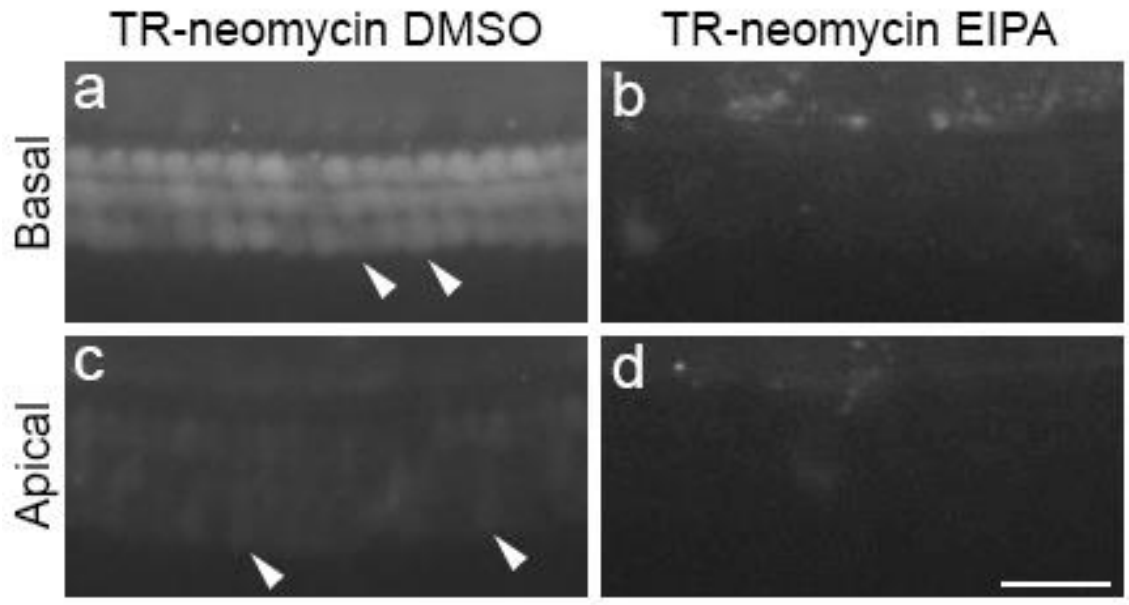

Figure 3.44. High magnification images of hair cells in the middle of basal-coil (**a,b**) and middle of apical-coil (**c,d**) cochlear cultures treated with neomycin Texas Red in the presence of DMSO as a control (**a,c**) or 100 µM EIPA (**b,d**). A reduction in neomycin loading was observed in EIPA treated cultures in both the basal and apical coil OHCs. The culture treated with DMSO, loaded neomycin in the majority of hair cells with a gradient running from the basal end of the basal coil to the apical end of the apical coil. White arrowheads indicate hair cells loaded with Texas Red neomycin. Scale bar = 20 µm.

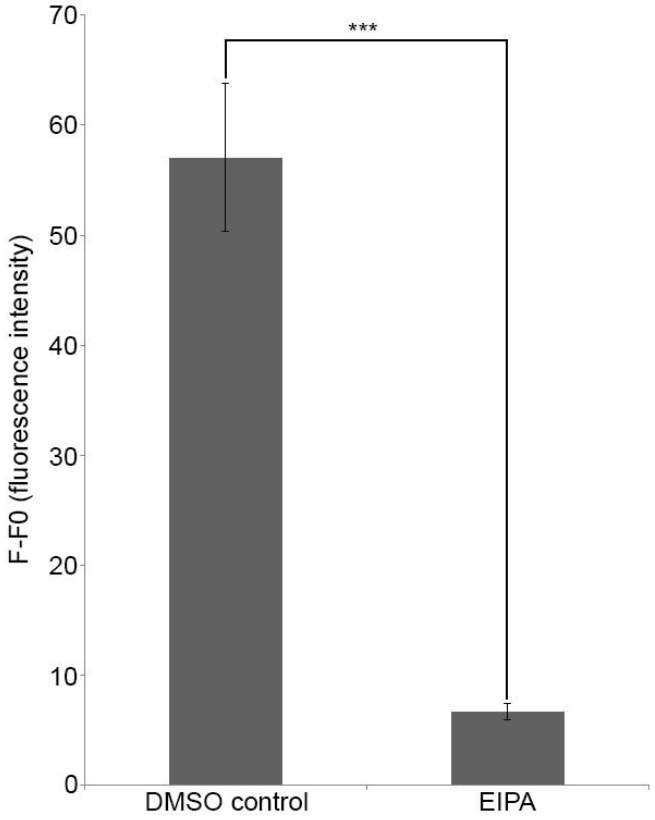

Figure 3.45. Quantification of neomycin Texas Red fluorescence intensity from OHCs pre-treated with DMSO as a control or 100 µM EIPA. Neomycin Texas Red fluorescence was significantly more intense in OHCs treated with DMSO when compared to EIPA treated cultures. *** Indicates a significance level of $p < 0.001$. The statistical test used was an unpaired t test. Error bars represent SEM.

Number of OHCs measured:

DMSO control n = 20 OHCs (mean = 57.05, SEM ± 6.74).

100 µM EIPA n = 20 OHCs (mean = 6.691, SEM ± 0.77).

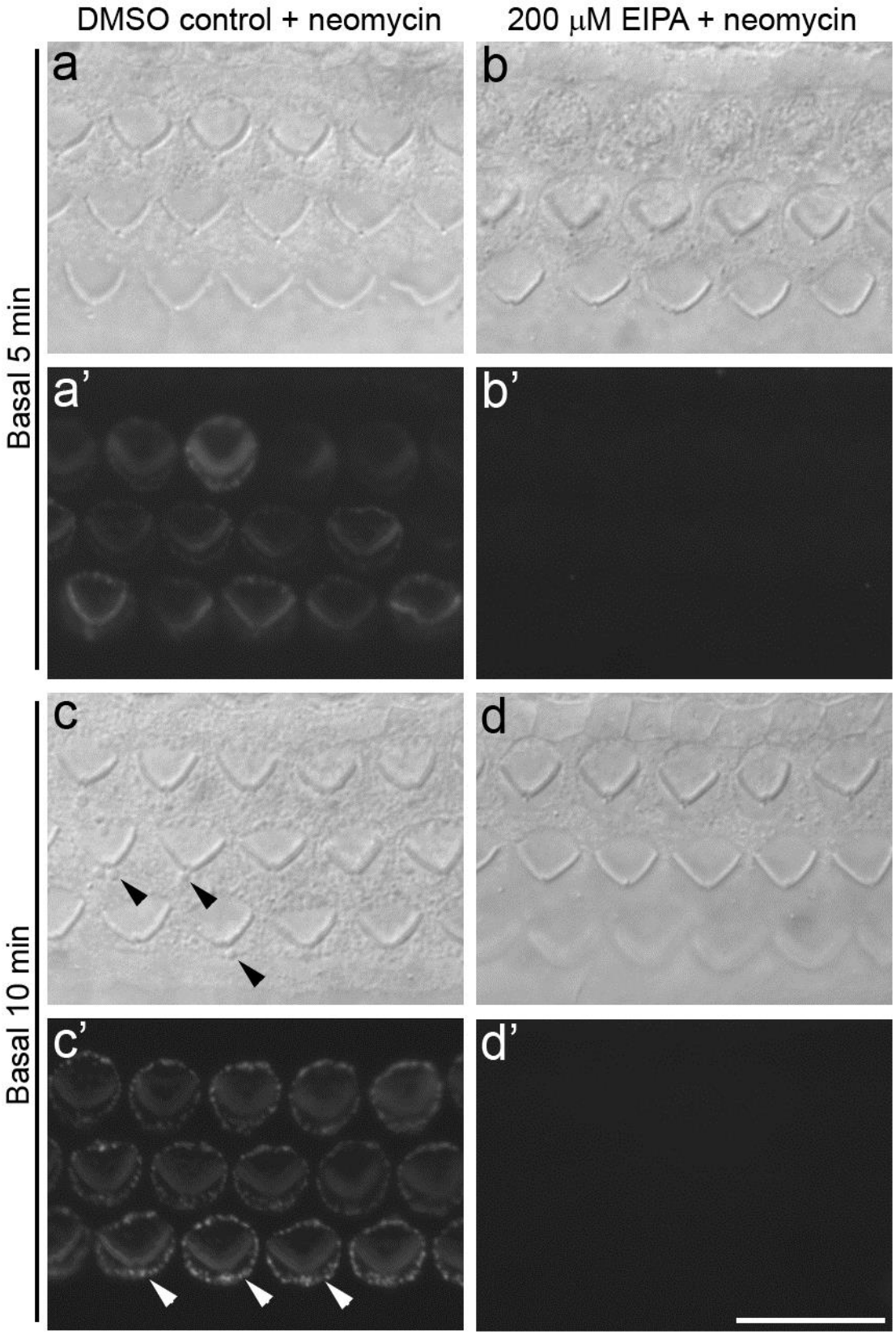

Figure 3.46. Live imaging of hair cells in the middle of basal-coil cochlear cultures 5 minutes after neomycin treatment (**a-b'**) and 10 minutes after neomycin treatment (**c-d'**). Membrane blebs formed in the control cultures (**a,c**) but not in the EIPA cultures (**b,d**). Annexin V-488 labelling was detected in control cultures (**a',c'**) but was absent in EIPA treated cultures (**b',d'**). Arrowheads indicate membrane blebs. Scale bar = 10 μm.

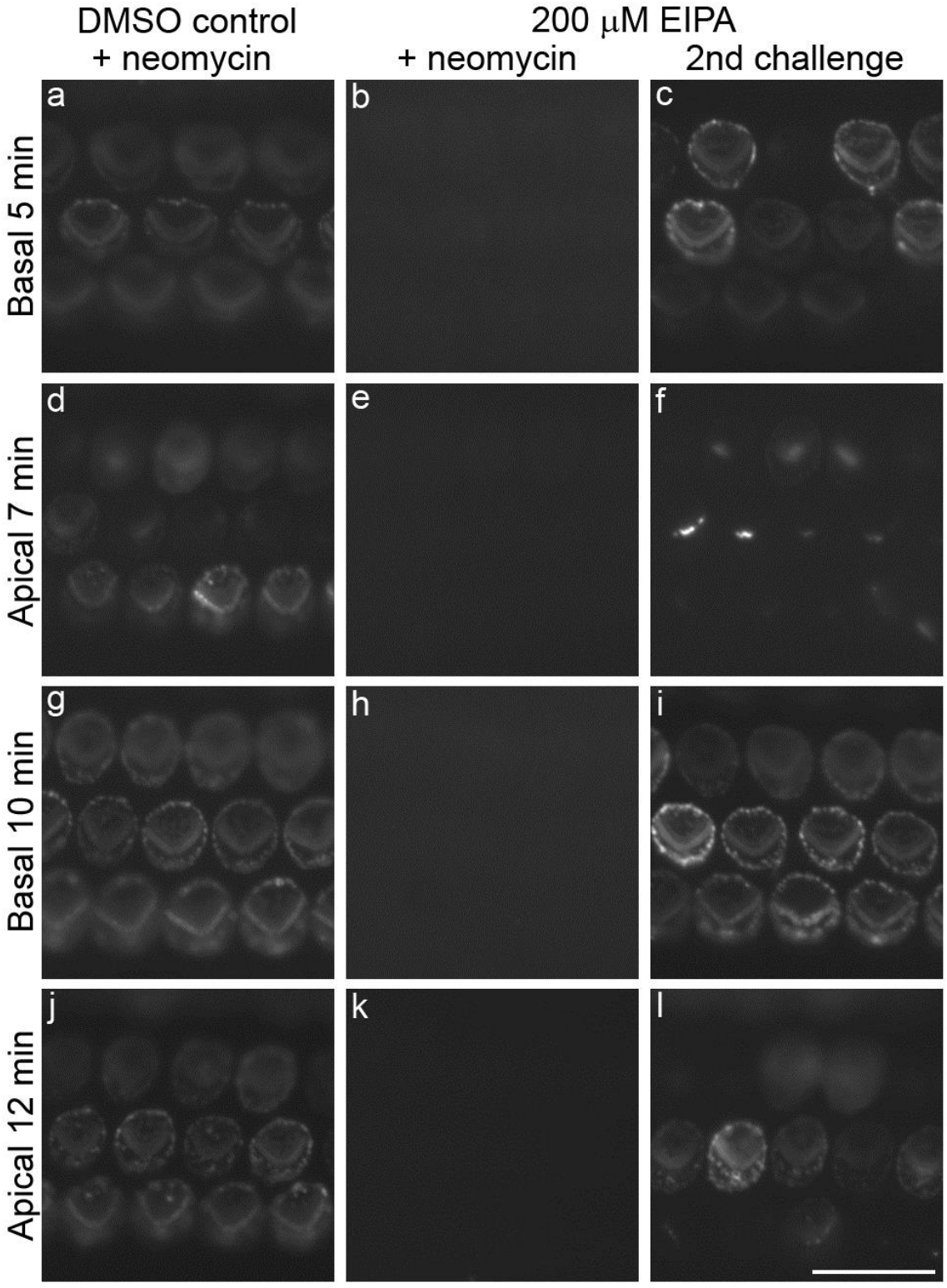

Figure 3.47. Live imaging of hair cells in the middle of basal-coil cochlear cultures pre-treated with DMSO as a control (**a,d,g,j**) or 200 μM EIPA (**b,e,h,k**) for 5 minutes before the addition of 1 mM neomycin in the presence of annexin V-488 for 15 minutes. The culture pre-treated with EIPA was washed and rechallenged with neomycin in the presence of annexin V-488 (**c,f,i,l**). Scale bar = 10 μm.

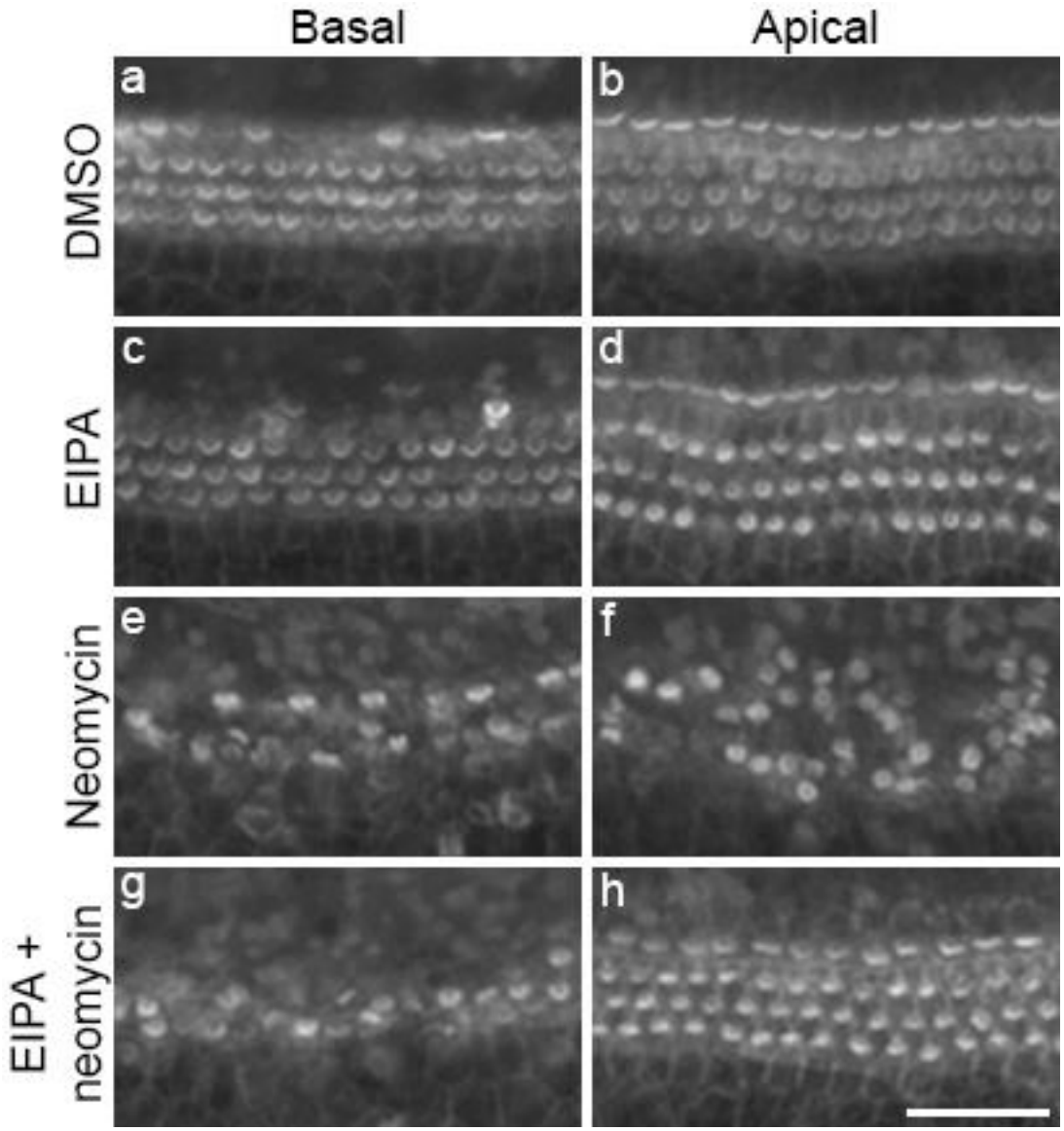

Figure 3.48. High magnification images of phalloidin stained hair cells in the middle of basal-coil (**a**) and middle of apical-coil (**b**) cochlear cultures treated with DMSO, 50 µM EIPA (**c,d**), 250 µM neomycin (**e,f**) or 50 µM EIPA with 250 µM neomycin (**g,h**) for 24 hours, washed and labelled with Texas Red phalloidin. Scale bar = 20 µm.

4 DISCUSSION

4.1 Summary of key findings

The main aim of this thesis was to understand how cochlear hair cells repair the membrane damage caused by short-term exposure to aminoglycoside antibiotics. There were several key findings which are summarised below:

1. The damage repair process does not require clathrin, caveolae, the clathrin-independent carrier (CLIC) pathway, autophagy or macropinocytosis.

2. Actin dynamics play a role in retrieval of damaged membrane in recovering hair cells.

3. Protein kinase A is required for internalisation of damaged membrane during hair cell repair.

4. Hair cells from mice lacking proteins involved in membrane turnover and maintenance of phospholipid asymmetry are able to repair membrane damage caused by aminoglycoside exposure.

5. The amiloride derivative, EIPA reversibly blocks aminoglycoside entry into hair cells and protects apical coil hair cells from aminoglycoside ototoxicity in vitro.

4.2 Clathrin, dynamin, the CLIC pathway, autophagy and macropinocytosis are not necessary for damage repair

4.2.1 Myosin II is not essential for membrane bleb formation

Transmission electron microscopy was used to investigate the ultrastructural features of hair cells recovering from neomycin damage. Numerous membrane blebs form on the apical surface of hair cells in response to neomycin exposure. These blebs appear rapidly and are completely removed following drug washout and incubation in media for 30 minutes at 37°C. The membrane blebs are usually filled with cytoplasm but are devoid of mitochondria and other organelles. Membrane blebs form at the periphery of the apical surface of hair cells, adjacent to the hair bundle and on the stereocilia. The membrane bounding the blebs that form in response to neomycin treatment is, in contrast to the apical plasma membrane of untreated hair cells, not uniformly labelled by cationic ferritin. This suggests part of the plasma membrane forming membrane blebs lacks anionic binding sites for cationic ferritin (Wessells et al., 1976). The plasma membrane of neomycin-induced blebs lacks cholesterol (Forge and Richardson, 1993). It is therefore likely membrane blebs form by the addition of new membrane to the hair-cell apical surface. This is supported by capacitance recordings which show an increase in the plasma membrane surface area of hair cells following neomycin treatment (Goodyear et al., 2008). The rapid formation of membrane blebs in response to neomycin exposure is unlikely to be a sign of apoptosis but is possibly a process exploited by aminoglycosides for self-promoted uptake into hair cells and has been described previously as a mechanism in bacteria (Hancock, Raffle, and Nicas, 1981). In bacteria, aminoglycosides cause disruption of the entire cell envelope, allowing direct entry of aminoglycosides. Gentamicin competes with Ca^{2+} and Mg^{2+} for binding sites on the outer membrane of bacteria,

destabilising the outer membrane and leading to extensive membrane bleb formation (Kadurugamuwa et al., 1993). Disruption of the plasma membrane allows further entry of aminoglycosides into the bacterial cytosol where they exert their ototoxic effects by halting protein synthesis (Kadurugamuwa et al., 1993).

Blebbistatin is an inhibitor of myosin II ATPase and blocks bleb formation in many cell types (Cheung et al., 2002; Charras et al., 2005; Norman et al., 2011). Blebbistatin, however, did not inhibit neomycin induced membrane blebbing in hair cells, indicating the process is not driven by myosin II activity. It is possible therefore that other myosin motors may drive the formation of membrane blebs or that the membrane protrusions formed during neomycin treatment are in fact not membrane blebs at all. The formation of membrane blebs is dependent on the activity of Rho-associated kinase 1 (ROCK1), an upstream activator of myosin II (Coleman et al., 2001) . Inhibition of ROCK1 activity by the inhibitor Y27632 reduced membrane bleb formation in fibroblasts (Coleman et al., 2001). Membrane bleb formation in mouse cochlear cultures in response to neomycin treatment was, however, not inhibited by Y27632 (Richardson and Goodyear, unpublished observations). These data suggest the blister-like protrusions formed in response to neomycin in sensory hair cells are not membrane blebs. It is likely that a different mechanism underlies membrane remodeling during neomycin-induced damage.

When cultures were incubated in media containing the actin stabilising compound jasplakinolide, the membrane blebs that formed following neomycin treatment were much larger than those observed without jasplakinolide pre-treatment. Membrane bleb size depends on actomyosin cortical tension, with increased tension leading to the formation of larger blebs (Tinevez et al., 2009). Treatment of fibroblasts with compounds that regulate actin turnover leads to an increase in cortical tension and increased membrane bleb size (Tinevez et

al., 2009), which could also be how jasplakinolide increases the volume of neomycin-induced blebs in hair cells.

4.2.2 Clathrin-mediated endocytosis underlies apical membrane turnover but is not necessary for damage repair

Ultrastructural analysis of hair cells during repair revealed many features typical of different pathways of endocytosis. These included clathrin-coated pits that were present at the apical surface of hair cells during recovery and were also observed in hair cells which had not been treated with neomycin. To test the potential role of this pathway in the repair process, hair cells were treated with pharmacological inhibitors of clathrin-mediated endocytosis. Inhibition of clathrin coated pit formation by Pitstop 2 did not completely block recovery, nor did rhodadyn or dynasore which inhibit dynamin- a protein required for clathrin-mediated endocytosis. Damage repair was not complete following exposure to Pitstop 2 and rhodadyn, suggesting these two compounds impeded but did not block the repair process. Antibodies to clathrin heavy chains also did not colocalise with annexin V-488 bound to externalised phosphatidylserine (PS) at the apical surface of hair cells. This indicates that clathrin-mediated endocytosis is not essential for damage repair. Coated pits are also seen in untreated hair cells that did not receive neomycin treatment making it likely that clathrin-mediated endocytosis regulates apical membrane turnover (Kachar et al., 1997; Forge and Richardson, 1993), and is not essential for damage repair. It is, however, possible a proportion of membrane externalising PS becomes internalised in coated pits during apical membrane turnover.

4.2.3 Caveolae

Ultrastructural studies also revealed structures resembling caveolae at the apical surface of hair cells during repair from neomycin-induced damage, and also in hair cells that had not been treated with neomycin. Scission of caveolae from the plasma membrane is dependent on dynamin GTPase. As the dynamin inhibitors dynasore and rhodadyn did not block internalisation of damaged membrane, it is unlikely caveolae are required for the repair process. Further studies using antibodies to caveolin 1, a major component of caveolae, revealed caveolin 1 and PS-annexin V-488 complexes are not co-localised at the apical surface of hair cells, again suggesting it is highly unlikely membrane repair is caveolae-dependent. As caveolae are seen in hair cells in the absence of neomycin treatment, caveolae could provide an alternate function to damage repair. In the absence of neomycin-induced membrane stress, caveolae are located at the surface of cells as surface-connected invaginations. Upon mechanical stress caused by membrane stretching during the early stages of membrane bleb formation, the caveolae buffer membrane tension by flattening out across the surface of the plasma membrane in an ATP-dependent process (Nassoy and Lamaze, 2012) (Figure 4.1). The flattening of caveolae during neomycin treatment could minimize cell damage resulting from mechanical stress (Nassoy and Lamaze, 2012).

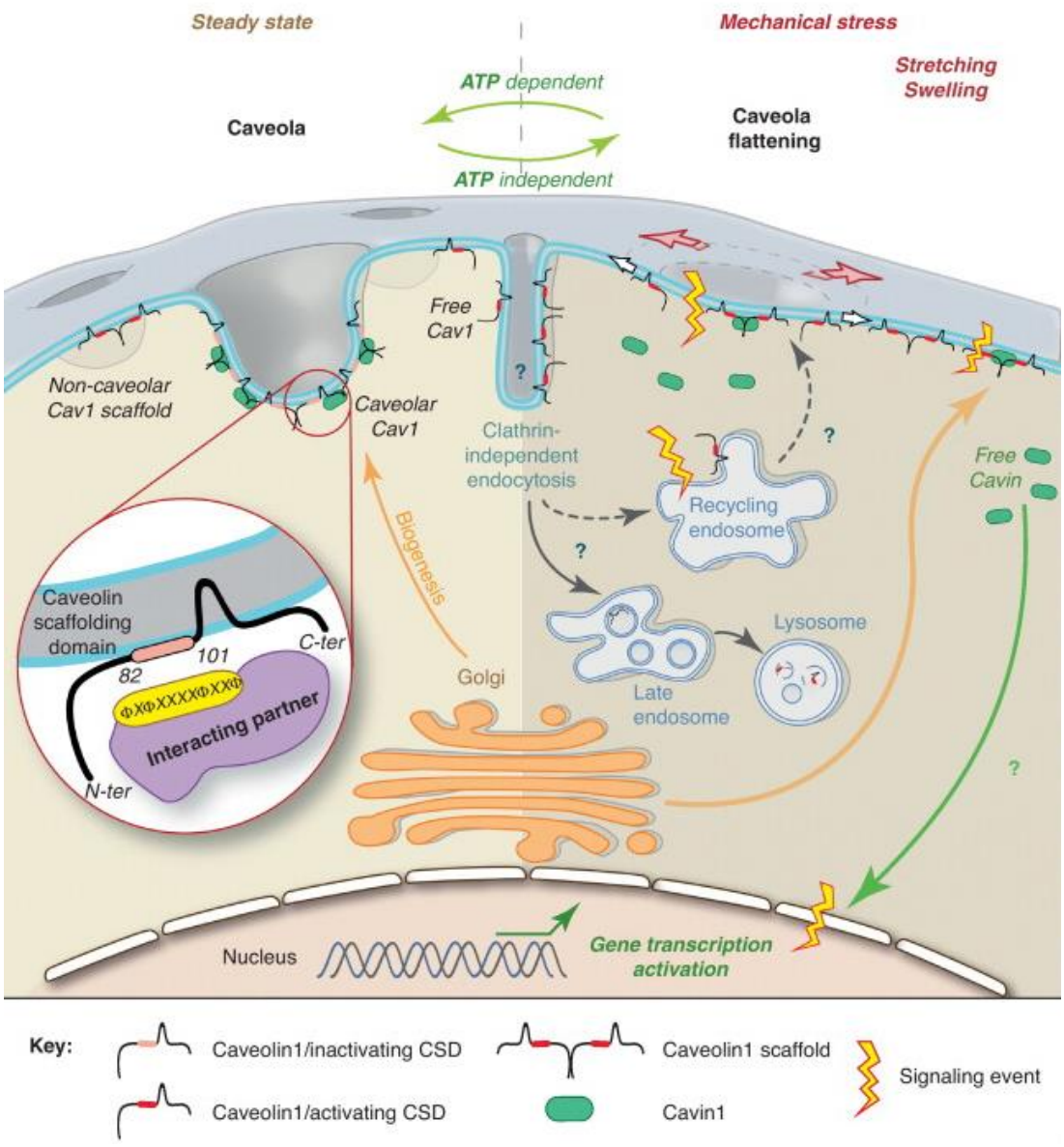

Figure 4.1. The molecular mechanisms underlying **c**aveolar flattening (Nassoy and Lamaze, 2012).

4.2.4 CLIC

Long tubular invaginations were observed in hair cells recovering from neomycin exposure. In addition ring-like structures resembling GPI-AP(glycosylphosphatidyl-inositol anchored proteins)-enriched early endosomal compartments (GEECs) were also present, which are features of the CLIC pathway. Although these structures were seen in hair cells recovering from neomycin-induced damage, inhibition of the CLIC pathway by EIPA did not abolish repair, suggesting the CLIC pathway is not necessary for damage repair in hair cells. Cholera toxin B binds to the GM1 ganglioside receptor on the plasma membrane and is predominantly internalised by the CLIC pathway. Attempts were made to see if CTxB entry would colocalise with internalised annexin V during hair-cell repair. There was, however, only a very small amount of CTxB labelling on the surface of hair cells and the majority of labelling was detected on the supporting cells. The reduced labelling that was observed is likely due to a lack of GM1 (the binding site for CTxB) on the plasma membrane of hair cells (Zhao et al., 2012).

4.2.5 Macropinocytosis

Features typical of macropinocytosis were observed in hair cells recovering from neomycin damage. Membrane blebs collapsing and fusing with the underlying plasma membrane were seen during repair. The collapse of large membrane protrusions is a common mechanism for removing large areas of plasma membrane (Mercer and Helenius, 2009) and macropinocytosis is also a mechanism of virus entry (Mercer and Helenius, 2012). The process of macropinocytosis can be activated by the presence of PS in the outer leaflet of the plasma membrane (Hoffmann et al., 2001) or by detecting PS on the surface of viruses (Mercer and Helenius, 2012). Macropinocytosis is typically susceptible to PI3K inhibitors (Falcone et al.,

2006) and EIPA (Kalin et al., 2010). In the case of hair cells, pharmacological inhibition with the PI3K inhibitors wortmannin and LY294002 did not block or impede the internalisation of membrane blebs or externalised PS bound to annexin V. Recently studies have shown entry of viruses including Vaccinia virus (Mercer et al., 2010), mature virions (Schmidt et al., 2011) and HIV-1 (Carter et al., 2011) via macropinocytosis occurs in the presence of PI3K inhibitors. This suggests a process similar to macropinocytosis may occur in hair cells to remove damaged membrane that is independent of PI3K and is not susceptible to inhibition by EIPA. There are different types of macropinocytosis, for example bleb-associated or lamellepodia-associated (Mercer and Helenius, 2009) and these may involve a different set of signaling pathways. The process of macropinocytosis is dependent on actin remodeling and it has been shown that pharmacological disruption (section 3.2.5) and genetic perturbation (section 3.3.3) of actin dynamics inhibits the repair process. This is discussed in more detail in section 4.3.

4.2.6 Autophagy

Double-membraned vesicles were also observed in hair cells during the repair process, these are a typical feature of autophagy. The process of autophagy is thought to be involved in cellular housekeeping by preventing a build-up of defective cellular components. The rate of autophagy increases following cellular stress resulting from oxidative damage and aggregation of proteins. The process of autophagy is important for cell survival (Todde et al., 2009) but excessive activity can also lead to cell death (Lee, 2012). Autophagy is a degradation pathway which sequesters cellular components in an autophagosome, which is then delivered to the lysosome for degradation (Lee, 2012; Yang and Klionsky, 2010). The initiation of autophagy occurs with the formation of the phagophore which is an isolated area of cytoplasmic membrane. The phagophore then becomes elongated, capturing cellular components destined

for degradation before closing and becoming a complete double-membraned autophagosome. The outer membrane of the autophagosome then docks and fuses with the lysosome to form the autolysosome which is the site of degradation of the autophagosome contents (Yang and Klionsky, 2010). The process of autophagy is controlled by autophagy-related genes (ATG) which are in turn controlled upstream by mammalian target of rapamycin (mTOR) (Wu et al., 2010). Autophagy is stimulated by activation of mTOR which is in turn controlled by PI3K. Activation of mTOR occurs following deprivation of cellular nutrients. The process of autophagy can be blocked by using inhibitors of PI3K including wortmannin and LY294002 (Wu et al., 2010). Wortmannin and LY294002, however, failed to block repair showing autophagy is not regulating the damage repair process.

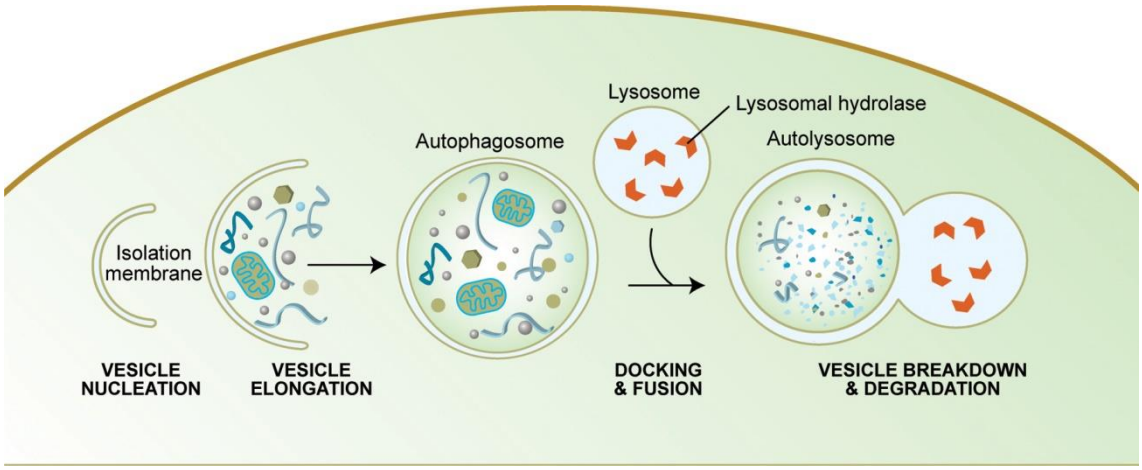

Figure 4.2. The process of autophagy. From Meléndez and Levine, 2009.

4.3 Actin dynamics play a role in damage repair

4.3.1 Inhibition of damage repair by jasplakinolide

Many cellular processes, including cytokinesis, cell migration and endocytosis require actin (Hertzog et al., 2010). There are many different mechanisms of endocytosis that are actin dependent, including clathrin-dependent and caveolae-mediated endocytosis, the CLIC pathway and macropinocytosis (Doherty and McMahon, 2009). Internalisation of neomycin-induced membrane blebs and PS-annexin V complexes are blocked by pre-treating hair cells with the actin stabilising compound jasplakinolide (see section 3.2.5). Membrane repair in hair cells is therefore actin-dependent. It is possible that a macropinocytosis-like mechanism is operating to internalise membrane blebs and annexin V bound to PS as clathrin-dependent endocytosis, caveolae-mediated endocytosis and the CLIC pathway are not essential for damage repair.

4.3.2 Eps8 mutants are able to repair

Actin dynamics are controlled by various actin binding proteins, including actin capping proteins which block proliferation of actin filaments (Hertzog et al., 2010). Eps8 is an actin capper that also has cross-linking capabilities allowing it to organise actin filaments into more complex structures (Hertzog et al., 2010). Eps8 is expressed in the tips of hair-cell stereocilia and plays a key role in the maintenance and growth of stereociliary hair bundles (Olt et al., 2014). Hair cells from cochlear cultures derived from mice lacking Eps8 are able to remove

neomycin-induced membrane blebs and internalise PS-annexin V complexes. This suggests the capping activity and actin-crosslinking abilities of Eps8 are not essential for damage repair.

4.4 PKA is required for membrane repair

Protein kinase activity is required for various mechanisms of endocytosis, although the exact function remains unclear (Doherty and McMahon, 2009). Endocytosis of urea transporter (UT)-A1 in MDCK cells is PKA dependent, increased by forskolin treatment and reduced by inhibition of PKA with H-89 (Su et al., 2012). Retrieval of membrane blebs and annexin V bound to PS was resistant to inhibition by the general protein kinase inhibitor staurosporine and did not require p21 activated kinase (PAK1) or protein kinase C (PKC) activity. The activity of PAK1 is essential for typical macropinocytosis (Dharmawardhane et al., 1997), suggesting damage repair in hair cells is not occurring via this pathway. Damage repair is PKA dependent as inhibiting this pathway with H-89 and KT5720 blocks retrieval of membrane blebs and internalisation of PS-annexin V complexes. The target of PKA in hair-cell membrane repair and the specific pathway of endocytosis it regulates remain to be elucidated although H-89 has been shown to expand the apical surface of hair cells from apical-coil cultures (Goodyear et al., 2014), indicating a possible role for PKA activity in regulating the surface area of the apical plasma membrane. Pharmacological inhibition of the repair process reveals apical membrane internalisation requires protein phosphorylation by PKA and normal actin dynamics. It is possible membrane internalisation during the repair process may be enhanced by stimulating PKA activity. Drugs that stimulate PKA could potentially be designed to be given alongside aminoglycoside antibiotics to ameliorate damage repair and protect hair cells in patients undergoing aminoglycoside treatment.

4.5 Mice lacking proteins involved in membrane turnover and phospholipid asymmetry are able to repair neomycin-induced membrane damage

4.5.1 Atp8b1 repair

Previous studies have shown mice with a mutation in the P4-ATPase Atp8b1 have a significant hearing loss as detected by an increase in auditory brainstem response (ABR) thresholds (Stapelbroek et al., 2009). This hearing impairment is associated with a progressive loss of hair cells from the cochlea. A hair bundle phenotype was previously reported at postnatal (P) day 16, with a normal development of bundles observed at P4 (Stapelbroek et al., 2009). This thesis, however, has shown that a bundle phenotype is present much earlier at P0. As the function of Atp8b1 is to maintain normal lipid asymmetry by pumping PS from the outer leaflet of the plasma membrane to the inner leaflet, it was hypothesised that hair cells from cochlear cultures prepared from Atp8b1 deficient mice would spontaneously accumulate PS in the outer leaflet of the plasma membrane. This was, however, not the case as there was little difference between spontaneous PS externalisation in hair cells from control mice and hair cells from mice lacking Atp8b1. This suggests other mechanisms must underlie spontaneous accumulation of PS in the outer plasmalemma of hair cells. Alternative mechanisms could include activity of other P4 ATPases. There are 14 different P4 ATPases in mammals which function as phospholipid flippases (Lopez-Marques et al., 2014). A recent study has shown the outer segment of the membrane from photoreceptors from mice lacking the P4-ATPase Atp8a2 had an accumulation of PS in the outer leaflet of the plasma membrane to the same extent as photoreceptors from wildtype mice in response to light exposure (Coleman et al., 2014). This also suggests alternate P4-ATPases may control flipping of PS from the outer leaflet

of the plasma membrane to the inner leaflet and therefore prevent accumulation of PS in the outer plasmalemma of photoreceptors. Hair cells from cochlear cultures of mice with a mutation in Atp8b1 are also able to repair the membrane damage caused by neomycin. Following recovery, membrane blebs are no longer detected and PS-annexin V complexes are internalised within hair cells to a similar extent in both hair cells from mutant mouse cochlear cultures and in hair cells from control mice. This finding may also show other P4-ATPases or alternative mechanisms control neomycin-induced PS externalisation.

4.5.2 Mice lacking Ptprq and mice with a TRPC3/6 double knockout are able to repair neomycin-induced membrane damage

The intracellular domain of Ptprq is believed to be associated with Eps15 homology domain containing 3 (EHD3), a protein involved in endocytosis (Nayak, 2010) . The exact role of EHD3 in the endocytic pathway remains unknown but some previous studies have shown EHD3 is required for transport from the early endosome to the endocytic recycling compartment (Naslavsky et al., 2006) and also from the early endosome to the Golgi network (Naslavsky et al., 2009). It was hypothesised that hair cells from mice lacking Ptprq may not be able to internalise neomycin-induced damaged membrane and transport it to the late endosome. It is possible endocytosis in these hair cells may be compromised due to deficient Ptprq which may therefore impede EHD3 function. Hair cells from cochlear cultures generated from Ptprq deficient mice are, however, able to remove membrane blebs and internalise PS-annexin V complexes during damage repair. Although transcytosis and membrane recycling were not studied, this may be an area to investigate further to see if Ptprq is involved in other membrane processes. Hair cells from TRPC3/6 double KO mice are also able to repair neomycin-induced membrane damage and it would appear the double deletion has no effect

on the repair process despite these mice having a significant hearing loss as detected by ABRs (Quick et al., 2012).

4.6 EIPA blocks aminoglycoside entry into hair cells

4.6.1 Neomycin entry block

EIPA is a derivative of amiloride and is an inhibitor of sodium-proton exchanger (NHE) activity (Vigne et al., 1983). Amiloride and its derivatives phenamil, benzamil, hexamethyleneiminoamiloride (HMA), dimethylamiloride (DMA) and 2'-methoxy-5'-nitroiodobenzamil (I-NMBA) are able to block MET currents in OHCs from cochlear cultures (Rusch et al., 1994). The compound EIPA blocks entry of FM1-43 (section 3.4.1) and aminoglycosides (section 3.4.2) into hair cells and consequently inhibits the short term ototoxic effects, membrane blebbing and PS externalisation (section 3.4.3). This block of membrane damage is almost entirely reversible (section 3.4.4) following EIPA washout and a rechallenge with neomycin. As amiloride has been shown to prevent entry of FM1-43 (Nishikawa and Sasaki, 1996) and uptake of the aminoglycoside gentamicin (Alharazneh et al., 2011) into hair cells by blocking the MET channel, it is possible the amiloride derivative EIPA is also blocking neomycin entry by the same mechanism. It was shown EIPA is also able to protect hair cells from neomycin-induced damage in apical-coil but not basal-coil cochlear cultures over a longer time period of 24 hours. Hair cells from P2 basal-coil cochlear cultures are more susceptible to neomycin damage than hair cells from apical-coil cochlear cultures which matches a gradient of maturation (Richardson and Russell, 1991) and could explain why EIPA was not able to protect hair cells in basal-coil cultures. At the concentration tested EIPA

alone does not appear to cause damage to hair cells in any region of the cochlea suggesting EIPA could have potential as an otoprotectant.

4.7 Future directions

The damage repair process is blocked by pretreating hair cells with the PKA inhibitors H-89 and KT5920. At the concentration used, H-89 is considered to specifically inhibit PKA activity. At slightly higher concentrations H-89 is also known to block other kinases including CaM kinase II and Rho kinase II. Testing multiple inhibitors of both of these kinases could confirm the specific involvement of PKA in the damage repair process.

It would be useful to see if the damage repair process can be stimulated by activating PKA. The activity of PKA is cAMP dependent and by increasing cAMP levels with forskolin and 9-bromo-cAMP, this could potentially ameliorate the repair process. If activating PKA enhances the repair process then this will also support the involvement of PKA in damage repair. In addition, the targets of PKA at present remain unknown and so this should be a focus of future work.

5 CONCLUSIONS

Previous studies have shown hair cells are able to repair membrane damage caused by short term exposure to aminoglycoside antibiotics in vitro. Following drug washout and incubation in medium at 37°C membrane blebs are no longer detected on the apical surface of hair cells and plasma membrane containing externalised phosphatidylserine is endocytosed. The exact mechanisms underlying membrane repair were previously unknown but this current study has uncovered the molecular mechanisms involved in damage repair.

This thesis has shown retrieval of membrane blebs and endocytosis of membrane containing externalised phosphatidylserine, is dependent on protein kinase A (PKA) activity and normal functioning actin dynamics. The targets of PKA in the repair process, however, are yet to be identified. Other protein kinases including protein kinase C and p21 activated kinase are not necessary for repair from neomycin-induced damage. It is unlikely a classical mechanism of endocytosis underlies membrane retrieval as clathrin-mediated and caveolae-dependent endocytosis, in addition to the clathrin-independent carrier (CLIC) pathway and autophagy, are not necessary for retrieval of damaged membrane. It is worth noting, however, the endocytic pathways may operate in parallel and by blocking one specific pathway others may become upregulated as a compensatory mechanism. As the repair process is actin-dependent it is likely a non-typical mechanism similar to macropinocytosis operates to remove large areas of damaged membrane. Classical macropinocytosis is not involved in the repair process as inhibiting molecules associated with this pathway does not abolish or impede membrane retrieval.

Work in this thesis has also identified the otoprotective potential of the amiloride derivative EIPA. Aminoglycoside entry and subsequent damage to hair cells in vitro, can be blocked by treating cochlear cultures with EIPA prior to aminoglycoside exposure.

6 REFERENCES

Ahmed, Z. M., Goodyear, R., Riazuddin, S., Lagziel, A., Legan, P. K., Behra, M., and Friedman, T. B. (2006). The Tip-Link Antigen, a Protein Associated with the Transduction Complex of Sensory Hair Cells, Is Protocadherin-15. *The Journal of Neuroscience*, *26*(26), 7022–7034.

Alberts, B., Johnson, A., Lewis, J., Raff, M., Roberts, K., and Walter, P. (2008). *Molecular biology of the cell* (5th ed.). New York, USA: Garland Science.

Alharazneh, A., Luk, L., Huth, M., Monfared, A., Steyger, P. S., Cheng, A. G., and Ricci, A. J. (2011). Functional Hair Cell Mechanotransducer Channels Are Required for Aminoglycoside Ototoxicity. *PLoS ONE*, *6*(7).

Anniko, M., and Møller, A. R. (1978). A physiological and morphological study of the cochlea of the rat following treatment with atoxyl and neomycin. *Acta Oto-Laryngologica*, *86*(3-4), 201–211.

Apodaca, G. (2001). Endocytic traffic in polarized epithelial cells: role of the actin and microtubule cytoskeleton. *Traffic (Copenhagen, Denmark)*, *2*(3), 149–159.

Bird, J. E., Daudet, N., Warchol, M. E., and Gale, J. E. (2010). Supporting cells eliminate dying sensory hair cells to maintain epithelial integrity in the avian inner ear. *The Journal of Neuroscience: The Official Journal of the Society for Neuroscience*, *30*(37), 12545–12556.

Blommaart, E. F., Krause, U., Schellens, J. P., Vreeling-Sindelárová, H., and Meijer, A. J. (1997). The phosphatidylinositol 3-kinase inhibitors wortmannin and LY294002 inhibit autophagy in isolated rat hepatocytes. *European Journal of Biochemistry / FEBS*, *243*(1-2), 240–246.

Bohdanowicz, M., and Grinstein, S. (2013). Role of Phospholipids in Endocytosis, Phagocytosis, and Macropinocytosis. *Physiological Reviews*, *93*(1), 69–106.

Bokoch, G. M. (2003). Biology of the p21-activated kinases. *Annual Review of Biochemistry*, *72*, 743–781.

Bratton, D. L., Fadok, V. A., Richter, D. A., Kailey, J. M., Guthrie, L. A., and Henson, P. M. (1997). Appearance of phosphatidylserine on apoptotic cells requires calcium-mediated nonspecific flip-flop and is enhanced by loss of the aminophospholipid translocase. *The Journal of Biological Chemistry*, *272*(42), 26159–26165.

Bubb, M. R., Spector, I., Beyer, B. B., and Fosen, K. M. (2000). Effects of Jasplakinolide on the Kinetics of Actin Polymerization AN EXPLANATION FOR CERTAIN IN VIVO OBSERVATIONS. *Journal of Biological Chemistry*, *275*(7), 5163–5170.

Carter, G. C., Bernstone, L., Baskaran, D., and James, W. (2011). HIV-1 infects macrophages by exploiting an endocytic route dependent on dynamin, Rac1 and Pak1. *Virology*, *409*(2), 234–250.

Charras, G. T. (2008). A short history of blebbing. *Journal of Microscopy*, *231*(3), 466–478.

Charras, G. T., Coughlin, M., Mitchison, T. J., and Mahadevan, L. (2008). Life and times of a cellular bleb. *Biophysical Journal*, *94*(5), 1836–1853.

Charras, G. T., Yarrow, J. C., Horton, M. A., Mahadevan, L., and Mitchison, T. J. (2005). Non-equilibration of hydrostatic pressure in blebbing cells. *Nature*, *435*(7040), 365–369.

Chen, Y., Huang, W.G., Zha, D.J., Qiu, J.H., Wang, J.L., Sha, S.H., and Schacht, J. (2007). Aspirin attenuates gentamicin ototoxicity: from the laboratory to the clinic. *Hearing Research*, *226*(1-2), 178–182.

Cheung, A., Dantzig, J. A., Hollingworth, S., Baylor, S. M., Goldman, Y. E., Mitchison, T. J., and Straight, A. F. (2002). A small-molecule inhibitor of skeletal muscle myosin II. *Nature Cell Biology*, *4*(1), 83–88.

Clerici, W. J., Hensley, K., DiMartino, D. L., and Butterfield, D. A. (1996). Direct detection of ototoxicant-induced reactive oxygen species generation in cochlear explants. *Hearing Research*, *98*(1-2), 116–124.

Coleman, J. A., Zhu, X., Djajadi, H. R., Molday, L. L., Smith, R. S., Libby, R. T., and Molday, R. S. (2014). Phospholipid flippase ATP8A2 is required for normal visual and auditory function and photoreceptor and spiral ganglion cell survival. *Journal of Cell Science*, *127*(5), 1138–1149.

Coleman, M. L., Sahai, E. A., Yeo, M., Bosch, M., Dewar, A., and Olson, M. F. (2001). Membrane blebbing during apoptosis results from caspase-mediated activation of ROCK I. *Nature Cell Biology*, *3*(4), 339–345.

Corey, D. P., and Hudspeth, A. J. (1979). Ionic basis of the receptor potential in a vertebrate hair cell. *Nature*, *281*(5733), 675–677.

Dharmawardhane, S., Sanders, L. C., Martin, S. S., Daniels, R. H., and Bokoch, G. M. (1997). Localization of p21-activated kinase 1 (PAK1) to pinocytic vesicles and cortical actin structures in stimulated cells. *The Journal of Cell Biology*, *138*(6), 1265–1278.

Doherty, G. J., and Lundmark, R. (2009). GRAF1-dependent endocytosis. *Biochemical Society Transactions*, *37*(Pt 5), 1061–1065.

Doherty, G. J., and McMahon, H. T. (2009). Mechanisms of endocytosis. *Annual Review of Biochemistry*, *78*, 857–902.

Eker, P., Holm, P. K., van Deurs, B., and Sandvig, K. (1994). Selective regulation of apical endocytosis in polarized Madin-Darby canine kidney cells by mastoparan and cAMP. *The Journal of Biological Chemistry*, *269*(28), 18607–18615.

Fackler, O. T., and Grosse, R. (2008). Cell motility through plasma membrane blebbing. *The Journal of Cell Biology*, *181*(6), 879–884.

Falcone, S., Cocucci, E., Podini, P., Kirchhausen, T., Clementi, E., and Meldolesi, J. (2006). Macropinocytosis: regulated coordination of endocytic and exocytic membrane traffic events. *Journal of Cell Science*, *119*(22), 4758–4769.

Fallon, R. J., and Danaher, M. (1992). The effect of staurosporine, a protein kinase inhibitor, on asialoglycoprotein receptor endocytosis. *Experimental Cell Research*, *203*(2), 420–426.

Farris, H. E., LeBlanc, C. L., Goswami, J., and Ricci, A. J. (2004). Probing the pore of the auditory hair cell mechanotransducer channel in turtle. *The Journal of Physiology*, *558*(Pt 3), 769–792.

Fiala, J. C. (2005). Reconstruct: a free editor for serial section microscopy. *Journal of Microscopy*, *218*(Pt 1), 52–61.

Forge, A., and Richardson, G. (1993a). Freeze fracture analysis of apical membranes in cochlear cultures: differences between basal and apical-coil outer hair cells and effects of neomycin. *Journal of Neurocytology*, *22*(10), 854–867.

Forge, A., and Richardson, G. (1993b). Freeze fracture analysis of apical membranes in cochlear cultures: differences between basal and apical-coil outer hair cells and effects of neomycin. *Journal of Neurocytology*, *22*(10), 854–867.

Forge, A., and Schacht, J. (2000). Aminoglycoside Antibiotics. *Audiology and Neuro-Otology*, *5*, 3–22.

Gale, J. E., Marcotti, W., Kennedy, H. J., Kros, C. J., and Richardson, G. P. (2001). FM1-43 dye behaves as a permeant blocker of the hair-cell mechanotransducer channel. *The Journal of Neuroscience: The Official Journal of the Society for Neuroscience*, *21*(18), 7013–7025.

Galovic, M., Xu, D., Areces, L. B., Kammen, R. van der, and Innocenti, M. (2011). Interplay between N-WASP and CK2 optimizes clathrin-mediated endocytosis of EGFR. *Journal of Cell Science*, *124*(12), 2001–2012.

Garcia, M., Ray, S., Brown, I., Irom, J., and Brazill, D. (2014). PakD, a putative p21-activated protein kinase in Dictyostelium discoideum, regulates actin. *Eukaryotic Cell*, *13*(1), 119–126.

Goodyear, R. J., Legan, P. K., Wright, M. B., Marcotti, W., Oganesian, A., Coats, S. A., and Richardson, G. P. (2003). A Receptor-Like Inositol Lipid Phosphatase Is Required for the Maturation of Developing Cochlear Hair Bundles. *The Journal of Neuroscience*, *23*(27), 9208–9219.

Goodyear, R. J., Forge, A., Legan, P. K., and Richardson, G. P. (2010). Asymmetric Distribution of Cadherin 23 and Protocadherin 15 in the Kinocilial Links of Avian Sensory Hair Cells. *The Journal of Comparative Neurology*, *518*(21), 4288–4297.

Goodyear, R. J, Gale, J. E., Ranatunga, K. M., Kros, C. J., and Richardson, G. P. (2008). Aminoglycoside-induced phosphatidylserine externalization in sensory hair cells is regionally restricted, rapid, and reversible. *The Journal of Neuroscience: The Official Journal of the Society for Neuroscience*, *28*(40), 9939–9952.

Goodyear, R. J, Marcotti, W., Kros, C. J., and Richardson, G. P. (2005). Development and properties of stereociliary link types in hair cells of the mouse cochlea. *The Journal of Comparative Neurology*, *485*(1), 75–85.

Goodyear, R. J., Ratnayaka, H. S. K., Warchol, M. E., and Richardson, G. P. (2014). Staurosporine-induced collapse of cochlear hair bundles. *Journal of Comparative Neurology*, *522*(14), 3281–3294.

Grati, M., and Kachar, B. (2011). Myosin VIIa and sans localization at stereocilia upper tip-link density implicates these Usher syndrome proteins in mechanotransduction. *Proceedings of the National Academy of Sciences of the United States of America*, *108*(28), 11476–11481.

Hancock, R. E., Raffle, V. J., and Nicas, T. I. (1981). Involvement of the outer membrane in gentamicin and streptomycin uptake and killing in Pseudomonas aeruginosa. *Antimicrobial Agents and Chemotherapy*, *19*(5), 777–785.

Hansen, C. G., Howard, G., and Nichols, B. J. (2011). Pacsin 2 is recruited to caveolae and functions in caveolar biogenesis. *Journal of Cell Science*, *124*(Pt 16), 2777–2785.

Hashino, E., and Shero, M. (1995). Endocytosis of aminoglycoside antibiotics in sensory hair cells. *Brain Research*, *704*(1), 135–140.

Heller, J. (1984). Effect of some simple manoeuvres on the course of acute renal failure after gentamycin treatment in rats. *International Urology and Nephrology*, *16*(3), 243–251.

Hertzog, M., Milanesi, F., Hazelwood, L., Disanza, A., Liu, H., Perlade, E., and Scita, G. (2010). Molecular Basis for the Dual Function of Eps8 on Actin Dynamics: Bundling and Capping. *PLoS Biology*, *8*(6).

Hoffmann, P. R., deCathelineau, A. M., Ogden, C. A., Leverrier, Y., Bratton, D. L., Daleke, D. L., and Henson, P. M. (2001). Phosphatidylserine (PS) induces PS receptor-mediated macropinocytosis and promotes clearance of apoptotic cells. *The Journal of Cell Biology*, *155*(4), 649–659.

Horvath, C. A. J., Vanden Broeck, D., Boulet, G. A. V., Bogers, J., and De Wolf, M. J. S. (2007). Epsin: Inducing membrane curvature. *The International Journal of Biochemistry & Cell Biology*, *39*(10), 1765–1770.

Howe, A. K. (2004). Regulation of actin-based cell migration by cAMP/PKA. *Biochimica Et Biophysica Acta*, *1692*(2-3), 159–174.

Humphries, A. C., and Way, M. (2013). The non-canonical roles of clathrin and actin in pathogen internalization, egress and spread. *Nature Reviews Microbiology*, *11*(8), 551–560.

Huth, M. E., Ricci, A. J., and Cheng, A. G. (2011). Mechanisms of aminoglycoside ototoxicity and targets of hair cell protection. *International Journal of Otolaryngology*, *2011*, 937861.

Iscla, I., Wray, R., Wei, S., Posner, B., and Blount, P. (2014). Streptomycin potency is dependent on MscL channel expression. *Nature Communications*, *5*, 4891.

Jiang, H., Sha, S.-H., and Schacht, J. (2006). Kanamycin alters cytoplasmic and nuclear phosphoinositide signaling in the organ of Corti in vivo. *Journal of Neurochemistry*, *99*(1), 269–276.

Johnson, K. E. (1976). Circus movements and blebbing locomotion in dissociated embryonic cells of an amphibian, Xenopus laevis. *Journal of Cell Science*, *22*(3), 575–583.

Kachar, B., Parakkal, M., Kurc, M., Zhao, Y., and Gillespie, P. G. (2000). High-resolution structure of hair-cell tip links. *Proceedings of the National Academy of Sciences of the United States of America*, *97*(24), 13336–13341.

Kachar, B., Battaglia, A., and Fex, J. (1997). Compartmentalized vesicular traffic around the hair cell cuticular plate. *Hearing Research*, *107*(1–2), 102–112.

Kadurugamuwa, J. L., Clarke, A. J., and Beveridge, T. J. (1993). Surface action of gentamicin on Pseudomonas aeruginosa. *Journal of Bacteriology*, *175*(18), 5798–5805.

Kalin, S., Amstutz, B., Gastaldelli, M., Wolfrum, N., Boucke, K., Havenga, M., and Greber, U. F. (2010). Macropinocytotic Uptake and Infection of Human Epithelial Cells with Species B2 Adenovirus Type 35. *Journal of Virology*, *84*(10), 5336–5350.

Kerr, M. C., and Teasdale, R. D. (2009). Defining Macropinocytosis. *Traffic*, *10*(4), 364–371.

Kirkham, M., and Parton, R. G. (2005). Clathrin-independent endocytosis: new insights into caveolae and non-caveolar lipid raft carriers. *Biochimica Et Biophysica Acta*, *1745*(3), 273–286.

Kleinegris, M. C., Koek, G. H., Mast, K., Mestrom, E. H. C., Wolfs, J. L. N., and Bevers, E. M. (2012). Ribavirin-induced externalization of phosphatidylserine in erythrocytes is predominantly caused by inhibition of aminophospholipid translocase activity. *European Journal of Pharmacology*, *693*(1–3), 1–6.

Laser-Azogui, A., Diamant-Levi, T., Israeli, S., Roytman, Y., and Tsarfaty, I. (2014). Met-induced membrane blebbing leads to amoeboid cell motility and invasion. *Oncogene*, *33*(14), 1788–1798.

Lee, J. A. (2012). Neuronal autophagy: a housekeeper or a fighter in neuronal cell survival? *Experimental Neurobiology*, *21*(1), 1–8.

Lim, D. J. (1976). Ultrastructural cochlear changes following acoustic hyperstimulation and ototoxicity. *The Annals of Otology, Rhinology, and Laryngology*, *85*(6 PT. 1), 740–751.

Lopez-Marques, R. L., Theorin, L., Palmgren, M. G., and Pomorski, T. G. (2014). P4-ATPases: lipid flippases in cell membranes. *Pflugers Archiv*, *466*(7), 1227–1240.

Ludwig, A., Howard, G., Mendoza-Topaz, C., Deerinck, T., Mackey, M., Sandin, S., and Nichols, B. J. (2013). Molecular Composition and Ultrastructure of the Caveolar Coat Complex. *PLoS Biology*, *11*(8).

Mahaut-Smith, M. P. (2013). A role for platelet TRPC channels in the Ca2+ response that induces procoagulant activity. *Science Signaling*, *6*(281), pe23.

Marcotti, W., van Netten, S. M., and Kros, C. J. (2005). The aminoglycoside antibiotic dihydrostreptomycin rapidly enters mouse outer hair cells through the mechano-electrical transducer channels. *The Journal of Physiology*, *567*(Pt 2), 505–521.

Martin, N. L., and Beveridge, T. J. (1986). Gentamicin interaction with Pseudomonas aeruginosa cell envelope. *Antimicrobial Agents and Chemotherapy*, *29*(6), 1079–1087.

McDowell, B. (1982). Patterns of cochlear degeneration following gentamicin administration in both old and young guinea pigs. *British Journal of Audiology*, *16*(2), 123–129.

McGee, J., Goodyear, R. J., McMillan, D. R., Stauffer, E. A., Holt, J. R., Locke, K. G., and Richardson, G. P. (2006). The very large G-protein-coupled receptor VLGR1: a component of the ankle link complex required for the normal development of auditory hair bundles. *The Journal of Neuroscience: The Official Journal of the Society for Neuroscience*, *26*(24), 6543–6553.

Meléndez, A., and Levine, B. (2009). Autophagy in C. elegans. *WormBook: The Online Review of C. Elegans Biology*, 1–26.

Mercer, J., and Helenius, A. (2009). Virus entry by macropinocytosis. *Nature Cell Biology*, *11*(5), 510–520.

Mercer, J., and Helenius, A. (2012). Gulping rather than sipping: macropinocytosis as a way of virus entry. *Current Opinion in Microbiology*, *15*(4), 490–499.

Mercer, J., Knébel, S., Schmidt, F. I., Crouse, J., Burkard, C., and Helenius, A. (2010). Vaccinia virus strains use distinct forms of macropinocytosis for host-cell entry. *Proceedings of the National Academy of Sciences of the United States of America*, *107*(20), 9346–9351.

Meshki, J., Douglas, S. D., Lai, J. P., Schwartz, L., Kilpatrick, L. E., and Tuluc, F. (2009). Neurokinin 1 receptor mediates membrane blebbing in HEK293 cells through a Rho/Rho-associated coiled-coil kinase-dependent mechanism. *The Journal of Biological Chemistry*, *284*(14), 9280–9289.

Michalski, N., Michel, V., Bahloul, A., Lefèvre, G., Barral, J., Yagi, H., and Petit, C. (2007). Molecular Characterization of the Ankle-Link Complex in Cochlear Hair Cells and Its Role in the Hair Bundle Functioning. *The Journal of Neuroscience*, *27*(24), 6478–6488.

Myrdal, S. E., Johnson, K. C., and Steyger, P. S. (2005). Cytoplasmic and intra-nuclear binding of gentamicin does not require endocytosis. *Hearing Research*, *204*(1-2), 156–169.

Naslavsky, N., McKenzie, J., Altan-Bonnet, N., Sheff, D., and Caplan, S. (2009). EHD3 regulates early-endosome-to-Golgi transport and preserves Golgi morphology. *Journal of Cell Science*, *122*(3), 389–400.

Naslavsky, N., Rahajeng, J., Sharma, M., Jović, M., and Caplan, S. (2006). Interactions between EHD Proteins and Rab11-FIP2: A Role for EHD3 in Early Endosomal Transport. *Molecular Biology of the Cell*, *17*(1), 163–177.

Nassoy, P., and Lamaze, C. (2012). Stressing caveolae new role in cell mechanics. *Trends in Cell Biology*, *22*(7), 381–389.

Nayak, G. D. (2010). *The hair cell antigen/Ptprq: Lipid phosphatase activity, intracellular domain interactions, Apical targeting and Evidence that it is a Proteoglycan*. University of Sussex.

Nayak, G. D., Ratnayaka, H. S. K., Goodyear, R. J., and Richardson, G. P. (2007). Development of the hair bundle and mechanotransduction. *The International Journal of Developmental Biology*, *51*(6-7), 597–608.

Nishikawa, S., and Sasaki, F. (1996). Internalization of styryl dye FM1-43 in the hair cells of lateral line organs in Xenopus larvae. *Journal of Histochemistry & Cytochemistry*, *44*(7), 733–741.

Nonnenmacher, M., and Weber, T. (2011). Adeno-Associated Virus 2 Infection Requires Endocytosis through the CLIC/GEEC Pathway. *Cell Host & Microbe*, *10*(6), 563–576.

Norman, L., Sengupta, K., and Aranda-Espinoza, H. (2011). Blebbing dynamics during endothelial cell spreading. *European Journal of Cell Biology*, *90*(1), 37–48.

Olt, J., Mburu, P., Johnson, S. L., Parker, A., Kuhn, S., Bowl, M., and Brown, S. D. M. (2014). The actin-binding proteins eps8 and gelsolin have complementary roles in regulating the growth and stability of mechanosensory hair bundles of mammalian cochlear outer hair cells. *PloS One*, *9*(1), e87331.

Osborne, M. P., Comis, S. D., and Pickles, J. O. (1988). Further observations on the fine structure of tip links between stereocilia of the guinea pig cochlea. *Hearing Research*, *35*(1), 99–108.

Parton, R. G., and Simons, K. (2007). The multiple faces of caveolae. *Nature Reviews. Molecular Cell Biology*, *8*(3), 185–194.

Peterson, A. A., Hancock, R. E., and McGroarty, E. J. (1985). Binding of polycationic antibiotics and polyamines to lipopolysaccharides of Pseudomonas aeruginosa. *Journal of Bacteriology*, *164*(3), 1256–1261.

Pickles, J. (1988). *An Introduction to the Physiology of Hearing* (Second ed.). London: Academic Press.

Pirvola, U., Xing-Qun, L., Virkkala, J., Saarma, M., Murakata, C., Camoratto, A. M., and Ylikoski, J. (2000). Rescue of hearing, auditory hair cells, and neurons by CEP-1347/KT7515, an inhibitor of c-Jun N-terminal kinase activation. *The Journal of Neuroscience: The Official Journal of the Society for Neuroscience*, *20*(1), 43–50.

Purves, D. (2008). *Neuroscience*. Sunderland, Mass.: Sinauer.

Quick, K., Zhao, J., Eijkelkamp, N., Linley, J. E., Rugiero, F., Cox, J. J., and Wood, J. N. (2012). TRPC3 and TRPC6 are essential for normal mechanotransduction in subsets of sensory neurons and cochlear hair cells. *Open Biology*, *2*(5).

Ravichandran, K. S. (2011). Beginnings of a good apoptotic meal: the find-me and eat-me signaling pathways. *Immunity*, *35*(4), 445–455.

Richardson, G. P., Forge, A., Kros, C. J., Fleming, J., Brown, S. D., and Steel, K. P. (1997). Myosin VIIA is required for aminoglycoside accumulation in cochlear hair cells. *The Journal of Neuroscience: The Official Journal of the Society for Neuroscience*, *17*(24), 9506–9519.

Richardson, G. P., and Russell, I. J. (1991). Cochlear cultures as a model system for studying aminoglycoside induced ototoxicity. *Hearing Research*, *53*(2), 293–311.

Rivard, R. L., Birger, M., Gaston, K. J., and Howe, A. K. (2009). AKAP-Independent Localization of Type-II Protein Kinase A to Dynamic Actin Microspikes. *Cell Motility and the Cytoskeleton*, *66*(9), 693–709.

Rizzi, M. D., and Hirose, K. (2007). Aminoglycoside ototoxicity. *Current Opinion in Otolaryngology & Head and Neck Surgery*, *15*(5), 352–357.

Rusch, A., Kros, C. J., and Richardson, G. P. (1994). Block by amiloride and its derivatives of mechano-electrical transduction in outer hair cells of mouse cochlear cultures. *The Journal of Physiology*, *474*(1), 75–86.

Russell, I. J., and Richardson, G. P. (1987). The morphology and physiology of hair cells in organotypic cultures of the mouse cochlea. *Hearing Research*, *31*(1), 9–24.

Rybak, L. P., and Ramkumar, V. (2007). Ototoxicity. *Kidney International*, *72*(8), 931–935.

Sandvig, K., Torgersen, M. L., Raa, H. A., and van Deurs, B. (2008). Clathrin-independent endocytosis: from nonexisting to an extreme degree of complexity. *Histochemistry and Cell Biology*, *129*(3), 267–276.

Sato, H., and Frank, D. W. (2014). Intoxication of Host Cells by the T3SS Phospholipase ExoU: PI(4,5)P2-Associated, Cytoskeletal Collapse and Late Phase Membrane Blebbing. *PLoS ONE*, *9*(7).

Schacht, J. (1993). Biochemical basis of aminoglycoside ototoxicity. *Otolaryngologic Clinics of North America*, *26*(5), 845–856.

Schacht, J., Talaska, A. E., and Rybak, L. P. (2012). Cisplatin and Aminoglycoside Antibiotics: Hearing Loss and Its Prevention. *Anatomical Record (Hoboken, N.J. : 2007)*, *295*(11), 1837–1850.

Schatz, A., Bugle, E., and Waksman, S. A. (1944). Streptomycin, a Substance Exhibiting Antibiotic Activity Against Gram-Positive and Gram-Negative Bacteria.∗†. *Experimental Biology and Medicine*, *55*(1), 66–69.

Schmidt, F. I., Bleck, C. K. E., Helenius, A., and Mercer, J. (2011). Vaccinia extracellular virions enter cells by macropinocytosis and acid-activated membrane rupture. *The EMBO Journal*, *30*(17), 3647–3661.

Segawa, K., Suzuki, J., and Nagata, S. (2011). Constitutive exposure of phosphatidylserine on viable cells. *Proceedings of the National Academy of Sciences of the United States of America*, *108*(48), 19246–19251.

Sha, S. H., Zajic, G., Epstein, C. J., and Schacht, J. (2001). Overexpression of copper/zinc-superoxide dismutase protects from kanamycin-induced hearing loss. *Audiology & Neuro-Otology*, *6*(3), 117–123.

Sheppard, A., Hayes, S. H., Chen, G. D., Ralli, M., and Salvi, R. (2014). Review of salicylate-induced hearing loss, neurotoxicity, tinnitus and neuropathophysiology. *Acta Otorhinolaryngologica Italica*, *34*(2), 79–93.

Shi, X., Gillespie, P. G., and Nuttall, A. L. (2005). Na+ influx triggers bleb formation on inner hair cells. *American Journal of Physiology. Cell Physiology*, *288*(6), C1332–1341.

Shvets, E., Ludwig, A., and Nichols, B. J. (2014). News from the caves: update on the structure and function of caveolae. *Current Opinion in Cell Biology*, *29*, 99–106.

Siemens, J., Lillo, C., Dumont, R. A., Reynolds, A., Williams, D. S., Gillespie, P. G., and Müller, U. (2004). Cadherin 23 is a component of the tip link in hair-cell stereocilia. *Nature*, *428*(6986), 950–955.

Sorkin, A. (2004). Cargo recognition during clathrin-mediated endocytosis: a team effort. *Current Opinion in Cell Biology*, *16*(4), 392–399.

Stan, R. V. (2005). Structure of caveolae. *Biochimica Et Biophysica Acta*, *1746*(3), 334–348.

Stapelbroek, J. M., Peters, T. A., van Beurden, D. H. A., Curfs, J. H. A. J., Joosten, A., Beynon, A. J., and Houwen, R. H. J. (2009). ATP8B1 is essential for maintaining normal hearing. *Proceedings of the National Academy of Sciences of the United States of America*, *106*(24), 9709–9714.

Su, H., Carter, C. B., Laur, O., Sands, J. M., and Chen, G. (2012). Forskolin stimulation promotes urea transporter UT-A1 ubiquitination, endocytosis, and degradation in MDCK cells. *American Journal of Physiology. Renal Physiology*, *303*(9), F1325–1332.

Sun, X., and Whittaker, G. R. (2007). Role of the actin cytoskeleton during influenza virus internalization into polarized epithelial cells. *Cellular Microbiology*, *9*(7), 1672–1682.

Tinevez, J. Y., Schulze, U., Salbreux, G., Roensch, J., Joanny, J. F., and Paluch, E. (2009). Role of cortical tension in bleb growth. *Proceedings of the National Academy of Sciences of the United States of America*, *106*(44), 18581–18586.

Todde, V., Veenhuis, M., and van der Klei, I. J. (2009). Autophagy: Principles and significance in health and disease. *Biochimica Et Biophysica Acta (BBA) - Molecular Basis of Disease*, *1792*(1), 3–13.

Tsuprun, V., Goodyear, R. J., and Richardson, G. P. (2004). The Structure of Tip Links and Kinocilial Links in Avian Sensory Hair Bundles. *Biophysical Journal*, *87*(6), 4106–4112.

van den Anker, J. N. (2014). How to optimize the evaluation and use of antibiotics in neonates. *Early Human Development*, *90 Suppl 1*, S10–12.

van der Mark, V. A., Oude Elferink, R. P. J., and Paulusma, C. C. (2013). P4 ATPases: Flippases in Health and Disease. *International Journal of Molecular Sciences*, *14*(4), 7897–7922.

Verpy, E., Leibovici, M., Michalski, N., Goodyear, R. J., Houdon, C., Weil, D., and Petit, C. (2011). Stereocilin connects outer hair cell stereocilia to one another and to the tectorial membrane. *The Journal of Comparative Neurology*, *519*(2), 194–210.

Vigne, P., Frelin, C., Cragoe, E. J., and Lazdunski, M. (1983). Ethylisopropyl-amiloride: a new and highly potent derivative of amiloride for the inhibition of the Na+/H+ exchange system in various cell types. *Biochemical and Biophysical Research Communications*, *116*(1), 86–90.

von Kleist, L., Stahlschmidt, W., Bulut, H., Gromova, K., Puchkov, D., Robertson, M. J., and Haucke, V. (2011). Role of the Clathrin Terminal Domain in Regulating Coated Pit Dynamics Revealed by Small Molecule Inhibition. *Cell*, *146*(3), 471–484.

Wang, J., Van De Water, T. R., Bonny, C., de Ribaupierre, F., Puel, J. L., and Zine, A. (2003). A peptide inhibitor of c-Jun N-terminal kinase protects against both aminoglycoside and acoustic trauma-induced auditory hair cell death and hearing loss. *The Journal of Neuroscience: The Official Journal of the Society for Neuroscience*, *23*(24), 8596–8607.

Welsch, T., Endlich, K., Giese, T., Büchler, M. W., and Schmidt, J. (2007). Eps8 is increased in pancreatic cancer and required for dynamic actin-based cell protrusions and intercellular cytoskeletal organization. *Cancer Letters*, *255*(2), 205–218.

Wessells, N. K., Nuttall, R. P., Wrenn, J. T., and Johnson, S. (1976). Differential labeling of the cell surface of single ciliary ganglion neurons in vitro. *Proceedings of the National Academy of Sciences of the United States of America*, *73*(11), 4100–4104.

Wickman, G., Julian, L., and Olson, M. F. (2012). How apoptotic cells aid in the removal of their own cold dead bodies. *Cell Death and Differentiation*, *19*(5), 735–742.

Wu, Y. T., Tan, H. L., Shui, G., Bauvy, C., Huang, Q., Wenk, M. R., and Shen, H. M. (2010). Dual Role of 3-Methyladenine in Modulation of Autophagy via Different Temporal Patterns of Inhibition on Class I and III Phosphoinositide 3-Kinase. *The Journal of Biological Chemistry*, *285*(14), 10850–10861.

Xie, J., Talaska, A. E., and Schacht, J. (2011). New developments in aminoglycoside therapy and ototoxicity. *Hearing Research*, *281*(1-2), 28–37.

Yang, Q., Zhang, X. F., Van Goor, D., Dunn, A. P., Hyland, C., Medeiros, N., and Forscher, P. (2013). Protein kinase C activation decreases peripheral actin network density and increases central nonmuscle myosin II contractility in neuronal growth cones. *Molecular Biology of the Cell*, *24*(19), 3097–3114.

Yang, Z., and Klionsky, D. J. (2010). Eaten alive: a history of macroautophagy. *Nature Cell Biology*, *12*(9), 814–822.

Zhao, H., Williams, D. E., Shin, J. B., Brügger, B., and Gillespie, P. G. (2012). Large membrane domains in hair bundles specify spatially constricted radixin activation. *The Journal of Neuroscience: The Official Journal of the Society for Neuroscience*, *32*(13), 4600–4609.